ISSN 2087-2852

The Journal of Experimental Life Science

Discovering Living System Concept through Nano, Molecular and Cellular Biology

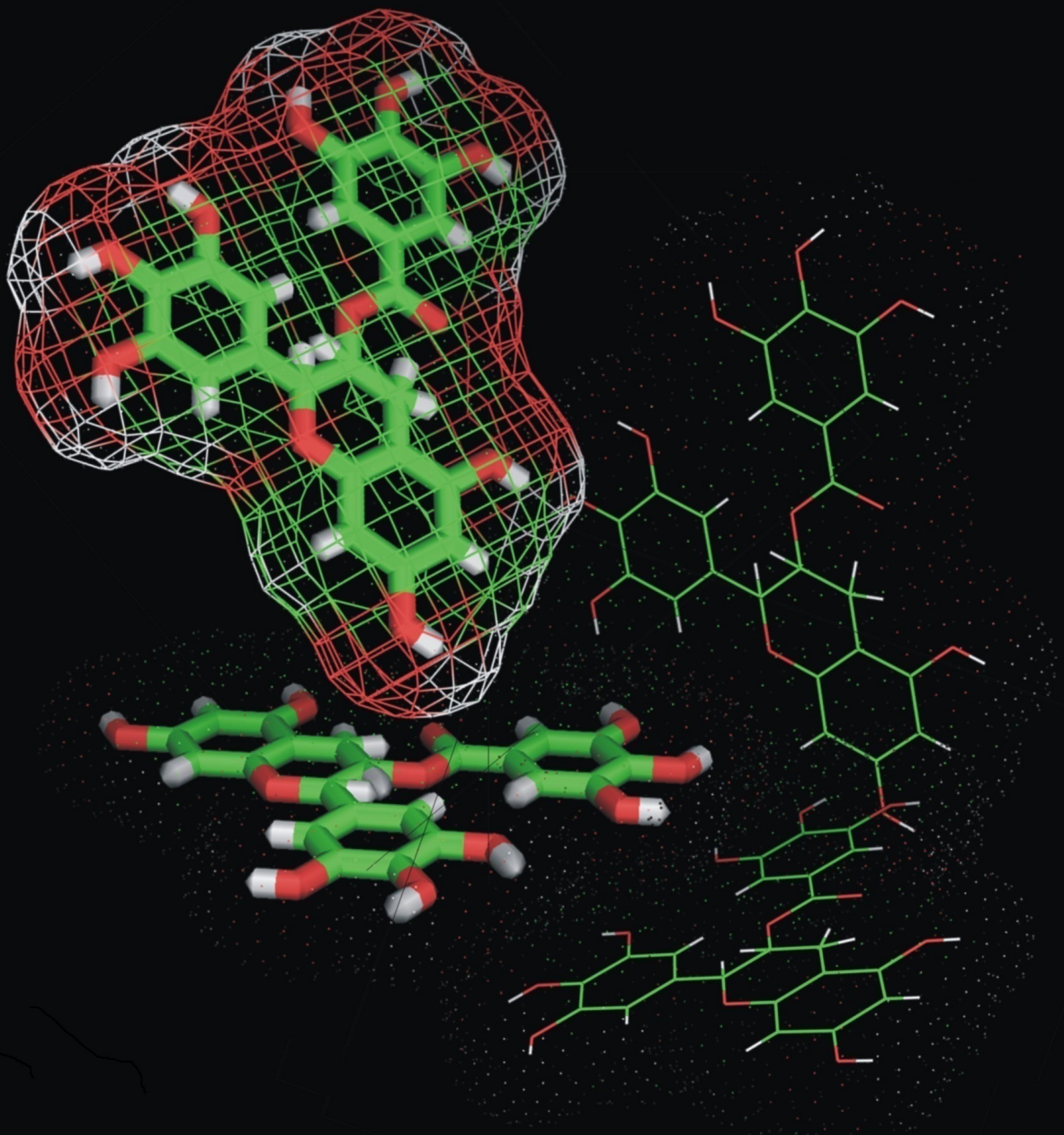

J. Exp. Life. Sci. | Vol. 8 | No. 2 | pages. 71-132 | June 2018

Published by

Graduate Program, University of Brawijaya
in Cooperation With
Masyarakat Nano Indonesia (MNI)

ISSN. 2087-2852
E-ISSN. 2338-1655

The Journal of Experimental Life Science

Discovering Living System Concept through Nano, Molecular and Cellular Biology

Editorial Board

Address
The Journal of Experimental Life Science
Building E, 2nd Floor, Postgraduate School, University of Brawijaya
Jl. Mayor Jenderal Haryono 169, Malang, 65145
Telp: (0341) 571260 ; Fax: (0341) 580801
Email: jels@ub.ac.id
Web: http://www.jels.ub.ac.id

ISSN. 2087-2852
E-ISSN. 2338-1655

Table of Content

Geographically and Temporally Weighted Regression Modeling in Analyzing Factors Affecting the Spread of Dengue Fever in Malang

A. Fahmi Indrayani[1*], Henny Pramoedyo[2], Atiek Iriany[2]

[1]Master Program of Mathematics, Faculty of Mathematics and Natural Sciences, University of Brawijaya, Malang, Indonesia

[2]Department of Mathematics, Faculty of Mathematics and Natural Sciences, University of Brawijaya, Malang, Indonesia

Abstract

Geographically and Temporally weighted regression (GTWR) modeling has been developed to evaluate spatial heterogeneity and temporal heterogeneity in factors influencing the spread of dengue fever in Malang city. By using the monthly data in 2012-2015 as the temporal unit of each urban village in Malang and village is considered as a spatial unit. GTWR model is compared with the GWR model using several statistical criteria. GTWR model shows that the relationship between dengue incidence with population density and monthly average temperature significantly affects each Village in Malang.

Keywords: dengue hemorrhagic fever, Geographically and Temporally weighted regression, spatiotemporal pattern.

INTRODUCTION

Dengue hemorrhagic fever (DHF) is a disease caused by the dengue virus that is found in tropical and subtropical areas. The number of sufferers and the extent of their spreading areas increases with increasing mobility and population density. In Indonesia, the disease transmitted by *Aedes aegypti* mosquitoes was first discovered in Surabaya and Jakarta in 1968 [1].

For the last three years, patients with dengue fever in Malang continue to increase (Health Office of City Government of Malang, 2016, unpublished). Various programs have been implemented for disease prevention and control, but DHF in Malang remains high. High dengue cases require serious efforts to prevent the spread of DHF endemic disease by analyzing the risk factors associated with dengue virus infection. Many research on the factors that cause the spread of dengue virus in the community were conducted [2].

Previous study used the Geographically Weighted Regression (GWR) model in its analysis; where GWR statistical methods adjusted the global framework with local regression models allowing estimation regression parameters for each spatial unit [3]. And it is reported that rainfall significantly affects the spread of DHF. However, this research is limited to spatial effects and rainfall factors, where the relationship between dengue fever and rainfall varies greatly in each location of observation. As a result, its conclusions only look at the spatial effects and one factor, not paying attention to the influence of time and other factors that can also affect the spread of dengue in the area.

In many cases, data structures are not only owned by geographic location but also related to the time factor. One method for examining spatial and temporal influences is geographically and temporally weighted regression (GTWR). This statistic method is developed from GWR. It is expexted that this model can accommodate spatial influence, and also able to analyze the temporal influence which present in the data simultaneously [4].

The purpose of this study is to extend the GTWR modeling framework in analyzing factors causing dengue extensively by observing the presence of spatial heterogeneity and temporal heterogeneity in the modeling. The GTWR model obtained is compared with the GWR model using several statistical tests. The results of this study will practically be useful for the authorities in regulating the prevention program of DHF infection locally and at certain times.

MATERIAL AND METHOD

Study Area

Location of this research is Malang City, East Java, which consists of 57 urban villages. Total area of Malang is 252.10 km^2 which is located on Java island about 7^{o}06 '- 8^{o}07' latitude and 112^{o}06 '- 112^{o}07' longitude [5]. Village is used as a spatial unit in this study, there are 57 villages and the month as a temporal unit, consisting of 48 months.

* Correspondence address:
A. Fahmi Indrayani
Email : fahmi.indrayani@gmail.com
Address : Dept. Mathematics, Faculty of Mathematics and Natural Science, University of Brawijaya, Veteran Malang, Malang 65145.

Data Collection

Data on the number of DHF patients in each Village and each month during the year 2012 - 2015 was obtained from the Health Office of Malang city government. Monthly data as a temporal unit in each Village, one Village is defined as one spatial unit. For population density data, the number of *Puskesmas* (health center) in each Village, as well as the height of the place in each Village obtained from Malang Central Agency on Statistics publication [5-8]. Data of rainfall and average temperature obtained from Karangploso Agency for Meteorological, Climatological and Geophysics.

Number of DHF patients selected as response variable (Y), population density (X_1), Number of health center auxiliary (X_2), rainfall (X_3), average temperature (X_4) and altitude of place from sea level (X_5) as predictors variable.

Statistical Methods

The relationship between DHF incidence and factors considered to affect the spread of DHF was analyzed by comparing the results of GWR model and GTWR model. If GTWR model is better than GWR model, the relation between respondent variable and the predictor variables is spatially and temporally different for each Village.

GWR model is a simple model and is usually used in research. The spatial heterogeneity of the relationship between the occurrence of DHF and factors influencing it was analyzed by the GWR model allowing estimation of different regression parameters in each Village [3].

$$Y_i = \beta_0(u_i, v_i) + \sum_{k=1}^{p} \beta_k(u_i, v_i) X_{ik} + \varepsilon_i \quad \text{.....1}$$

Where $\beta_0(u_i, v_i)$and $\beta_k(u_i, v_i)$ is the coefficient of GWR in each Village i; (u_i, v_i) is the location point of the Village is the definition of the longitude and latitude coordinates ; and ε_i is an error that is assumed to be normal distribution with mean 0 and its variant known.

The GTWR model is formed by using the spatial weight function and the temporal weighting function in estimating its parameters [4].

$$Y_{it} = \beta_0(u_i, v_i, t_i) + \sum_{k=1}^{p} \beta_k(u_i, v_i, t_i) X_{ik} + \varepsilon_i \quad \text{.....2}$$

Where (u_i, v_i, t_i) is the location of Village i^{th} and the observation time for the observation location. Longitude and Latitude coordinate defined by (u_i, v_i, t_i); Y_{it} is a response variable, X_{ik} is a factor that may affect and ε_i is an error of observation at location i^{th}. The first step for GTWR modeling to define the coordinates of Longitude and Latitude for each Village at *t* time. Geographical coordinates are used to determine the euclidean distance between villages observed at t time

$$d_{ij} = \sqrt{\lambda\left[(u_i - u_j)^2 + (v_i - v_j)^2\right] + \mu(t_i - t_j)^2} \quad \text{.....3}$$

λ and μ are scale factors used to measure location and time difference. Distance in equation (3) as a basis in weighting data to estimate GTWR model parameters. The closer the distance between the expected points each village, the greater the weight of the data during the estimation. In this study, data weighting is done by using the adaptive Gaussian kernel function

$$w_{ij} = \exp\left(-(d_{ij}/h)^2\right) \quad \text{.....4}$$

Where, h is the constant bandwidth performed by the Incremental Spatial Autocorrelation (ISA) method [9]. The Adaptive Gaussian kernel function is used in forming a weighted matrix.

$$\mathbf{W}(u_i, v_i, t_i) = diag(W_1(u_i, v_i, t_i), \cdots, W_n(u_i, v_i, t_i)) \quad \text{.....5}$$

Each observed data has one weighted matrix $W(u_i, v_i, t_i)$ in estimating the parameters. Using the algebraic matrix approach, and using the Weighted least square (WLS) method the parameter estimation can be written [4]

$$\hat{\beta}(u_i, v_i, t_i) = (X'\mathbf{W}(u_i, v_i, t_i)X)^{-1} X\mathbf{W}(u_i, v_i, t_i)Y \quad \text{.....6}$$

Significant test of GTWR model is given on [10]. Where the null hypothesis of test indicates the function $\beta_k(u_i, v_i)$ for each coordinate (u_i, v_i) of the research location. If the null hypothesis is rejected, then the GTWR model is accepted to describe the data. Meanwhile, tests for the variation of each set of β_k for the entire study site will be used in F_3 statistics [10]. The identification of the GTWR model will also be shown by coefficient determination (R^2). The comparison of the GWR model and the GTWR model will be shown with Root mean square error. According to RMSE the regression model that has the smallest RMSE value is defined as the best model.

ISSN. 2087-2852
E-ISSN. 2338-1655

RESULT AND DISCUSSION

Result of GWR Model

Using the spatial weighting, the parameter estimation ratios (regression coefficients) for the obtained GWR model are shown in Table 1. In this model the value of obtained R^2 = 51.1% and RMSE = 13.13. Further analysis of the model indicates that the error approaches normal distribution.

Table 1. Summary for Coefficient of GWR Model

Parameter	Minimun	Median	Maximum
θ_0	0.9138619705260	0.9138767081168	0.9138948801913
θ_1	0.0000010683522	0.0000010684401	0.0000010685115
θ_2	-0.2121692197872	-0.2121678107572	-0.2121659143796
θ_3	0.0004221212435	0.0004221221469	0.0004221234641
θ_4	2.0687979109140	2.0687998269883	2.0688021917249
θ_5	282.8140409500290	282.8165895808340	282.8184768167160

Result of GTWR Model

By using ISA [9], GTWR modeling has bandwidth Optimum *h* = 3947.54. Table 2 shows the estimated estimation of the GTWR model parameters. The GTWR model has a value of RMSE = 1.22, which is smaller than the RMSE value of the GWR model. And the coefficient of determination (R^2 = 69.13%) is higher than the GWR model.

Positive value on coefficient for koefisien β_1, β_2, β_3, β_4 and β_5 shows that predictor variables of population density, number of puskesmas / puskesmas auxiliaries, rainfall, temperature and altitude of the sea surface contribute positively to the response variable, this indicates that if these variables increase, then the number of dengue fever patients every month in Village it will increase.

To determine the factors that influence the incidence of DHF in each Village, conducted statistical calculation of GTWR model parameters test for each urban village in Malang. Value of *t* compared with t_{table} (0.05; 2730) = 2.24264. If $|t_{cal}| > t_{table}$ then it is decided reject H_0 which means the significant k^{th} parameter of i^{th} location.

Table 2. Summary for coefficient of GTWR Model

Parameter	Minimun	Median	Maximum
θ_0	0.1511224153094	0.1511827937156	0.1512318270934
θ_1	0.0000823500371	0.0000823518679	0.0000823541227
θ_2	0.0019856156327	0.1985769641700	0.0019859593066
θ_3	0.0000149726542	0.0001497344800	0.0000149740928
θ_4	0.0208599179654	0.0208606080060	0.0208614577425
θ_5	0.0004859141711	0.0048598685785	0.0004860763600

CONCLUSION

In this paper, a discrete fractional-order Population density and temperature are significant variables on the number of dengue fever occurrences in Malang. Residents living in densely populated locations have a higher risk of dengue transmission. So also if there is an increase in temperature then the risk of transmission of dengue virus will also be greater.

ACKNOWLEDGEMENT

We thank to Health Office of Malang city government, Malang Central Agency on Statistics, and Karangploso Agency for Meteorological, Climatological and Geophysics for supporting data.

REFERENCES

[1] Aiken, S., C. Leigh. 1978. Dengue Hemorrhagic fever in South-East Asia. *Trans. Inst. Br. Geogr*. 3(4). 476-497.

[2] Baharuddin, Suhariningsih, B. Ulama. 2014. Geographically Weighted Regression Modeling for analyzing spatial heterogeneity on relationship between Dengue Hemorrhagic Fever incidence and rainfall in Surabaya, Indonesia. *Mod. Appl. Sci.* 8(3). 85-91.

[3] McMillen, D. P. 2002. Geographically Weighted Regression - the analysis of Spatially Varying Relationships. *Am. J. Agric. Econ.* 86(2). 554-556.

[4] Huang, B., B. Wu, M. Barry. 2010. Geographically and Temporally Weighted Regression for modelling spatio-temporal

variation in house prices. *Int. J. Geogr. Inf. Sci.* 24(3). 383-401.
[5] Central Agency on Statistics. 2013. Malang in figures 2013. Central Agency on Statistics. Malang.
[6] Central Agency on Statistics. 2014. Malang in figures 2014. Central Agency on Statistics. Malang.
[7] Central Agency on Statistics. 2015. Malang in figures 2015. Central Agency on Statistics. Malang.
[8] Central Agency on Statistics. 2016. Malang in figures 2016. Central Agency on Statistics. Malang.
[9] Ge, L., Y. Zhao, Z. Sheng, N. Wang, K. Zhou, X. Mu, L. Guo, T. Wang, Z. Yang, X Huo. 2016. Contruction of Seasonal Difference-Geographically and Temporally Weighted Regression (SD-GTWR) model and comparative analysis with GWR-Based Models for Hemorrhagic Fever with Renal Syndrome (HFRS) in Hubei Province (China). Int. J. Environ. Res. Public Health. 13(11). pii: E1062.
[10] Xuan, H., S. Li, M. Amin. 2015. Statistical inference of Geographically and Temporally Weighted Regression Model. *Pakistan J. Statist.* 31(3). 307-325.
[11] Hii, Y. L., H. Zhu, N. Ng, L.C. Ng, J. Rocklov. 2012. Forecast of Dengue Incidence Using Temperature and Rainfall. PLOS Neglected Tropical Diseases. Available at: https://doi.org/10.1371/journal.pntd.0001908.

ISSN. 2087-2852
E-ISSN. 2338-1655

The Effect of *Elephantopus scaber* Extract to TNF-α and TGF-β on Mice under Carcinogen Treatment

Rizki Amalia[1*], Sri Widyarti[2], Moch. Sasmito Djati[2]

[1]Master Program of Biology, Faculty of Mathematics and Natural Sciences, University of Brawijaya, Malang, Indonesia
[2]Department of Biology, Faculty of Mathematics and Natural Sciences, University of Brawijaya, Malang, Indonesia

Abstract

Carcinogen compounds are the compounds that cause DNA damage and trigger cancer. TNF-α and TGF-β are cytokines produced by immune cells and serve to maintain body homeostasis. *Elephantopus scaber* is a plant that prevents the cancer progression, and improve the body's immune system, so this study was conducted to determine the effect of *E. scaber* extract on TNF-α and TGF-β after the administration of carcinogen compounds. The study was conducted by administering the carcinogen compound DMBA with a dosage of 0.56 mg kg^{-1} BW and estradiol with a dose of 0.0504 mg kg^{-1} BW which was given alternately for 8 weeks to the *Mus musculus* test animals. The study was conducted in 3 groups: K- (the normal group of mice), K + (a carcinogen-induced group of mice), and P (a group of carcinogen-induced mice and *E. scaber* extract). The treatment was done in 1 week, 2 weeks, and 3 weeks. Immune cells were isolated from splenocytes and performed immunostaining for flow cytometry analysis. The computed relative amount is TNF-α produced by macrophages CD11b and TGF-β produced by Treg CD4CD25. The relative number of cells was analyzed by two-way ANOVA and advanced Tukey test with 95% confidence level (α = 0.05). The results showed no significant differences in the number of cytokines TNF-α and TGF-β in both the carcinogen-induced mice group and the mice group was given the extract of *Elephantopus scaber* for 1 week, 2 weeks and 3 weeks.

Keywords: Carcinogen, *Elephantopus scaber*, TNF-α, TGF-β.

INTRODUCTION*

Carcinogens are various substrates that can cause cancer or carcinogenesis. Carcinogenic compounds do not always cause direct poisoning, but can be in a very long time [1]. When the carcinogen compound enter the body, it will be detoxified by the liver through a biotransformation process to transform the toxic compounds to become water-soluble so it can be easily removed from the body. However, in some cases, this process can change the non-toxic compounds to be more toxic [2].

One of the most carcinogenic compounds that widely used in cancer modeling research was DMBA (7.12-Dimethylbenz [a] anthracene), the immunosuppressor compound and potent cancer-promoting agent [3]. The DMBA bioactivation process on microsomal P-450 by NADPH produced 7-Hydroxymethyl-12-methylbenz [a] anthracene (7-HMBA) metabolite which then cytosolic sulfotransferase by PAPS into more mutagenic compound 7-HMBA sulfate [4]. Mutagenic compounds which have the potential to damage DNA occurs to cause errors during the process of replication, resulting in the occurrence of mutations and alteration epigenetic [5]. Such epigenetic mutations and alterations may be replicated as cells proliferate, thereby altering gene function or expression of the gene that would potentially be a cancer-triggering agent.

Previous research has shown that increased DNA damage on cultured cells was responded by activating oncogenic factors [6]. Stress at the time of cell replication coincides with the inactivation of mutated gene caused by DNA damage, lead to downregulation or loss of DNA damage response mechanisms, resulting in cell loss of ability to perform DNA repair, senescence, and cell death programs (apoptosis), and trigger the occurrence of cancer [7]. The body has a natural response to control the repairing process caused by DNA damage. One of the body's natural factors that act as the body defending system is immune cells.

The immune system has the ability to detect the presence of cell abnormalities in the body, and provides a natural response to apoptosis programs so that the balance of the body defending system is maintained [8]. Through pro-inflammatory and anti-inflammatory responses, the immune system works to induce body homeostasis. One of the cytokines that play a role in this process is TNF-α and TGF-β. Tumor necrosis factor α (TNF-α) is a signal protein that plays an important role in inflammatory regulation, and produced most by macrophages

* Correspondence address:
Rizki Amalia
Email : rizkiamalia_93@yahoo.co.id
Address : Dept. Biology, Faculty of Mathematics and Natural Science, University of Brawijaya, Veteran Malang, Malang 65145.

ISSN. 2087-2852
E-ISSN. 2338-1655

[9]. TNF-α can induce cell death pathways by activating NF-κB, activating MAPK pathway or by activation of caspase-8 [10,11,12].

In addition to TNF-α, Transforming Growth Factor β (TGF-β) is also a cytokine that plays an important role in the regulation of immune system. TGF-β is anti-inflammatory cytokine that produced by all the immune cells, which serves to induce gene transcription for differentiation, chemotaxis, proliferation, and activation of immune cells [13,14]. Both TNF-α and TGF-β are important signal proteins to maintain body immune system through inflammatory and anti-inflammatory responses.

One of the plants that have anti-inflammatory activity is *Elephantopus scaber* [15]. *E. scaber* has long been used in traditional medicine in Brazil [16]. *E. scaber* contains deoxyelephantopin active compounds that are able to inhibit the growth of HCT116 collecting cancer by inducing apoptosis and cell cycle retention [17]. Deoxyelephantopin is also capable of inhibiting the growth of breast tumors and the proliferation of lung cancer metastases [18]. Deoxyelephantopin was able to fight cancer by inducing the activation of PPAR-γ (Peroxisome proliferator-activated receptor gamma), inhibiting NF-κB, has antiproliferation effects, and inducing apoptosis in tumors [19]. Due to some of the things mentioned earlier, in this study researchers wanted to know the effect of *Elephantopus scaber* plant extract on relative number of TNF-α and TGF-β in mice under carcinogen compounds tratment.

MATERIAL AND METHOD

Animal Trial

The experiment animals used in this study were BALB/c female mice with an average weight of 15-20 grams aged 5 weeks and obtained from Malang Murine Farm, Singosari. The procedure for the use and maintenance of experiment animals in this study is in accordance with the procedure and has been approved by the Research Ethics Committee of Brawijaya University with no. 648-KEP-UB.

Elephantopus scaber Extract

E. scaber leaf simplicia was obtained from Materia Medica Batu, extracted with 96% ethanol. The extract with a dose of 50 mg kg^{-1} BW then dissolved in warm distilled water 0.5 mL volume.

Carcinogen Treatment

Mice were given DMBA carcinogen with a dose of 0.56 mg kg^{-1} BW obtained from Sigma Aldrich company, and injected subcutaneously in the mammary gland area with a 4 mm diameter syringe needle. Injection was done 4 times in 8 weeks. To accelerate the occurrence of cancer, sex hormone estradiol was also added. Estradiol is an esterogen, which functions for the growth and differentiation of reproductive organs [20], so in this study estradiol was used as an induction to accelerated the proliferation of mammary glands to formed cancer cells. Estradiol was obtained from the company Tokyo Chemical Industry (TCM), dissolved in corn oil with a dose of 0.0504 mg kg^{-1} BW. Injection of estradiol was performed subcutaneously in the mammary gland area with a 4 mm diameter syringe needle. Injection of estradiol was performed 4 times in 8 weeks given alternately with DMBA.

Elephantopus scaber Extract Treatment

E. scaber leaf extract was given after the induction of carcinogen compound DMBA and Estradiol has finished. Based on previous research [21], the optimal dose of *E. scaber* extract to maintain immune system was 50 mg kg^{-1} BW, the extract was administered orally with cannula (sonde) with a total volume of 500 µL. The extract was administered daily for 1 week, 2 weeks, and 3 weeks.

Flow cytometry Analysys

Mice was sacrified by neck dislocation, then the spleen organ was obtained. The spleen organ crushed with cold PBS to collected spleenocytes. The collecting cells then was washed until there is no residue remained. The resulting cells were extracellularly stained by adding 50 µL of monoclonal antibodies obtained from Biolegend, i.e. Fluorescein Isothiocyanate (FITC) anti-mouse CD11b, CD4, CD25 with a concentration of 0.5 mg mL^{-1} respectively and then incubated in cold dark spaces.

Before Intracellular staining was performed, the Fixation buffer (Paraformaldehyde 4%) of Biolegend was added to the suspension and incubated in dark cold spaces. After that added the Permeabilization Wash Buffer (wash/ferm) from Biolegend to wash the remaining of the fixation buffer. Then the cells were stained with intracellular antibodies from Biolegend, ie PE anti-mouse TNF-α and TGF-β Antibody with each concentration of 0.2 mg mL^{-1} and incubated in dark cold spaces. The stained sample were then analyzed by flowcytometry BD FCS Calibur. Furthermore, acquire is selected and will count the total cell count as well as the number of cells

ISSN. 2087-2852
E-ISSN. 2338-1655

detected by the antibody label. The results obtained are then processed with BD cellquest ProTM software.

Data Analysis

Data presented and analyses statisticaly by two way Anova with signifance p<0.

RESULT AND DISCUSSION

The induction of DMBA and Estradiol carcinogen compounds for 8 weeks induced the formation of breast cancer

7,12-Dimethylbenz[a]anthracene (DMBA) was a carcinogen compound that has an aromatic hydrocarbon chain and has been widely used in research as an inducer in breast cancer modeling [22,23,24]. Estradiol is a steroid the sex hormone that useful in female reproductive cycle in regulation of estrous and menstrual cycles. Estradiol has functions as transcription factor and gene expression, the bonding of estradiol with both uncontrolled receptors can trigger the development and progression of cancer cells such as breast cancer, ovarian cancer, and endometrial cancer [25-28]. In addition, estradiol along with progesterone regulates proliferation of breast epithelial cells, thus inducing the occurrence of breast cancer [29]. In this study, breast cancer was formed after induction of DMBA and Estradiol for 2 months.

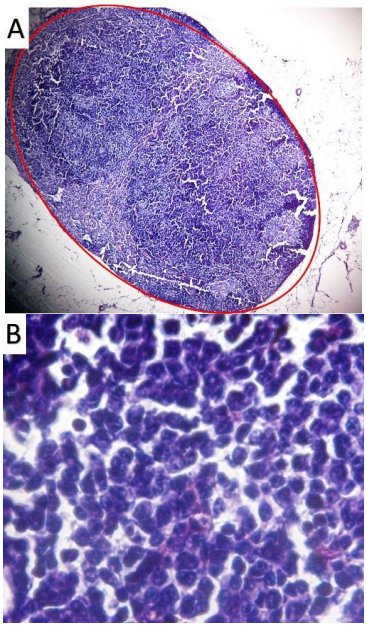

Figure 1. Histologic observation of mice breast tissue induced by carcinogen for 8 weeks at 40 times (A), and 1000 times (B) magnification with H & E staining. Higher cell density appears in red circled areas, indicating high cell proliferation or neoplasm. The resulting neoplasm was solid lobular carcinoma.

Neoplasm is an abnormal cell growth and often referred as a tumor, which formed a mass [30,31]. Provision of carcinogen compounds for 8 weeks in this study induced the formation of neoplasms in mice breast tissue. Based on histologic observations (Fig. 1), some breast tissue mice have transformed into a solid invasive lobular carcinoma. This carcinoma was derived from the lobular ducts, but the cells were mixed and ducts were no longer visible, made it hard to distinguish its cell types.

Invasive lobular carcinomas have characteristics such as round-to-polygonal cells with fewer cytoplasmic ratios when compared to nuclei (enlarged nucleus), small cells with undifferentiated nuclei and cytoplasm, mitotic and hyperchromatin images rarely seen, cell cohesion low, normal epithelial cell layer has been ruined by the proliferation of neoplastic cells above the pagetoid spread. The use of E-cadherin in immunohistochemical staining will make it easier to distinguish lobular carcinoma with the carcinoma ducts [32].

***E. scaber* extract treatment does not affect the relatives number of TNF-α and TGF-β**

TNF-α is an endogenous pyogenic that plays an important role in immune cells regulation, to induces fever, cell death (apoptosis), cachexia, inflammation, and to inhibit tumorigenesis [33]. In this study, TNF-α cytokine profiles of CD11b macrophages were observed to investigate the effect of *E. scaber* extract on inflammation response induced by carcinogenic compounds.

TGF-β is an anti-inflammatory cytokine which under normal conditions serves to stop the cell cycle in G1 phase, and induces apoptosis. TGF-β can suppress the epithelial cell proliferation and cancer growth in early stage, and inactivated mutations in some tumors through TGF-β signaling pathway [34,35,36]. In the case of severe cancer, TGF-β undergoes mutation and loss of control, thus becoming an immune-suppressor agent, and inducing angiogenesis that causes the cancer to become more invasive [37]. In this study, the relative amount of TGF-β was observed to investigate the effect of carcinogenic compounds induction as well as the effect of *E. scaber* extract on TGF-β relatives number fluctuations.

The results showed that there were an increasing number of TNF-α cytokine by macrophage CD11b in the K + mice group of 6.95% when compared with the K- group of K- by 4.58% in the first week (Fig. 2A). However, the

ISSN. 2087-2852
E-ISSN. 2338-1655

differences occurred in the second and third weeks in which TNF-α in the K + group mice decreased by 6.37% and 6.48% respectively, when compared to the K-groups of 10.75% and 16.16%, respectively. The administration of *E. scaber* extract in group P for 1 week and 2 weeks increased TNF-α profile by 14.28% and 15.92% (Fig. 2A).

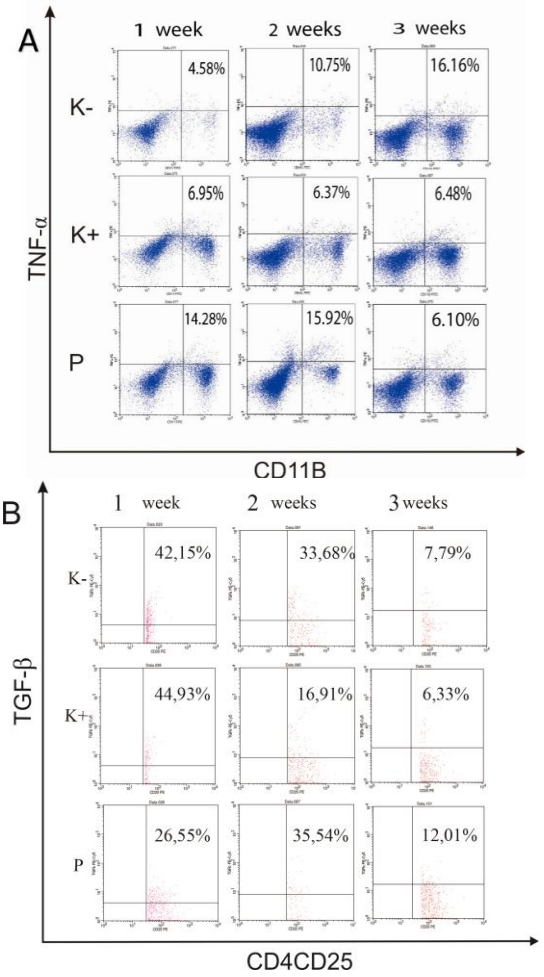

Figure 2. The flow cytometry results of the relative number of TNF-α (A) and TGF-β (B) isolated from macrophages and Treg, with K- (normal group), K + (cancer group with carcinogen induction), P (group of cancer-treated mice extract of *E. scaber*).

The result of the relative number (%) of TGF-β in flow cytometry was obtained by purifying CD4 and CD25 T cell, after which, the cell expressed CD4CD25 was purified again to obtained CD4CD25 T cells that expressed TGF-β. The results showed that in the K + mice group from 1 week to 3 weeks the relative number (%) of TGF-β ranged from 7.79% to 42.15%. While in group of K- week 1 to week 3 ranged between 6.33% - 44.93%, and in group of P week 1 to week 3 ranged from 12.01% -35.54%. The number of TGF-β continues to decrease weekly (Fig. 2B).

Based on statistical analysis using Tukey test, there were no significant difference in relative number (%) of TNF-α based on treatment group and time of extract with significance (p <0,05) (Table 1). In the TGF-β cytokine, there was a relative decreased in the number of relative (%) at week 3 by 8,712 ± 2,531 when compared with the relative number of (%) TGF-β at week 1 and 2 each of which were 37.877 ± 5.512 and 28.708 ± 2.639 (Table 1). Based on the treatment group, there was no significant difference in the relative number (%) of TGF-β between the K-, K +, and P mice (Table 1).

Table 1. The relative number (%) of TNF-α and TGF-β after administration of *E. scaber* for 1 week, 2 weeks, and 3 weeks

	TNF-α	**TGF-β**		
	E. scaber treatment			
	1,2,3, weeks	**1 week**	**2 weeks**	**3 weeks**
K-	9.733[a]	37,88[b]	28,71[b]	8,71[a]
K+				
P				

Notes: The relative numbers (%) of TNF-α and TGF-β based on duration of 1 week, 2 weeks, and 3 weeks, with K- (normal group), K + (cancer group with carcinogen induction), P (group of cancer-treated mice extract of *E. scaber*), Signification (p <0.05).

Tumour Necrosis Factor-α (TNF-α) is a pro-inflammatory cytokine produced by macrophages, was a protein involved in the inflammatory process, and cause hemorrhagic necrosis to induce tumor cell death. TNF-α activate the 3 different cell responses, namely cell defense and proliferation, pro-inflammatory gene transcription, and cell death. TNF-α has 2 receptors, TNFR1 and TNFR2. Binding of TNF-α to its receptor TNFR1 leads to activation of transcription factor NF-κB, pro-inflammatory gene, and self defense. In other cases, TNF-α bound to its receptor TNFR2 may initiate the IKK phosphorylation that causes translocation of NF-κB via the same signal path as TNFR1. What distinguishes TNFR1 signal pathway with TNFR2 is TNFR2 can activate endothelial/epithelial tyrosine kinase Etk involved in adhesion, migration, proliferation, and cell defense. In endothelial cells, TNFR-2 activates Etk via tyrosine phosphorylation of the intracellular VEGFR2 resulting in a single VEGF involved in the angiogenesis response by activating Akt [38].

ISSN. 2087-2852
E-ISSN. 2338-1655

In other hand, TNF-α was also a factor that caused cachexia, which is wasting syndrome that makes the sufferer lose weight, muscle atrophy, excessive fatigue, and the body becomes very weak [39]. Approximately 50% of cancer patients suffer from cachexia, this is because the condition of cancer can cause symptoms cachexia which is a side effect of chemotherapy that causes decreased quality of life, and is considered a cause of death in many cases of cancer patients [40,41].

In this study, there were no significant fluctuations in the relative numbers of TNF-α in both carcinogenic induced or in groups with *E. scaber* extract treatment (Table 1). Based on this results, the researcher assume that cancer induction by carcinogen compounds DMBA and Estradiol for 2 months has not resulted in excessive inflammatory reactions to cause cachexia syndrome. In rats model, DMBA can cause cachexia after 195 days of administration, while in 1 month administration of DMBA was not enough to promote cachexia syndrome [42,43]. TNF-α is cytokines that play major role to cause cachexia syndrom, and the increasing number of TNF-α can be considered as cachexia symtomps, because TNF-α responsible to degradation of myofibrillar and soleus muscle proteins [44]. The administration of *E. scaber* extract did not affect the inflammatory response, because it contains various phenolic compounds that have antioxidant and anti-inflammatory functions [45].

The immune system works in harmony interconnected with each other, where the function of immune cells will not work properly without other factors affecting it, and immune cells work to influenced each other [34,35,36]. Carcinogenic compounds induction by DMBA and estradiol not only affect the pro-inflammatory cytokines alone but also the anti-inflammatory cytokine expressed by CD4CD25 Treg cells.

Transforming Growth Factor-β (TGF-β), is a multifunctional cytokine which is a protein signal and is produced by many types of immune cells, including Treg [34]. TGF-β under normal conditions serves to stop the cell cycle in G1 phase, and induced apoptosis. TGF-β suppressed epithelial cell proliferation and early cancer growth, and may inactivated mutations in some tumors via TGF-β signal [46]. TGF-β in the early stage of cancer formation, serves to stop the cell cycle in G1 phase and induce cell apoptosis [46]. TGF-β otherwise secreted by Treg cells, was also secreted by cancer cells itself to attract Treg cells [37].

In this study, the relative number (%) of TGF-β continued to decline weekly (Table 1), but the induction of carcinogenic and *E. scaber* extract did not affect the fluctuations of TGF-β relative number (%) produced by Treg CD4CD25 (Table 1). Because of this, researchers assume that carcinogenic compounds DMBA and Estradiol induction for 2 months was in early stage induction of cancer so it has not affected the relative number of TGF-β, because in more advanced cases, the TGF-β was usually increased because it also produced by the tumor cells themselves to attract Treg and as an immuno-suppressor to escape from the immune cells [47].

In the case of severe cancer, the TGF-β undergoes mutation and loss of control, thus becoming an immuno-suppressor agent, and inducing angiogenesis that causes the cancer to become more invasive [40,41]. TGF-β has a very important and crucial role in maintaining cellular homeostasis. In normal epithelial cells, TGF-β plays a role in antiproliferation response, promotes cell differentiation, and cell apoptosis induction. Thus TGF-β has a very important role as an anti-proliferative agent in early stage cancer [44].

Based on relative number of TNF-α and TGF-β fluctuation, the administration of DMBA and Estradiol for 1 week, 2 weeks, and 3 weeks does not cause severe inflammation response, but the inflammation response does not affected only by TNF-α and TGF-β, various number of pro-inflammatory and anti-inflammatory cytokines involved in inflammation response. Further examination is necessary to find out the inflammatory response caused by carcinogenic compound DMBA and Estradiol, and the various dose of *E. scaber* extract administration is necessary to find out the most effective dose of *E. scaber* extract that have anti-inflammation effect against carcinogenic induction.

CONCLUSION

The induction of carcinogen compounds in the form of DMBA and Estradiol for 8 weeks can trigger the occurrence of breast cancer, but has not been able to change the fluctuations in the relative number of cytokines TNF-α and TGF-β produced by macrophages CD11b and Treg CD4CD25. Administration of *E. scaber* extract for 1 week, 2 weeks, and 3 weeks did not change the relative number of the TNF-α and TGF-β

ISSN. 2087-2852
E-ISSN. 2338-1655

cytokines produced by CD11b and Treg CD4CD25 macrophages.

ACKNOWLEDGEMENT

This research was financiallly supported by Ministry of Research, Technology and Higher Education of the Republic of Indonesia, and the financial grant does not involved in this design of study.

REFERENCES

[1] Ames, B.N., L.S. Gold. 2000. Paracelsus to parascience: the environmental cancer distraction. *Mutat. Res. Mol. Mech. Mutagen.* 447(1). 3-13.

[2] Eaton, D.L., E.P. Gallagher. 1994. Mechanisms of aflatoxin carcinogenesis. *Annu. Rev. Pharmacol. Toxicol.* 34(1). 135-172.

[3] Miyata, M., M. Furukawa, K. Takahashi, F.J. Gonzalez, Y. Yamazoe. 2001. Mechanism of 7,12-Dimethylbenz[a]anthracene-Induced Immunotoxicity: role of metabolic activation at the target organ. *Jpn. J. Pharmacol.* 86(3). 302-309.

[4] Watabe, T., T. Ishizuka, M. Isobe, N. Ozawa. 1982. A 7-hydroxymethyl sulfate ester as an active metabolite of 7,12-dimethylbenz [alpha]anthracene. *Science.* 215(4531). 403-405.

[5] O'Hagan, H.M., H.P. Mohammad, S.B. Baylin. 2008. Double Strand breaks can initiate gene silencing and SIRT1-Dependent Onset of DNA methylation in an exogenous promoter CpG Island. *PLoS Genet.* 4(8). e1000155.

[6] Bartkova, J., Z. Horejsí, K. Koed, A. Krämer, F. Tort, K. Zieger, P. Guldberg, M. Sehested, J.M. Nesland, C. Lukas, T. Ørntoft, J. Lukas, J. Bartek 2005. DNA damage response as a candidate anti-cancer barrier in early human tumorigenesis. *Nature.* 434(7035). 864-870.

[7] Halazonetis, T.D., V.G. Gorgoulis, J. Bartek. 2008. An Oncogene-Induced DNA damage model for cancer development. *Science.* 319(5868). 1352-1355.

[8] Chen, D. S., I. Mellman. 2013. Oncology meets immunology: the cancer-immunity cycle. *Immunity.* 39(1). 1-10.

[9] Beutler, B., A. Cerami. 1989. The biology of cachectin/TNF -- a primary mediator of the host response. *Annu. Rev. Immunol.* 7(1). 625-655.

[10] Chen, G., D.V. Goeddel. 2002. TNF-R1 signaling: a beautiful pathway. *Science.* 296(5573). 1634-1635.

[11] Gaur, U., B.B. Aggarwal. 2003. Regulation of proliferation, survival and apoptosis by members of the TNF superfamily," *Biochem. Pharmacol.* 66(8). 1403-1408.

[12] Kant, S., W. Swat, S. Zhang, Z.Y. Zhang, B.G. Neel, R.A. Flavell, R.J. Davis. 2011. TNF-stimulated MAP kinase activation mediated by a Rho family GTPase signaling pathway. *Genes Dev.* 25(19). 2069-2078.

[13] Massagué, J. 2012. TGFβ signalling in context. *Nat. Rev. Mol. Cell Biol.* 13(10). 616-630.

[14] Nakao, A., M. Afrakhte, A. Morén, T. Nakayama, J.L. Christian, R. Heuchel, S. Itoh, M. Kawabata, N.E. Heldin, C.H. Heldin, P. ten Dijke. 1997. Identification of Smad7, a TGFβ-inducible antagonist of TGF-β signalling. *Nature.* 389(6651). 631-635.

[15] Krishna, V., K. Mankani, B. Manjunatha, S. Vidya, Y. Manohara, S.J. Singh. 2005. Wound healing activity of the leaf extracts and deoxyelephantopin isolated from *Elephantopus scaber* Linn. *Indian J. Pharmacol.* 37(4). 238-242.

[16] Poli, A., M. Nicolau, C.M. Oliveira Simões, R.M. Ribeiro-do-Valle Nicolau, M. Zanin. 1992. Preliminary pharmacologic evaluation of crude whole plant extracts of Elephantopus scaber. Part I: in vivo studies. *J. Ethnopharmacol.* 37(1). 71-76.

[17] Chan, C., G. Chan, K. Awang, H. Abdul Kadir, 2016. Deoxyelephantopin from *Elephantopus scaber* inhibits HCT116 human colorectal carcinoma cell growth through apoptosis and cell cycle arrest. *Molecules*. 21(3). 385.

[18] Huang, C.C. C.P. Lo, C.Y. Chiu, L.F. Shyur. 2010. Deoxyelephantopin, a novel multifunctional agent, suppresses mammary tumour growth and lung metastasis and doubles survival time in mice. *Br. J. Pharmacol.* 159. 856-871.

[19] Zou, G., Z. Gao, J. Wang, Y. Zhang, H. Ding, J. Huang, L. Chen, Y. Guo, H. Jiang, X. Shen. 2008. Deoxyelephantopin inhibits cancer cell proliferation and functions as a selective partial agonist against PPARgamma. *Biochem. Pharmacol.* 75. 1381-1392.

[20] Lubahn, D.B., J.S. Moyer, T.S. Golding, J.F. Couse, K.S. Korach, O. Smithies. 1993. Alteration of reproductive function but not prenatal sexual development after

insertional disruption of the mouse estrogen receptor gene. *Proc. Natl. Acad. Sci.* 90(23). 11162-11166.

[21] Roffico, R., M.S. Djati. 2014. Efektivitas pemberian ekstrak ethanol daun *Polyscias obtusa* dan *Elephantopus scaber* terhadap modulasi Sel T CD4+ dan CD8+ pada mencit bunting BALB/c. *Biotropika J. Trop. Biol.* 2(3). 174-180.

[22] Liu, Z., T. Kundu-Roy, I. Matsuura, G. Wang, Y. Lin, Y.R. Lou, N.J. Barnard, X.F. Wang, M.T. Huang, N. Suh, F. Liu. 2016. Carcinogen 7,12-dimethylbenz[a]anthracene-induced mammary tumorigenesis is accelerated in Smad3 heterozygous mice compared to Smad3 wild type mice. *Oncotarget.* 7(40). 64878-64885.

[23] Linjawi, S.A.A., W.K.B. Khalil, M.M. Hassanane, E.S. Ahmed. 2015. Evaluation of the protective effect of *Nigella sativa* extract and its primary active component thymoquinone against DMBA-induced breast cancer in female rats. *Arch. Med. Sci.* 11(1). 220-229.

[24] Abba, M.C., Y. Zhong, J. Lee, H. Kil, Y. Lu, Y. Takata, M.S. Simper, S. Gaddis, J. Shen, C.M. Aldaz. 2016. DMBA induced mouse mammary tumors display high incidence of activating Pik3caH1047 and loss of function Pten mutations. *Oncotarget*. 7(39). 64289–64299.

[25] Hall, J.M., D.P. McDonnell. 1999. The estrogen receptor β-Isoform (ERβ) of the human estrogen receptor modulates ERα transcriptional activity and is a key regulator of the cellular response to estrogens and antiestrogens 1. *Endocrinology*. 140(12). 5566–5578.

[26] Schneider, H.P., C. Jackisch. 1998. Potential benefits of estrogens and progestogens on breast cancer. *Int. J. Fertil. Womens. Med.* 43(6). 278–285.

[27] Galtier-Dereure, F., F. Capony, T. Maudelonde, H. Rochefort. 1992. Estradiol stimulates cell growth and secretion of procathepsin D and a 120-kilodalton protein in the human ovarian cancer cell line BG-1. *J. Clin. Endocrinol. Metab.* 75(6). 1497-1502.

[28] Vivacqua, A., D. Bonofiglio, A.G. Recchia, A.M. Musti, D. Picard, S. Andò, M. Maggiolini. 2006. The G protein-coupled receptor GPR30 mediates the proliferative effects induced by 17β-estradiol and hydroxytamoxifen in endometrial cancer cells. *Mol. Endocrinol.* 20(3). 631-646.

[29] Foidart, J.M., C. Colin, X. Denoo, J. Desreux, A. Béliard, S. Fournier, B. de Lignières. 1998. Estradiol and progesterone regulate the proliferation of human breast epithelial cells. *Fertil. Steril.* 69(5). 963-969.

[30] Cooper, G.M. 1992. Elements of human cancer. Jones and Bartlett Publishers. London.

[31] Newman Dorland, W.A. 2012. Dorland's illustrated medical dictionary. W.B. Saunders. Elsevier. Melbourne.

[32] Selvi, R. 2015. Fibrocystic change: proliferative changes. In: Breast Diseases, Springer India. New Delhi. 151-155.

[33] Locksley, R.M., N. Killeen, M.J. Lenardo. 2001. The TNF and TNF receptor review superfamilies: integrating mammalian biology the receptors and ligands in this superfamily have unique structural attributes that couple them directly to signaling pathways for cell proliferation, survival, and differentiation. Thus, they have assumed prominent roles in the generation of tissues and transient microen. *Cell.* 104. 487-501.

[34] Blobe, G.C., W.P. Schiemann, H.F. Lodish. 2000. Role of Transforming Growth Factor β in human disease. N. Engl. J. Med. 342(18). 1350–1358.

[35] Carl-Henrik, H., L. Marene, M. Aristidis. 2009. Mechanism of TGF-β signaling to growth arrest, apoptosis, and epithelial–mesenchymal transition. *Curr. Opin. Cell Biol.* 21(2). 166-176.

[36] Hanahan, D., Weinberg R.A. 2000. The hallmarks of cancer. *Cell.* 100(1). 57-70.

[37] Yang, J., R.A. Weinberg. 2008. Epithelial-mesenchymal transition: at the crossroads of development and tumor metastasis. *Dev. Cell*. 14(6). 818-829.

[38] Waters, L.S., B.K. Minesinger, M.E. Wiltrout, S. D'Souza, R.V. Woodruff, G.C. Walker. 2009. Eukaryotic translesion polymerases and their roles and regulation in DNA damage tolerance. *Microbiol. Mol. Biol. Rev.* 73(1). 134-54.

[39] Ceramil, A., B. Beutler. 1988. The role of cachectin/TNF in endotoxic shock and cachexia. *Immunol. Today.* 9(1). 28-31.

[40] Alhamarneh, O., F. Agada, L. Madden, N. Stafford, J. Greenman. 2011. Serum IL10 and circulating CD4+CD25high regulatory T cell numbers as predictors of clinical outcome and survival in patients with head

and neck squamous cell carcinoma. *Head Neck.* 33(3). 415-423.
[41] Fearon, K.C.H., A.G.W. Moses. 2002. Cancer cachexia. *Int. J. Cardiol.* 85(1). 73-81.
[42] Jabara, A.G., G.N. Marks, J.E. Summers, P.S. Anderson. 1979. Effects of progesterone on mammary carcinogenesis by DMBA applied directly to rat mammae. *Br. J. Cancer.* 40(2). 268-273.
[43] C. Bartsch et al., 1999. Serial transplants of DMBA-induced mammary tumors in fischer rats as a model system for human breast cancer. *Oncology.* 56(2). 169-176.
[44] Patel, H.J., B.M. Patel. 2017. TNF-α and cancer cachexia: Molecular insights and clinical implications. *Life Sci.* 170. 56-63.
[45] Kabiru, A., L.Y. Por. 2013. *Elephantopus* species: traditional uses, pharmacological actions and chemical composition. *Adv. Life Scie. Tech.* 15. 6-13.
[46] Weinberg, R.A. 2014. Garland Science - Book: the biology of cancer + 2, 2nd Ed. Garland Science, Taylor & Francis Group, LLC. New York and London.
[47] Oleinika, K., R.J. Nibbs, G.J. Graham, A.R. Fraser. 2013. Suppression, subversion and escape: the role of regulatory T cells in cancer progression. *Clin. Exp. Immunol.* 171(1). 36-45.

ISSN. 2087-2852
E-ISSN. 2338-1655

The Alteration Tissue Structure of Digestive Diverticulum of *Anodonta woodiana* Induced by Lead

Renanda Baghaz Dzulhamdhani Surya Putra[1], Sri Andayani[2], Hartati Kartika Ningsih[2], Diana Arfiati[2], Asus Maizar Suryanto Hertika[2*]

[1]Master Program of Fisheries and Marine Sciences, Faculty of Fisheries and Marine Sciences, University of Brawijaya, Malang, Indonesia

[2]Faculty of Fisheries and Marine Sciences, University of Brawijaya, Malang, Indonesia

Abstract

Accumulated the toxic compound such as lead in *A. woodiana* caused an alteration in the tissue. The aim of the study is observation through histology to determine the alteration of the structure of digestive diverticulum tissue. *Anodonta woodiana* were maintained in water tub that treated with lead II nitrate exposure ($Pb(NO_3)_2$) 0, 15, 25, 35 $mg.L^{-1}$ for 7 days to determine the alteration of the damaged structure of the digestive diverticulum and determining water quality such temperature, DO and pH. The highest damage occurs in digestive diverticulum which treated with 35 $mg.L^{-1}$ due to many alteration on the tissue structure such as hyperplasia, edema, atrophy, and necrosis with the percentage of total damage about 35%. The lowest alteration tissue structure occurs in 15 $mg.L^{-1}$ treatment group of the digestive diverticulum. The temperature was observed about 25.3 – 26.4°C, pH about 6-7, and DO about 6.1-6.7 $mg.L^{-1}$. Thus, the increment of lead dose treatment induces increment of tissue structure alteration in digestive diverticula tissue, therefore, might promote the death of *A. woodiana*.

Keywords: *Anodonta woodiana*, digestive diverticulum, histology.

INTRODUCTION

The common pollutant of heavy metals such as lead (Pb) are considered as toxic pollutants. In addition, the natural aquatic ecology also contaminated with the heavy metals released by domestic activity [1]. The organism or biomass contaminated with the heavy metals may have effect on human health risks [2,3].

As bivalve, the suspension feeding activity of mussel represents the main pathway for heavy metal uptake and accumulation [4,5]. Mussels are suspension feeders both aqueous and dietary; such as material resuspended from sediments. Therefore, it consisted of high-molecular-weight substances, microorganisms, fecal pellets and detritus [6,7]. Mussels are organisms that commonly used to assess the ecotoxicological research in nature to analyze the effects of the compound that released from anthropogenic activities [8,9]. In the previous study, Mussel was used to evaluate *In Situ* metal contamination in wastewater effluent and in aquatic ecosystems [10,11]. The concentration metal in the tissue of mussel was increased concomitantly with the elevating of metal absorption or uptake and it showed the various metal bioaccumulation levels in different tissues of mussel [12,13].

Lead is a very toxic heavy metal [14] which cumulative [15] in the gills [16] and gastric [17]. With histopathological analyses, we could observe the alteration of damaged tissue, such as gills and gastric [18] which affected by the contaminants. Lead penetrated the tissues of the body through the respiratory tract [19] and gastrointestinal [20]. It induces the alteration tissue and a functional disorder in *A. woodiana* [21].

Anodonta woodiana (Kijing Taiwan) is a freshwater mussel found in waters with the muddy substrate. Kijing Taiwan lives in bottom waters and is relatively settled. Kijing Taiwan is a filter feeder organism that can filter water and is able to survive in the polluted environment, so it can be used as a bio-indicator of a water body. Lead induces the tissue damage which caused alteration of tissue structure in *A. woodiana*. The previous study, the histopathology of *A. woodiana* used to monitoring the pollution in aquatic environments and alteration structure of gill and kidney tissue observed [22]. In another study, they observed enlargement of the gastric wall and diverticulum of *A. woodiana* due to exposure to pesticides [23]. The other research on hyperplasia, atrophy, and necrosis occur in the gills of *A. woodiana* due to the Cadmium exposure [24]. However, the tissue structure alteration of digestive diverticulum in *A.*

* Correspondence address:
Asus Maizar Suryanto Hertika
Email : asusmaizar@yahoo.com
Address : Faculty of Fisheries and Marine Sciences, University of Brawijaya, Veteran Malang, Malang 65145.

woodiana still unknown. The aim of this study was to observed the alteration tissue structure of digestive diverticulum of *A. woodiana* induced by lead II nitrate exposure treatment for 7 days.

MATERIAL AND METHOD

Data Collection

The descriptive qualitative method is used in determining the alteration histology digestive diverticulum of *A. woodina* and water quality in each treatment and data was collected with 3 times experiment repeatition. *Anodonta woodiana* in size 8-10 cm obtained from Freshwater Cultivation Management Unit (UP-BAT) Punten Batu, Malang and maintained in Workshop Laboratory in Faculty of Fisheries and Marine Science, University of Brawijaya, Malang. Six of *A. woodiana* were induced with Lead Nitrate for 7 days in each treatment and maintained in the circulation system water tub (30 liter volume).

Lead II nitrate [$Pb(NO_3)_2$] dissolved and diluted in the following concentration 0 $mg.L^{-1}$, 15 $mg.L^{-1}$, 25 $mg.L^{-1}$, and 35 $mg.L^{-1}$. Furthermosre, the water quality such as temperature, pH, and DO in each water tub was measured once in a day for 7 days. After 7 days, the stomach of mussels in each water tub was harvested and immediately, preserved in ddH_2O containing 10% of formaldehyde. The stomachs were ready for staining and histology analysis.

Histotology analysis

Histology analysis was conducted according to Elsayed et al. [25]. Briefly, the stomach of *A. woodiana* in each treatment was harvested after treatment and immediately fixed in neutral buffered formaldehyde 10%. Further, the stomachs were dehydrated using ascending grades of ethanol (70, 80, 90, and 100% for 1 hour in each concentration). The samples were then cleared in xylene. After blocking using soft paraffin, the stomachs were cut using the microtome to serial sections of 4 µm thickness. Then, sections were stained using hematoxylin-eosin stain. After staining, the stomachs were observed with microscope Olympus BX41 and scanned using Olympus CX21FS. The percentage of organ damage is calculated based on the following formula.

$$\text{Organ damage (\%)} = \frac{\text{amount of damaged tissue}}{\text{amount of tissue analyzed}} \times 100\%$$

Statistical Analysis

Data are expressed as mean ± SD. Statistical significance of pairwise differences among three or more groups was determined using one-way analysis of variance (ANOVA) followed by LSD test. $P<0.05$ was considered statistically significant. The analysis was performed using SPSS for Windows (SPSS Inc., Version 20.0, Chicago, IL, USA). The Graph was performed using GraphPad Prism 7 (GraphPad Software, Inc. USA).

RESULT AND DISCUSSION

The Morphology of Digestive Diverticulum Tissue Alteration

The alteration of digestive diverticulum tissue of *A. woodiana* in each treatment was shown in Figure 1. The digestive diverticulum induced with 15 $mg.L^{-1}$ of Lead appeared edema and hyperplasia. The epithelia of digestive diverticulum showed swollen and some cells were grown more (Fig 1B). Further, the atrophy and necrosis of digestive diverticulum were found in *A. woodiana* which induced with 25 $mg.L^{-1}$ of Lead (Fig. 1C). The digestive diverticulum was narrowed and its epithelia showed damage. In this treatment, it was revealed that the *A. woodiana* was not resisted to this concentration of Lead. The digestive diverticulum of *A. woodiana* was then found with more necrosis (Fig. 1D). In this treatment group, many alterations of digestive diverticulum was found. It was suggested that above 15 $mg.L^{-1}$ of Lead, the *A. woodiana* was not resisted the toxicity of Lead. It might cause the death because the digestive diverticulum was damage and was not performed normally. Excretion of mucus is a form of *A.woodiana* self-protection against the toxic lead. The mucus contained the neutrophils that play a role in digesting foreign substances that penetrate to the body of this organism [24].

Previous study explained that the edema occurs as a form of cell adaptation to survive due to the influence of toxic materials [26]. Enzymes are out of cells along these substances will inhibit cell metabolism. This will ultimately result in cell death (necrosis) [23]. *Necrosis* is cell death that occurs because of hyperplasia redundant, so tissue no longer intact form or in other words, necrosis occurs accompanied by the death of an organism [27].

ISSN. 2087-2852
E-ISSN. 2338-1655

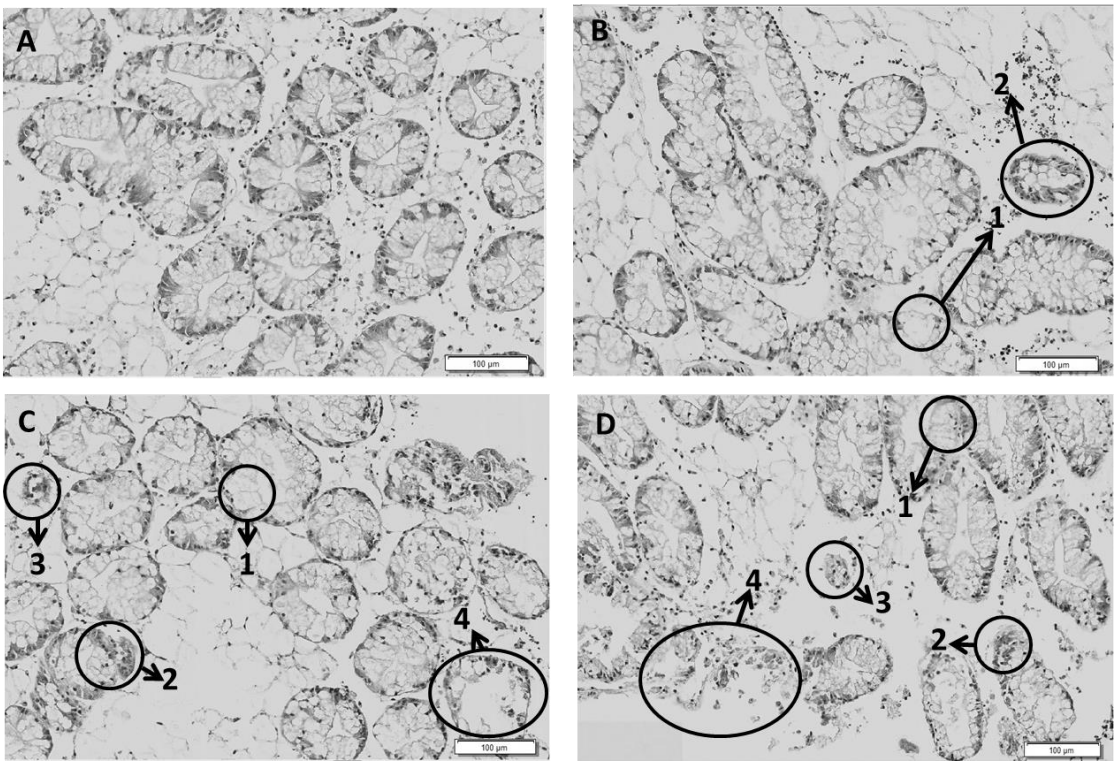

Figure 1. Digestive diverticulum of gastric tissue *A. woodiana* after Lead II Nitrate ($Pb(NO_3)_2$) exposure for 7 days 100 µm, (magnification 400x, Olympus BX41 microscope, Olympus DP 20 camera). **A.** treated 0 $mg.L^{-1}$ lead II nitrate, **B.** treated 15 $mg.L^{-1}$ lead II nitrate, **C.** treated 25 $mg.L^{-1}$ lead II nitrate, **D.** treated 30 $mg.L^{-1}$ lead II nitrate. **(1)** Edema; **(2)** Hyperplasia; **(3)** Atrophy; **(4)** Necrosis.

The Quantity of Digestive Diverticulum Alteration Analysis

The percentage of alteration on the digestive diverticulum induced by Lead was shown in Figure 2. The hyperplasia was increased significantly in 25 $mg.L^{-1}$ and 35 $mg.L^{-1}$ treatment groups about 7.8% and 9.6%, differently compared to 15 $mg.L^{-1}$ treatment group about 3%.

Moreover, the necrosis was increased significant in 35 $mg.L^{-1}$ treatment group around 12% compare than 25 $mg.L^{-1}$ treatment group around 3.1%. In the present study, the edema and atrophy were not significant differences in each treatment group. However, the alteration of digestive diverticulum induced 35 $mg.L^{-1}$ of Lead showed the highest hyperplasia and necrosis was also observed.

The total percentage of digestive diverticulum alteration was shown in Figure 3. The total alteration of digestive diverticulum was increased significantly in 35 $mg.L^{-1}$ compare to 15 $mg.L^{-1}$ and 25 $mg.L^{-1}$ treatment groups. At this moment, the 35 $mg.L^{-1}$ treatment group has the highest alteration tissue structure of 36% followed by 25 $mg.L^{-1}$ for 22% and 15 $mg.L^{-1}$ for 8%.

The alteration in gastric tissue begins with edema. The gastric has columnar epithelial cells. The Epithelial cells of the digestive organs column are eosinophilic with an elliptical core. Epithelial cells of the stomach started swelling due to growth. Hyperplasia in epithelial cells is a response of the epithelial cells which are eosinophils [28].

Eosinophils are immune properties of the body against substances that are toxic. On the composition of the cilia starting to look irregular. Thickening of cilia results in fusion of the cilium [29]. In some parts, the gastric walls look thinner. This is caused by cilia and epithelial cells start to shrink (atrophy). Atrophy of the epithelial cells is a form of adaptive reaction to toxic substances that cause digestive activity is not running perfectly so that the needs of the supply of nutrients and hormones is insufficient [30]. Edema and atrophy of the gastric epithelial cells cause the membrane of epithelial cells out of the proponent as well as causing dysfunction organ of the gastric and cause necrosis. Adaptive changes can develop into irreversible characterized by necrosis [31].

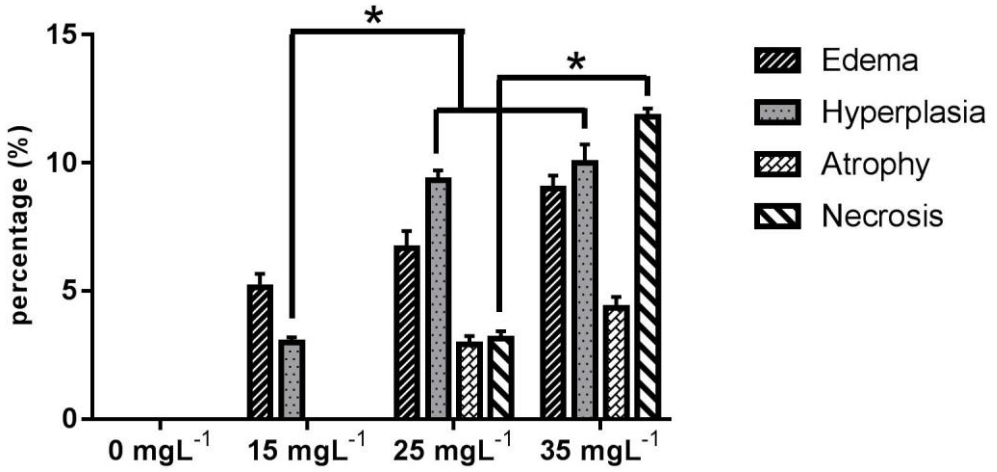

Figure 2. Percentage of each digestive diverticula alteration analysis after Lead II Nitrate ($Pb(NO_3)_2$) exposure for 7 days. Results were the mean ± SEM;. *p<0.0001 was significant.

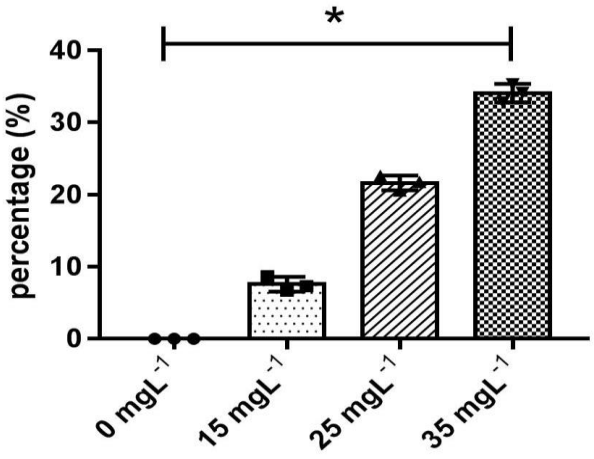

Figure 3. The total percentage of digestive diverticulum alteration of *A. woodiana* after Lead II Nitrate ($Pb(NO_3)_2$) exposure for 7 days Results were the mean ± SEM;. *p<0.0001 was significant.

Digestive diverticulum in bivalves accumulated pollutants, actively participates in the process of detoxification. Digestive diverticulum sensitive targets such as harmful pollutants. In the digestive diverticulum, occur Hyperplasia as indicated by increasing number of cells basophils seen by the assembly dots. Cells in the vesiculated digestive cell showed dominance in the digestive diverticulum. Depreciation cause the digestive diverticulum basophil cells occurred lyses and necrosis in the digestive diverticulum. Alteration in the gastrointestinal cells, basophils cell mass digestion, the out cells and alteration tissue such atrophy and necrosis of the digestive diverticulum, indicating the occurrence of chronic poisoning. This is consistent in previous research of Pillai [32]. Structural cell damage examination indicates that there is enlargement of cells that induce to digestive diverticulum enlarged structure of epithelial cells. cell enlargement resulted in an overall increase in cell volume due to the formation of lysosomes enlarged. then cause gastrointestinal cell atrophy and necrosis. The increment of concentration lead II nitrate treatment induces increment alteration tissue structure in gill tissue and gastric tissue.

ISSN. 2087-2852
E-ISSN. 2338-1655

Water Quality Analysis

The treatment of $Pb(NO_3)_2$ was not affected the water quality. The present study showed the temperature, pH and dissolved of oxygen (DO) were inappropriate for the ecological life of *A. woodiana*. A good temperature for the growth of freshwater mussels are temperatures between 15°C-27°C [33]. In the observation, pH and DO showed it is good for *A. woodiana* life. The pH is suitable for the environment for *A. woodiana* ranging from 6.5 to 7.8. If the pH in the water is more or less, the limit could affect the movement of cilia gills [24]. According to Subarijanti, oxygen content which not contained toxic compounds, amounting to a minimum of 2 $mg.L^{-1}$ is already sufficient to support the normal life of aquatic organisms [34]. In general, the oxygen obtained taken through gills that produce currents that go into his coat [35].

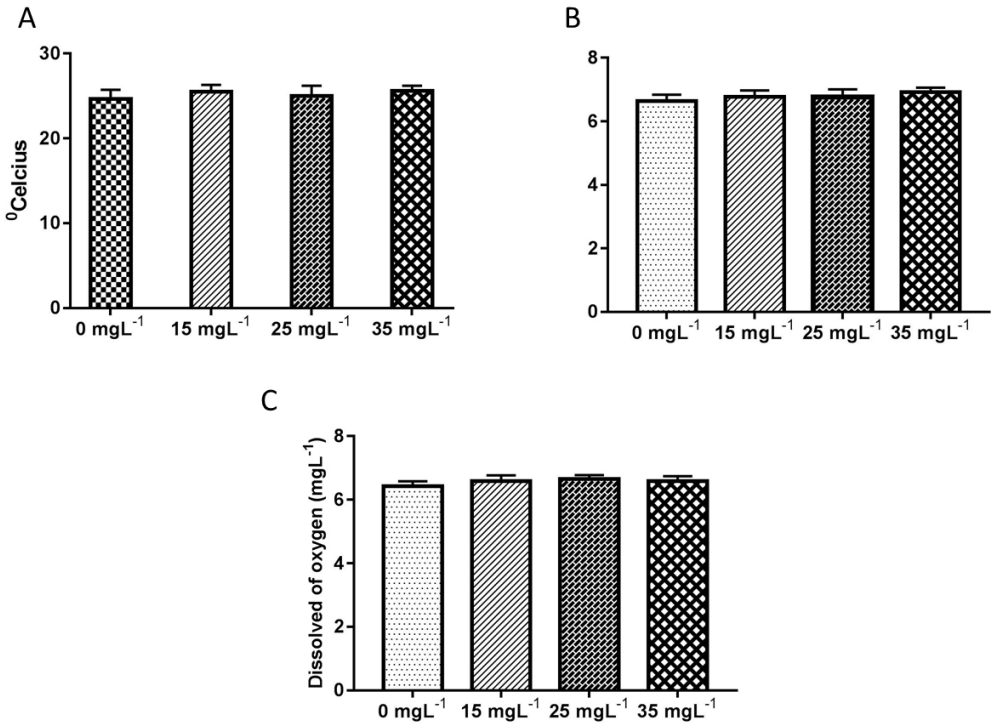

Figure 4. The water quality analysis in *Anodonta woodiana* tube after Lead II Nitrate ($Pb(NO_3)_2$) exposure for 7 days

CONCLUSION

These result showed that *A. woodiana* was not resisted with Lead toxicant in the concentration of Lead above 25 $mg.L^{-1}$. At concentration up to 25 $mg.L^{-1}$, the *A. woodiana* might death because the digestive diverticulum was not performed normally and it caused by any alteration of digestive diverticulum tissue structure.

REFERENCES

[1] Velez, D., R. Montoro. 1998. Arsenic speciation in manufactured seafood products: a review. *J. food. Protect.* 61(9). 1240-1245.

[2] Ja ¨rup. 2003. Hazards of heavy metal contamination. *Brit. Med. Bull.* 68. 167–182.

[3] Caussy, D., M. Gochfeld, E. Gurzau, C. Neagu, H. Ruedel. 2003. Lessons from case studies of metals: investigating exposure, bioavailability, and risk. *Ecotoxicol. Environ. Safe.* 56. 45–51.

[4] Pan, K., W.X. Wang. 2008. Validation of biokinetic model of metals in the scallop *Chlamys nobilis* in complex field environments. *Environ. Sci. Technol.* 42. 6285–6290.

[5] Metian, M., M. Warnau, J. L. Teyssie, P. Bustamante. 2011. Characterization of 241Am and 134Cs bioaccumulation in the king scallop *Pecten maximus*: investigation via three exposure pathways. *J. Environ. Radioactiv.* 102. 543–550.

[6] Galimany, E., M. Ramo´n, M. Delgado. First evidence of fiberglass ingestion by a marine invertebrate (*Mytilus galloprovincialis* L.) in a N.W. Mediterranean estuary. 2009. *Mar. Pollut. Bull.* 58. 1334–1338.

[7] Hull, M.S., P.J. Vikesland, I.R. Schultz. 2013. Uptake and retention of metallic nanoparticles in the Mediterranean mussel (*Mytilus galloprovincialis*). *Aquat. Toxicol.* 140–141. 89–97.

[8] Bocchetti, R., C.V. Lamberti, B. Pisanelli, E.M. Razzetti, C. Maggi, B. Catalano, G. Sesta, G. Martuccio, M. Gabellini, F. Regoli. 2008. Seasonal variations of exposure biomarkers, oxidative stress responses and cell damage in the clams, Tapes philippinarum, and mussels, Mytilus galloprovincialis, from Adriatic sea. *Mar. Environ. Res.* 66. 24–26.

[9] Guidi, P., G. Frenzilli, M. Benedetti, M. Bernardeschi, A. Falleni, D. Fattorini, F. Regoli, Scarcelli, M. Nigro. 2010. Antioxidant, genotoxic and lysosomal biomarkers in the freshwater bivalve (*Unio pictorum*) transplanted in a metal polluted river basin. *Aquat. Toxicol.* 100. 75–83.

[10] Gagnon, C., F. Gagné, P. Turcotte, I. Saulnier, C. Blaise, M.H. Salazar, S.M. Salazar. 2006. Exposure of caged mussels to metals in a primary-treated municipal wastewater plume. *Chemosphere.* 62. 998–1010.

[11] Gillis, P.L., F. Gagné, R. McInnis, T.M. Hooey, E.S. Choy, C. André, M.E. Hoque, C.D. Metcalfe. 2014. The impact of municipal wastewater effluent on field-deployed freshwater mussels in the Grand River (Ontario, Canada). *Environ. Toxicol. Chem.* 33(1). 134–143.

[12] Yeager-Armstead, M., J.L. Yeager. 2007. *In Situ* toxicity testing of unionids. In: Farris, J.L., J.H. Van Hassel (Eds). Freshwater Bivalve Ecotoxicology. Boca Raton (FL). CRC Press. 135–149.

[13] Jebali, J., L. Chouba, B. Mohamed, H. Bousetta. 2014. Comparative study of the bioaccumulation and elimination of trace metals (cd, Pb, Zn, Mn and Fe) in the digestive gland, gills and muscle of bivalve Pinna nobilis during a field transplant experiment. *J. Trace Elem. Med. Biol.* 28(2). 212–217.

[14] Supriyanto, C., Samin, Z. Kamal. 2007. Analyses of heavy metals contamination Pb, Cu, and Cd on freshwater fish Degan method Nyala atomic absorption spectrophotometry (AAS). Proceedings of the Third National Seminar on Human Resources for Nuclear Technology. Yogyakarta. 147-152.

[15] dan Gul, Y. 2003. Histopathological effects of cadmium and copper on the sea scallop Placopecten magellanicus. Marine Pollution and Physiology: Recent Advances. University of South Carolina Press. Columbia, SC. 187-198.

[16] Sunarto. 2007. Bioindikator pencemar logam berat Cadmium (Cd) dengan analisis struktur mikroanatomi, efisiensi fungsi insang, morfologi dan kondisi cangkang kerang air tawar (*Anodonta Woodiana* Lea). PhD Thesis. Airlangga University. Surabaya.

[17] Gopinathan, K. M., R. S. Amma. 2006. Bioaccumulation of toxic heavy metals in the edible soft tissues of green mussel (*Perna viridis* L.) of Mahe region. Project report submitted to the Department of Science, Technology and Environment (DSTE), Government of Pondicherry. India.

[18] Setyowati, A., D. Hidayati., P.D.N. Awik., N. Abdulgani. 2007. Studi histopatologi hati Ikan Belanak (*Mugil cephalus*) di Muara Sungai Aloo Sidoarjo. Research Report. Department of Biology. Sepuluh Nopember Institute of Technology. Surabaya.

[19] Erlania, A.I., Gubawan, Y.H. Prihadi. 2007. Cultivation potential Kijing Taiwan (*Anodonta woodiana*) In Cirata. Proceedings of the National Seminar Mollusks in Research, Conservation and Economic. Aquaculture Research Center. Jakarta.

[20] Galtsoff, P.S. 1964. The American oyster (*Crassostrea virginica*). Fishery Bulletin of The Fish and Wildlife Service. 489.

[21] Soegianto, A., N.A. Primarastri, D. Winarni. 2004. Pengaruh pemberian kadmium terhadap tingkat kelangsungan hidup dan kerusakan struktur insang dan hepatopankreas pada udang Regang *[Macrobrachium Sintangense (De Man)*. Berk. Penel. Hayati. 10. 59–66.

[22] Widiastuti. 1997. Kijing Air Tawar sebagai alat pemantau pencemaran perairan logam berat. Bachelor Thesis. Department of Biology, Bogor Agricultural University. Bogor.

[23] Lesmana, G.L., D. Arfiati, A. Maizar, 2013. Pengamatan jaringan lambung Kijing Taiwan (*Anodonta woodiana* Lea) yang terdedah pestisida Diazinon 60 EC pada beberapa konsnetrasi. *J. Exp. Life Sci.* 3(1). 37-39.

[24] Fitriawan, F. 2010. Analyses of change and variation pattern ribbon mikroanatomi isozyme at gills and kidneys freshwater mussels *Anodonta woodiana* against heavy

metal Cadmium exposure. Thesis. Sebelas Maret university. Surakarta.

[25] Elsayed, E.E., N.E. El Dien, M.A. Mahmoud. 2006. Ichthyophthiriasis: various fish susceptibility or presence of more than one strain of the parasite?. *Nat. Sci.* 4(3). 5-13.

[26] Widayati, D.E., Aunurohim, A. Nurlita. 2011. Histopatologi mempelajari Insang Ikan Mujair (*Oreochromis mossambicus*) pada konsentrasi subletal Air Lumpur Sidoarjo. Sepuluh Nopember Institute of Technology. Surabaya.

[27] Laksman, H. T. 2003. Medical Dictionary. Djambatan. Jakarta.

[28] Andrew, M., Stephen A.B. 2014. Histological atlas of freshwater mussels (Bivalvia, Unionidae): *Villosa nebulosa* (Ambleminae: Lampsilini), *Fusconaia cerina* (Ambleminae: Pleurobemini) and *Strophitus connasaugaensis* (Unioninae: Anodintini). *Malacologica.* 57(1). 99–239

[29] Hoey, D. A., M.E. Downs, C.R. Jacobs. 2012. The mechanics of the primary cilium: an intricate structure with complex function. *J. Biomech.* 45(1). 17-26.

[30] Sarjadi. 1999. Pathology and systematic. EGC Medical Book Publisher. Jakarta.

[31] Raza'i, T.S. 2008. Analisis histopatologi organ insang dan usus ikan Kerapu Lumpur (*Epinephelus coioides*) yang diberi Khamir Laut (Marine 5 Yeast) sebagai imunostimulan. Master Thesis. Faculty of Fisheries and Marine Sciences, University of Brawijaya. Malang.

[32] Pillai, S.P. 1993. Heavy metal toxicity in bivalve histological and histochemical enquiry. Thesis. Cochin University. India.

[33] Rachman, B., D. Hasbullah, Rahmat. 2006. Application of poly between shellfish (*Hyriopsis* Sp.) with the Tilapia and Mola in production efforts prospective parent and freshwater pearls. Engineering Annual Report. Freshwater Aquaculture Centres. Sukabumi.

[34] Subarijanti, H. 1990. Limnology. of Fisheries and Marine Sciences, University of Brawijaya. Malang.

[35] Nontji. 2002. Preservation and management of water resources in tropical coastal areas. PT. Gramedia Pustaka. Jakarta.

ISSN. 2087-2852
E-ISSN. 2338-1655

Biological Analysis of Blue Swimmer Crab (*Portunus pelagicus*) from Collectors in Lamongan, Tuban, Pasuruan, and Rembang, Java, Indonesia

Lini Murni[1*], Diana Arfiati[2], Andi Kurniawan[2], Yuni Kilawati[2], Herwati Umi Subarijanti[2], Suliswanto[2], Muhammad Nafar Amani Syams[2], Agum Bayu Gumelar[2], Alif Raditya Amirul Huda[2]

[1]Master Program of Fisheries and Marine Sciences, Faculty of Fisheries and Marine Sciences, University of Brawijaya, Malang, Indonesia
[2]Faculty of Fisheries and Marine Sciences, University of Brawijaya, Malang, Indonesia

Abstract

Blue swimmer crab (*Portunus pelagicus*) can increase the country's incomes due to its high demand of export. This study aims to determine biological analysis on the population of blue swimmer crab in Lamongan, Tuban, Pasuruan, and Rembang. The sampling location was based on the fishing area and the method used survey method from collectors in each location. The blue swimmer crab's biological characteristics which observed are the correlation on wide of carapace and blue swimmer crab weight, sex ratio, and gonad maturity level. The results showed the correlation between the wide and weight of carapace in Lamongan (male: 113.80-122.99 mm and 87.98-121.60 g then female: 108.21-117.27 mm and 71.80-99.74 g), Tuban (male: 113.26-117.74 mm and 89.63-102.76 g g then female: 114.36 mm and 106.51 g), Pasuruan (male: 87.66-94.43 mm and 39.68-49.90 g then female: 101.94-110.89 mm and 66.98-82.89 g), and Rembang (male: 120.30-126.69 mm and 93.53-118.43 g then female: 125.30-132.13 mm and 134.42-157.47 g); sex ratio (male: female) in Lamongan (1.4: 1), Tuban (1: 1.5), Pasuruan (2.8: 1), and Rembang (1: 1.46); and also gonad maturity level in Lamongan (dominant male at level III was 30.29%, female at level II and III was 30.40%), Tuban (dominant male at level II was 41.93%, female at level III was 33.33%), Pasuruan (dominant male at level III was 25.79%, female at level III was 48.10%), and Rembang (dominant male at level II was 32.35%, female at level II was 33.33%). These results indicate that the total of *Portunus pelagicus* which was being caught had fulfilled the standards rules by No.1/PERMEN-KP/2015. However, it requires continuous direct monitoring and counseling to maintain the stock of blue swimmer crab resources.

Keywords: Blue swimmer crab (*Portunus pelagicus*), gonad maturity level, sex ratio, wide and weight.

INTRODUCTION

Blue swimmer crab (*Portunus pelagicus*) is included as one of fishery commodities that has high economic value and becomes one of the primadonnas in the field of fisheries. Besides in the local market, the swimmer crabs can be one of the high levels and promising export commodities [1]. The request of Blue swimmer crab for every year is always increase makes fishery export commodity such as frozen meat without skin or processed meat in cans. Indonesia's export of blue swimmer crab in 2011 showed the high rate of 42,410 tons with ± Rp. 978 billion rupiahs [2].

The blue swimmer crab is an active swimmer, but in passive conditions it will bury themselves into sediment; only part of eye and antena which are not covered. Male of blue swimmer crab (*P. pelagicus*) has blue color whereas the female one has a brown-greenish color and has smaller claws than male [3]. The blue swimmer crab has lifecycle through a phase of zoea, megalopa, and instar I for 14-19 days. The phase of zoea I and II passed for 3-4 days each, a phase of zoea III and IV passed for 2-3 days each, and megalopa phase for 3-4 days. After megalopa phase, blue swimmer crab can metamorphose into first instar phase [4].

Eggs and larvae of blue swimmer crab (*P. pelagicus*) are planktonic. The eggs of blue swimmer crab can hatch for 15 days into larvae. The larvae of blue swimmer crab last for 26-45 days and located as far as 80 km in the coastal ocean. Before becoming young blue swimmer crab, it stays 6 weeks in loose waters and return to estuary area to grow and flourish then return to sea as adults and then lay eggs in the sea in summer of tropical waters or in spring of sub-tropical waters [5]. The intestines of blue swimmer crab captured in shallow sublittoral waters of Kunduchi Darussalam coast of Tanzania are estimated to be blue swimmer crabs, crustaceans, fish bones and other foods. The

* Correspondence address:
Lini Murni
Email : linimurni@gmail.com
Address : Faculty of Fisheries and Marine Sciences, University of Brawijaya, Veteran Malang, Malang 65145.

ISSN. 2087-2852
E-ISSN. 2338-1655

dominant food is the type of bivalve order of Mytiloida from *Arcuatula arcuatula* type [6].

However, the decline of blue swimmer crabs can be caused by nature of cannibalism, this often cases when molting makes their soft carapace and often preyed by other blue swimmer crabs as well as other predators [7]. It need guarantees on consistent availability and continuous of blue swimmer crab resources so that domestic and foreign market demand can be fulfilled.

One way to ensure the availability of blue swimmer crab resources is by maintaining the existing populations in nature by controlling the exploitation of blue swimmer crabs resources. However, the increasing of market demand for blue swimmer crab resources causes to a higher levels of exploitation in nature. Lack of knowledge levels of fisherman and enforcement of rules made by the government results in continuous catching regardless of size and timing of the catch. This matter, in the availability of blue swimmer crab stock is declining in nature. That is why it need a well designed program to maintain the availability of blue swimmer crab. One of them is by understanding the blue swimmer crab's biological characteristic for the fisherman. Therefore, the purpose of this research is to understand the correlation of wide of carapace and blue swimmer crab weight, sex ratio, and gonad maturity level caught by fisherman in Paciran Subdistrict (Lamongan Regency), Bancar Subdistrict (Tuban Regency), Kraton Subdistrict (Pasuruan Regency), Sluke Subdistrict (Rembang Regency), and the conformity of the rules applied by No.1/PERMEN-KP/2015 (Regulation of Ministry of Marine and Fisheries about Lobster, crabs, and blue swimmer crabs catching).

The blue swimmer crab (*P. pelagicus*) has similar morphology with crabs. It has greater width and length of carapace [8]. The blue swimmer crab caught in coastal waters generally have wide range of 8-13 cm carapace lengths with an average weight of ± 100 g at depth of 20 m with an average blue swimmer crab being obtained at 53.34 g with low weight of 30 g and maximum weight of 160 g [9]. The increased water depth, the weight of the captured blue swimmer crab is larger, but the number of tails obtained is not as much as the depth is relatively shallow [10]. The male blue swimmer crabs prefer to be in the waters with low salinity, thus spreading more in shallow area. This difference in gonad maturity can be due to several factors such as individual body condition and latitude [6].

MATERIAL AND METHOD

Study Area

This research was conducted from collectors which is the representative of blue swimmer crab catching area. Paciran Subdistrict, Lamongan geographical coordinates: 6°52'0'' South, 112°20'0'' East (Fig. 1); Bancar Subdistrict, Tuban 6°47'0'' South, 111°46'0'' East (Fig. 2); Kraton Subdistrict, Pasuruan 7°32'34''-8°30'20'' South, 112°33'55''-113°30'37'' East (Fig. 3); and Sluke Subdistrict, Rembang 6°30' - 7°6' South, 111°00' East as shown in Figure 4.

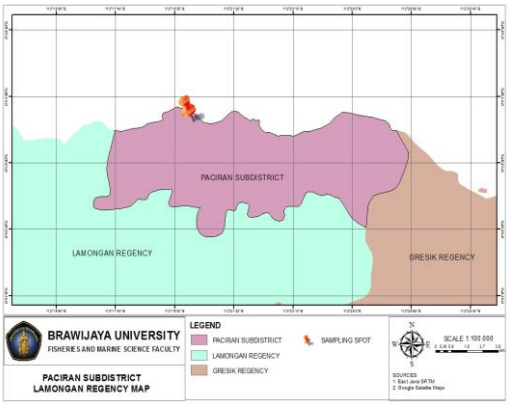

Figure 1. Paciran Subdistrict, Lamongan Regency

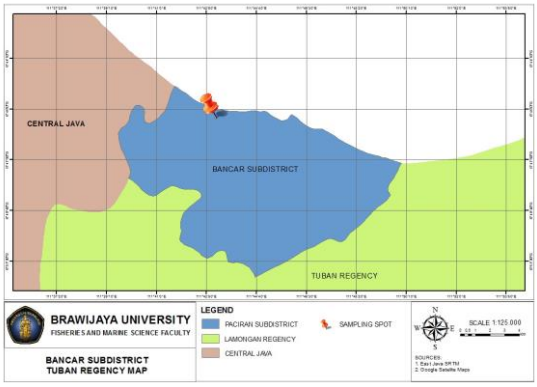

Figure 2. Bancar Subdistrict, Tuban Regency

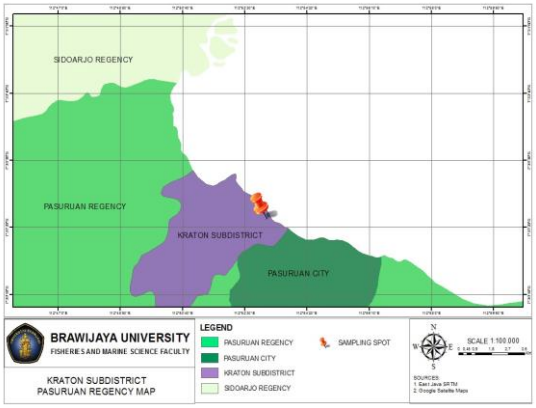

Figure 3. Kraton Subdistrict, Pasuruan Regency

ISSN. 2087-2852
E-ISSN. 2338-1655

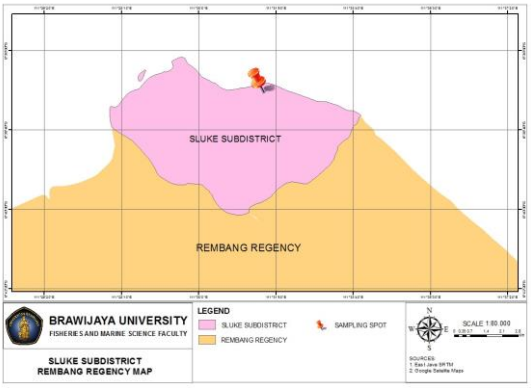

Figure 4. Sluke Subdistrict, Rembang Regency

Data Collection

This research used survey as the method of collecting the information from blue swimmer crab catchers and collectors representing population group. The sampling was done randomly in various water areas. Blue swimmer crab samples obtained by fisherman who were deposited to the collectors, shown in Table 1.

The tool used in the measurement of carapace wide was calipers with precision of 0.05 mm. Then, the measurement tool of sex ratio is making visual observation or seeing the morphological aspects and secondary sex features. The determination of genital blue swimmer crab can be seen from the color and shape of the abdomen. The calculation of sex was done by comparing the number of samples of male and female caught. The measurement of weight was using an analytical digital scale with precision of 0.01 g, while for measuring gonad weight and gonad observation is an analytical digital scales with accuracy of 0.01 g (sectio set and magnifying glass).

Table 1. The Sampling of Blue Swimmer Crab

Location (Regency)	Male (pcs)	Female (pcs)	Total	Sampling
Lamongan	175	125	300	wide-range of carapace and weight distribution
Tuban	116	184	300	
Pasuruan	221	79	300	
Rembang	122	178	300	
Lamongan	175	125	300	sex ratio
Tuban	116	184	300	
Pasuruan	221	79	300	
Rembang	122	178	300	
Lamongan	175	125	300	gonads maturity level
Tuban	31	69	100	
Pasuruan	221	79	300	
Rembang	34	66	100	

The wide of carapace and the distribution of blue swimmer crab weight and the correlation of carapace's wide to individual weights are closely related to the growth rate of the organism. In creating sustainable resources, growth is one of the key factors for determining it. The calculation of carapace wide correlation by weight can be seen from a value of b using the method based on Susanto [11], with formula :

$$b = \frac{N \times \Sigma(logW \times logL) - (\Sigma logW \times logL)}{N \times \Sigma Log^2 L - (\Sigma LogL)^2}$$

$$\textbf{Log a = (Log W/N) – bx (Log L/N)}$$

Description:
a = Condition factor
b = Correlation of wide and weight of blue swimmer crab
W = Blue swimmer crab weight (g)
N = Number of male or female(pcs)
L = Blue swimmer crab wide (mm)

The sex ratio of blue swimmer crab is calculated by comparing a total of male and female using methods based on Zahid and Charles [12], as follows:

$$\textbf{X = J : B}$$

Description:
X = Sex ratio
J = Total of male (pcs)
B = Total of female (pcs)

The gonad maturity level can be done by surgery from body at the abdomen and measured using digital scale with the accuracy of 0.01 g. Otherwise, morphological observations can be seen from color and occupation rate of blue swimmer crab gonad in female hepatic region, which is divided into five levels [13]. At level 1: gonad is immature, white or transparent; level 2: gonad start to mature, yellow/bright orange, not extend into the hapatic region; level 3: gonad in the process of mature, yellow/orange color does not extend/exceed the hepatic area; level 4: mature gonad, yellow/dark orange protruding into the hepatic area; and at level 5: ovigerous, females carry full-fledged eggs (pale eggs to dark yolks) on outside of body/abdomen.

RESULT AND DISCUSSION

The Correlation of Carapace Width and Weight of Blue Swimmer Crab

Each location showed different results. Sample in Lamongan Regency showed that the male blue swimmer crab have larger carapid. This can be due to the growth of female blue swimmer crab will decrease at the time of mature gonad rather than male or also caused by genetic factor of individual them self. The variety sizes of blue swimmer crab obtained can be caused by several factors such as season and depth of waters. The

ISSN. 2087-2852
E-ISSN. 2338-1655

correlation of carapace wide to individual weight of blue swimmer crab was done to know the growth pattern and population.

Based on the observations that have been done, the data obtained from total of 300 samples and analyzing the correlation of carapace wide with weight, it shows that the correlation of carapace wide and weight of male and female has a very close correlation, as well as growth pattern, reared allometric negative, because it is b<3 (male is b = 0.988 and female is b = 0.962). This is influenced by many factors, especially environment. The genetic factor contributing to the size of male blue swimmer crab reaching maturity at the same size. Generally male blue swimmer crab larger than female [14].

The amount of female blue swimmer crabs are higher than male. Catching location is one of the factors influencing the amount. Most of fisherman do the catching on the deep area in which they catch more female. It is because the female of blue swimmer crab prefer to be in the depth with high salinity for reproduction [15]. The factor of differences in the ratio between males and females are biological factor such as spawning. The female blue swimmer crabs like high salinity waters for spawning, thus spreading to deeper waters than male. Reversely, male blue swimmer crab like low salinity waters that spread in shallow waters [16].

Sample in Tuban Regency, the width of blue swimmer crab have a different pattern size of catch due to the different capture fisheries, where coastal waters of Bancar Subdistrict, Tuban Regency is cloudy so that fisherman catches in deeper waters. The weight distribution pattern of blue swimmer crab body dominated in 89.63-102.76 g class which was suspected due to the catching in shallow waters, where fisherman made the catch to easily set the Bubu (fish trap) by diving into the bottom of waters appropriately.

The correlation between the wide of carapace and weight of captured male blue swimmer crab shows negative allometric of b <3 (male is b = 2.532 and female is b = 2.490). Each increase in wide value is followed by an increase in weight value or the other way. The correlation of wide and weight of male blue swimmer crab shows closeness. The acquisition of the width of carapace in correlation with the weight of female blue swimmer crab had shown that the width increased higher than its weight. Besides, the width of carapace and the weight of female blue swimmer crab had close correlation.

The results obtained explain that growth rate of male blue swimmer crab is better than female. In coastal waters of Bancar Subdistrict, Tuban Regency has very few mangrove plants. This is an indication of lack organic material needed by primary organisms which later become bivalve food, gastropod, and mollusca as the main food of male and female blue swimmer crab. The research result said that there are no significant differences in food types during all seasons, regardless of the sexes and sizes. The body size differences do not affect the type of food but affect the amount of food [6].

Sampling in Pasuruan Regency measured the wider carapace on male blue swimmer crab than female. However, the total of male and female blue swimmer crab caught by fisherman has not been in accordance with the Minister of Marine and Fisheries regulations because many blue swimmer crab are caught below-set standards. While the weight of male blue swimmer crab in this study found that male blue swimmer crab is heavier than females. The correlation between the carapace width and body weight of both male and female blue swimmer crab had shown that the carapace width increased faster than the body weight. It indicated that the crabs were captured in small size. The correlation between the wide of carapace and weight of captured male blue swimmer crab shows negative allometric of b <3 (male is b = 2.802 and female is b = 2.771). This has factors such as the availability of feed in nature, genetics, and time of catch, as well as on female used more energy for reproduction so that weight growth is more hampered compared to the wide growth of the carapace. The weight difference between male and female blue swimmer crab suspected due to several factors such as water temperature or influence of growth rate [17].

Sampling in Rembang Regency of blue swimmer crab meet the standards set by No.1/PERMEN-KP/2015, both male and female; although 2% have wide carapace under the standard to be caught. The catch of blue swimmer crab can be done with size carapace > 10 cm. The blue swimmer crab in the laying state should neither be caught nor be recorded. The result could be dead or in unsuitable size. The correlation of the research, the wide of carapace and weight of captured male blue swimmer crab shows positive allometric is value of b >3 (male is b = 3.368 and female is b = 3.047). The

ISSN. 2087-2852
E-ISSN. 2338-1655

deployment of caught blue swimmer crab is sometimes on muddy and rocky substrates but more on sandy substrates. In addition, temperature and salinity factors are thought to affect size distribution of blue swimmer crab (*P. pelagicus*) [16].

The correlation of the wide carapace and weight captured have value of b=3. It is isometric growth pattern, a wide growth pattern equal to weight growth. If the value of b> 3 is positive, allometric growth pattern of weight growth is more dominant than wide growth, and if the value of b <3 is negative, allometric growth pattern of wide growth is more dominant than weight growth [18]. Deeper waters will result in relatively bigger blue swimmer crab (*P. pelagicus*) as well as many sandy substrate found. While the results of weight measurement of male are bigger compared to female. This is caused by metabolism in utilizing energy obtained from food. The correlation between wide of carapace and weight is an increase in the value of wide on blue swimmer crab followed by an increase of weight, shown in Figure 5. The results obtained in this study is larger male on blue swimmer crab than female.

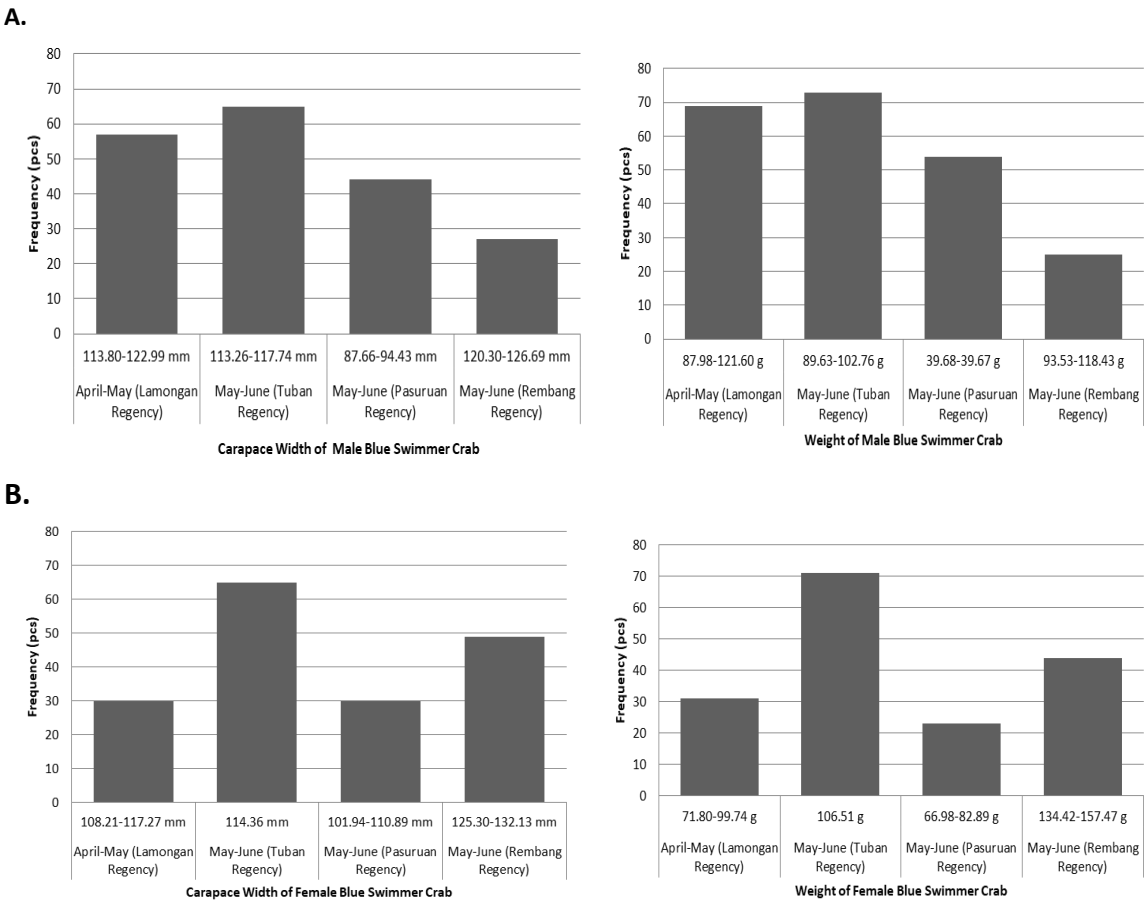

Figure 5. The Sampling of Wide and Weight of Blue Swimmer Crab. **A.** Wide and Weight of Male Blue Swimmer Crab Sample (*P. pelagicus*), and **B.** Wide and Weight of Female Blue Swimmer Crab Sample (*P. pelagicus*) from collectors.

Sex Ratio

Sex ratio is the ratio of males and females in the population. The sex ratio in each sampling site showed different results, can be seen in Table 2. The sampling in Lamongan Regency showed the composition of male and female blue swimmer crab are not balanced. The results of this observation indicate that those caught in dominance by male blue swimmer crab, it is probably due to April-May is spawning season for crab. While sampling in Tuban Regency shows male less than female, this is thought to be caused by spawning and fishing season but sampling in Pasuruan showed female is less than male means that composition of crab has an imbalance. The difference is caused by fisherman in an area of caught around the beach or in shallow waters by using a passive fishing trap. Differences in the total of caught are also caused by the male prefer shallow waters while female prefer deeper waters or waters that have high salinity for spawning.

ISSN. 2087-2852
E-ISSN. 2338-1655

However, sampling in Rembang Regency shows female is more than male or unbalanced. The factors that affect this sex ratio are influenced by migration and weather changes that may affect a population of blue swimmer crab [16].

Table 2. Distribution of *P. pelagicus*) quantities obtained during study at each time and location of taking from collectors.

Time (Location)	Sex Ratio	
	Male	Female
April-May (Lamongan Regency)	1.4	1
May-June (Tuban Regency)	1	1.5
May-June (Pasuruan Regency)	2.8	1
May-June (Rembang Regency)	1	1.46

Gonad Maturity Level

The maturity level of gonads in which gonad develop before and after spawning. The process of development body system gonad will undergo series of morphologic, histological, and cytologic changes. Observations obtained during the study at each time and location of sampling, can be seen in Table 3.

The results of gonad maturity level at each sampling site showed different results. Sampling in Lamongan Regency showed the composition of male and female blue swimmer crab (*P. pelagicus*) unbalanced in the maturity level of the gonad. It is because in April-May of female spawners began to migrate to the deeper ocean to hatch eggs. While sampling in Tuban Regency shows that highest level of male gonad maturity in a phase of maturity level of the gonad II. This possibility is because it depends on different fishing location in shallow waters so that it is dominated by a young crab that is not yet in a mature phase of the gonad.

Sampling in Pasuruan shows the highest level of female gonad maturity in a phase of maturity level II, possibly because it depends on the environment and caught. Sampling in Rembang Regency, it shows that highest level of gonad maturity in the female with a phase of maturity level of gonads II. It is because the least blue swimmer crabs were caught due to the species with mature gonad went on the deeper water. Blue swimmer crab (*P. pelagicus*) go to deeper areas to spawning peaks that occurred in July. However, sampling in Pasuruan shows that most gonad maturity level in the female with phase maturity level of gonads II. This is caused by maturity level of gonads I cell is not fully mature and mostly still in the form of egg cells. The maturity level of gonads II egg cells which begin to enter a stage of maturity, the ovari is still small and looks bright yellow. The maturity level of gonads III eggs begin to enter a stage of ovary has pale yellow color, maturity level of gonads IV egg cells have entered maturation phase and ready for fertilizing. The maturity level of gonads V eggs are located on outside of abdomen with pale until yellow color. Male blue swimmer crab like waters with low salinity so that spread more around in a relatively shallow coastal waters [6]. The maturity level of gonads III and IV occur with an indication of adult female blue swimmer crab laying eggs throughout the year. This occurs because reproduction is limited by warm temperatures in subtropical climates. In subtropical climates, female blue swimmer crab postpone development of gonad maturity during the winter season [19].

Table 3. Gonad Maturity Level of Blue Swimmer Crab (*P. pelagicus*)

Location	The Maturity Level of Gonads Dominant			
	M (pcs)	Freq	F (pcs)	Freq
Lamongan Regency	III Σ 175	53 (30.29%)	II & III Σ 125	38 (30.40%)
Tuban Regency	II Σ 31	13 (41.93%)	III Σ 69	23 (33.33%)
Pasuruan Regency	III Σ 221	57 (25.79%)	II Σ 79	38 (48.10%)
Rembang Regency	III Σ 34	11 (32.35%)	II Σ 66	22 (33.33%)

Note: M = Male, F = Female, Freq = Frequency, Pcs = Pieces, II and III= gonad maturity level

CONCLUSIONS

The correlation between width of carapace and weight of blue swimmer crab in different areas in Lamongan, Tuban, and Pasuruan have negative allometric growth patterns because they have b<3. This suggests that growth of carapace wide is faster than weight. But in Sluke Subdistrict, Rembang Regency, it has positive allometric growth pattern with b>3 (male is b = 3.368 and female is b = 3.047).

The sex ratio shows that ratio of males and females is in unbalanced conditions in which females are larger than males. The level of gonad maturity often found in stage II and III, and most rarely found in phase V so that fishing by fisherman in sampling area is in accordance with No.1/PERMEN-KP/2015, which prohibits the capture of blue swimmer crab in catch conditions

ISSN. 2087-2852
E-ISSN. 2338-1655

of gonad maturity level V. The percentage of crab obtained in this study based on an area of capture meet the standards set by No.1/PERMEN-KP/2015.

ACKNOWLEDGEMENT

The authors would like to thank the researcher, Collectors in Lamongan, Tuban, Pasuruan, Rembang Regency and also Department of Fisheries and Marine Science, University of Brawijaya, Indonesia for their help during this experiment.

REFERENCES

[1] Kembaren, D.D., E. Tri, Suprapto. 2012. Biologi dan parameter populasi rajungan (*Portunus pelagicus*) di perairan bone dan sekitarnya. Biology and Population Dynamics. Research Institute for Marine Fisheries. Jakarta.

[2] Ministry of Marine Affairs and Fisheries. 2012. Statistik perikanan tangkap indonesia tahun 2011. (ID): Directorate General of Capture Fisheries, Ministry of Marine Affairs and Fisheries. Jakarta.

[3] Svane, I., G.E Hooper. 2004. Blue swimmer crab (*Portunus pelagicus*) fishery. Fishery assessment report to PIRSA for the blue crab fishery management committee. South Australian Research and Development Institute (Aquatic Sciences). Adelaide. RD03/0274-2.

[4] Arshad, A., M.S. Efrizal, Kamarudin, C.R. Saad. 2006. Study on fecundity, embryology and larva development of blue swimming crab *Portunus pelagicus* (Linnaeus, 1758) under laboratory conditions. J. Fish. Hydrobiol. 1(1). 35-44.

[5] Kangas, M.I. 2000. Synopsis of the biology and exploitation of the blue swimmer crab; *Portunus pelagicus* Linnaeus, in Western Australia. *J. Fish. Res. Western Australia.* 12(1). 1-22.

[6] Chande, A.I., Y.D Mgaya. 2004. Food habits of the blue swimming crab *Portunus pelagicus* along the coast of Dar Es Salaam, Tanzania. *Western Indian Ocean J. Mar. Sci.* 3(1). 37-42.

[7] Josileen, J. 2011. Food and feeding of the blue swimmer crab, *Portunus pelagicus* (Linnaeus, 1758) (Decapoda, Brachyura) along the coast of Mandapam, Tamil Nadu, India. *Crustaceana.* 84(10). 1169-1180.

[8] Lovett, D.L. 1981. A guide to shirmps, prawns, lobster and crab of Malaysia and Singapore. Faculty of Fisheries and Marine Science, Universiti Pertanian Malaysia. Serdang, Selangor.

[9] Juwana, S., K. Romimohtarto. 2000. Rajungan: perikanan, cara budidaya dan menu masakan. Djambatan. Jakarta.

[10] Wulandari, W., R. Herry, B. Asriyanto. 2014. Analisis perbedaan kedalaman dan substrat dasar terhadap hasil tangkapan rajungan (*Swimming Crab*) dengan arad rajungan di perairan Wedung, Demak. *J. Fish. Resour. Util. Manage. Technol.* 3(4). 85-93.

[11] Susanto, A. 2011. Analisa beberapa aspek reproduksi kepiting bakau (*Scylla serata*) di perairan segara anakan, Kabupaten Cilacap, Jawa Tengah. *Jurnal Matematika Sains dan Teknologi.* 12(1). 30-36.

[12] Zahid, A., P.H.S Charles. 2009. Biologi reproduksi dan faktor kondisi Ikan Ilat-ilat *Cynoglossis bilineatus* (Lac.1820) (Pisces: Cynoglossidae) di perairan Pantai Mayangan Jawa Barat. *J. Indonesian Anthropol.* 9(1). 85-95.

[13] Sumpton, W.D., M.A. Potter, G.S Smith. 1994. Reproductions and growth of the commercial sand crab (*Portunus pelagicus*) in Moreton Bay Queensland. *Asian Fish. Sci.* 7. 103-133.

[14] Warner, G.F. 1977. The biology of crabs. Elek Science. London.

[15] Sunarto, D. Soedharma, E. Riani, S. Martasuganda. 2010. Performa pertumbuhan dan reproduksi Rajungan (*Portunus pelagicus*) di Perairan Pantai Kabupaten Brebes. *Omni-Akuatika.* 9(11). 75-82.

[16] Mehdi, H., V. Amir, P. Yaghob, M. Ali. 2012. Sex ratio, size distribution and seasonal abundance of blue swimming crab, *Portunus pelagicus* (Linnaeus, 1758) in Persian Gulf Coasts, Iran. *World Appl. Sci. J.* 17(7). 919-925.

[17] Lee, H.H., C.C. Hsu. 2003. Population biology of the swimming crab *Portunus sanguinolentus* in the waters off Northern Taiwan. *J. Crustacean Biol.* 23(3). 691-699.

[18] Effendie, M.I. 2002. Biologi perikanan. Yayasan Pustaka Nusantara. Yogyakarta.

[19] Kamrani, E., Sabili, N. Abdul, M. Yahyavi. 2010. Stock assessment and reproductive biology of the blue swimming crab, *Portunus pelagicus* in Bandar Abbas Coastal Waters, Northern Persian Gulf. *J. Persian Gulf (Mar. Sci.).* 1(2). 11-22.

ISSN. 2087-2852
E-ISSN. 2338-1655

Growth Rate and Chemical Composition of Secondary Metabolite Extracellular Polysaccharide (EPS) in Microalga *Porphyridium cruentum*

Nurul Mutmainnah[1*], Yenny Risjani[2], Asus Maizar Suryanto Hertika[3]

[1]Master Program of Aquaculture, Faculty of Fisheries and Marine Sciences, University of Brawijaya, Malang, Indonesia
[2]Central Laboratory of Life Sciences (LSIH), University of Brawijaya, Malang, Indonesia
[3]Department of Water Resources Management, Faculty of Fisheries and Marine Sciences, University of Brawijaya, Malang, Indonesia

Abstract

Porphyridium cruentum microalgae have great potential to be developed as a source of active ingredients in various fields of health. It excretes secondary metabolites in the form of extracellular polysaccharides (EPS), potentially as antibacterial, antihyperglycemic, and immunostimulant components. This study aims to obtain the best culture density of *P. cruentum*, the active component of *P. cruentum* (EPS), and the chemical composition of EPS. The *P. cruentum* was cultivated on 15%, 20% and 25% culture stock, with an addition of silicate, Fe and vitamins in sterile seawater medium with salinity 35‰, pH 8, temperature 25-27°C, with continuous aeration and 2500 lux continuous 24 hours, for 14 days of culture period. The results of this study indicate differences in growth rates and abundance of microalgae to each culture stock. The 15%, 20% and 25% culture stocks each showed stationary phase at days 10^{th}, 12^{th} and 14^{th}, with EPS concentrations of 10 ppt, 12 ppt, and 15 ppt, respectively. Variation of *P. cruentum* culture showed different EPS results, with a density of 25% capable of producing the highest EPS extract of 15,000 $mg.L^{-1}$. The EPS is known to contain glucose and carboxylic acid compounds that can be utilized in the health and industrial fields.

Keywords: culture, extracellular polysaccharides, *Porphyridium cruentum*.

INTRODUCTION

Porphyridium cruentum is one of the rare, single-celled, colon-free Rhodophyceae classes found in moist, freshwater, and dominant terrains found in marine waters [1,2]. The *P. cruentum* cell is about 4-9 µm in diameter, with cell structure consisting of nucleus, golgi body, mitochondria, chloroplasts, starch, mucus and vesicles. It contains red pigment phycoerythrin which is an additional pigment in the cell, dominant to cover the green color of chlorophyll. The pigment content is affected by the depth of the habitat, the deeper the habitas, phycoerythrin become more dominant, and it decrease in the shallower water. The *P. cruentum* contains chlorophyll a and has no chlorophyll b, but it has chlorophyll d. The red pigment *P. cruentum* masks the color of other photosynthetic pigments, so this red pigment becomes the main pigment that plays a role in the reception of light in the process of photosynthesis [1-4].

The *P. cruentum* cell is bound in the mucilago. Mucilago is a compound expressed by a cell constantly forming a capsule, and surrounds a cell, containing a sulfate polysaccharide or otherwise known as EPS. EPS is essentially a secondary metabolite of microalgae useful as a protective for microalga cell in the conditions that do not support its life survival. As a source of nutritional reserves in nutritional deficiencies, microalgae cell coatings keep the cells protected from extreme temperature changes. EPS becomes one of the important components in *P. cruentum* function as antioxidant, antibacterial, antiviral, and anti hyperglycemic [2,5,6]. In addition *P. cruentum* contains carotenoids which are useful in improving the immune system [7,8].

Porphyridium cruentum has a carbohydrate biomass composition value of 32.1% (w/w), 34.1% crude protein. Mineral contents in 100 g of dried biomass are Na (1130 mg), Mg (629 mg), Ca (4960 mg), K (1190 mg), and Zn (373 mg). The fatty acid content is 1.6% for 16:0, 0.4% for 18:2ώ6, 1.3% to 20:4ώ6, and 1.3% for 20:5ώ6. The biomass of *P. cruentum* contains pigment in the form of phycoerythrin characteristic of red color. Besides that, the biomass also contains vitamin K, tocopherol and carotene. These microalgae contain active components of phenol, sterols, terpenoids, flavonoids and polysaccharides that can be used as antiviral, antibacterial, antioxidant [2,9].

This microalgae is important to be explored because it has various benefits that can be applied in various fields, especially in medical field. Currently efforts to formulate alternative treat-

* Correspondence address:
Nurul Mutmainnah
Email : nurulmuhtar21@gmail.com
Address : Faculty of Fisheries and Marine Sciences, University of Brawijaya, Veteran Malang, Malang 65145.

ISSN. 2087-2852
E-ISSN. 2338-1655

ments are increasingly being made, requiring eco-friendly materials and abundant and accessible availability. One material that can be used as an alternative is to utilize microalgae, among others, the red microalgae *P. cruentum*. Microalgae is easily cultivated and able to grow quickly, in addition to the utilization of this microalga will increase the choice of raw materials that can be utilized in various fields both health and industry.

Efforts to explore the benefits of *P. cruentum* increasingly crowded, but the less of microalgae biomass is limiting the use of space to scale on in vitro only. So that method and modification of treatment to cultivate *P. cruentum* cultivation process must be developed, to obtain the right method to fulfill the needs of *P. cruentum* biomass on a wider scale. The purpose of this study is to obtain the best culture density of *P. cruentum*, the active component of *P. cruentum* (EPS), and the chemical composition of EPS in *P. cruentum*.

MATERIAL AND METHOD

The method used in this study is an experimental method, which is a deliberate method with certain controlled treatment in a place. This research was conducted at Fish Reproduction Laboratory and Parasitic and Fish Disease Laboratory, Faculty of Fisheries and Marine Sciences, University of Brawijaya, Malang.

Data Collection

Cultivation of Porphyridium cruentum

Porphyridium cruentum microalgae seeds used in this research were obtained from Brackish Water Aquaculture Center (BBAP) Situbondo. The cultivation media using seawater that has been in sterilization by boiling. The tools used were sterilized using chlorine 15 $g.L^{-1}$ diluent, after diluted chlorine sprayed sufficiently into a glass jar container of 1.5 L capacity which has been filled with plain water and allowed to stand for 24 hours. Furthermore, the water is drained and the container is allowed to dry until it is completely dry before the tool is used. Cultivation with the addition of Fe and silicates and vitamins as much as 1 $mL.L^{-1}$. The lighting 2500 lux and aeration is continuously with 15%, 20% and 25% culture stock [10,11,12]. The microalgae cultivation is in laboratory scale that carried out for 7-14 days, and observed the density of microalgae growth daily using hemositometer with the aid of 400x magnification light microscope [13].

Extracellular Polysaccharide Extraction (EPS)

The EPS extraction process was conducted based on Raposo et al. [14], where fresh *P. cruentum* in culture medium was centrifuged at 10,000 rpm for 20-30 min at 4°C. The formed pellets are removed and only take the supernatant containing EPS. The supernatant is placed under a ventilated hotte to obtain a suspension containing EPS. After 3-4 days, the sample is placed in water bath at 80°C for 1 hour. Suspensions containing EPS are filtered using simple filter paper and the extraction is refined by precipitation with two variations of cold ethanol volume (as required). After the EPS obtained, previously treated with freeze dryer before and after the dialysis process. The process of dialysis is carried out by resuspending dry EPS in distilled water and the process of dialysis using cellulose membranes. This process is done several times.

EPS Chemical Composition Analysis

The chemical composition test of EPS by FTIR method is based on Mishra and Jha [15] research. Fourier Transform Infrared (FTIR) in general aims to detect functional groups of certain compounds, so that the compiler compound can be known in a more detail than just phytochemical test. The test was carried out by homogenizing 200 mg of Kbr as well as 2 mg of EPS powder in the mortar. Samples that have been homogeneous compacted and fed into tensor 37. The test sample is measured at a wavelength of 4000-500 cm^{-1}, resulting in FTIR spectra showing the absorption peaks of the sample wave number. Functional groups are determined by the absorption peaks of expressed wave numbers.

RESULT AND DISCUSSION

Biomass production of *Porphyridium cruentum*

The *Porphyridium cruentum* microalga growth with 15%, 20%, and 25% culture stock density reached peak on 10^{th} day and decreased and stable on day 11 until day 14. Generally microalgae growth through several phases starting with phase lag (adjustment), logarithmic phase (growth), stationary phase (stop growing) and ending with death phase [13]. The abundance of *P. cruentum* which tends to be stable after passing through the stationary phase i.e. on the 8^{th} day, can be caused by continuous aeration and lighting treatment, and the availability of nutrients needed by the microalgae to grow. Until at certain times, the growth will be completely stopped and die, i.e. in the conditions

ISSN. 2087-2852
E-ISSN. 2338-1655

where nutrients are no longer available in the growth medium of *P. cruentum*. Through this study, the time occurs at week 5 of culture, without the addition of nutrients, where the aeration and lighting process continues.

The growth of *P. cruentum* is influenced by internal factors such as the quality of microalgae itself. It is also strongly influenced by external factors such as availability of light (2500-3000 lux), temperature (25-27°C), media quality (sterile), and availability of nutrients (vitamins , Fe, silicate, phosphate and nitrate) [2,16].

There is a difference in the rate of growth in the variation of the microalgae culture stock, which is due to the microalgae cell density itself, as well as the uneven nutritional and lighting requirements that support the variation in growth rate. Prayitno explained that cell culture density affects the growth pattern of microalgae [17], which in high culture stock can shorten the phase of lag (phase of adjustment), and exponential phase increases faster. Denser culture stock conditions cause increasing competition between cells to obtain light and nutrients. Thus in conditions of lack of light, it can disrupt the process of cell division. In addition, if aeration forces are reduced, nutrient transport does not occur thoroughly, causing microalgae cells to not undergo good cell division that affects the time of growth rate.

In 200 mL culture stock, we obtained faster growth rate so that it reaching stationary phase faster when compared with both other culture stocks, that is 150 mL and 250 mL. This become indication that at amount of growth media 1 L, using 200 mL microalga density, is the best to obtain a fast growth rate. The growth of *P. cruentum* microalgae was observed daily for 14 days of culture, to obtain the amount of *P. cruentum* density presented by growth graph in Figure 1.

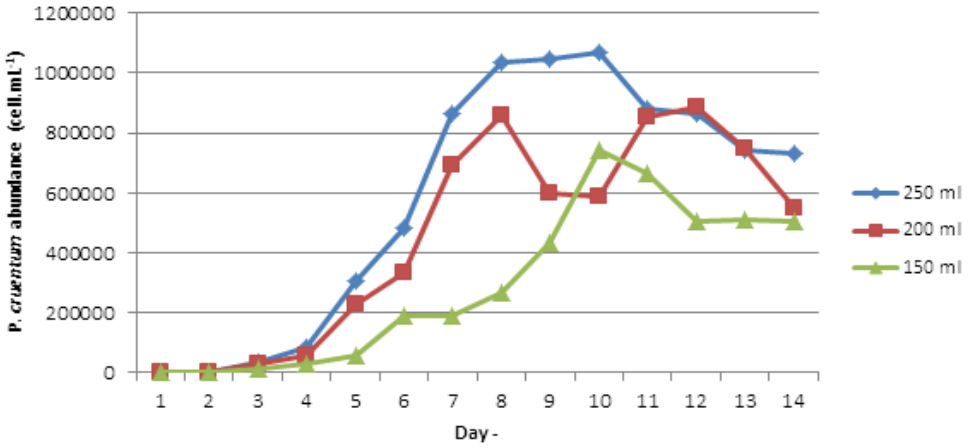

Figure 1. *Porphyridium cruentum* growth with 15%, 20% dan 25% culture stock density, with 2500 lux lighting and continuous aeration, for 14 days of culture.

Extracellular Polysaccharide (EPS)

The concentration of EPS was obtained by centrifugation process followed by the extraction process, used 96% ethanol solvent with media and solvent ratio of 1:0.75 v/v. Based on microalgae culture results for 14 days of rainy season, at 15% culture density obtained EPS + 10.000 mg.L^{-1} culture medium, 20% culture stock density obtained EPS + 12.000 mg.L^{-1}, and density stock culture 25% obtained EPS + 15.000 mg.L^{-1} (Table 1).

A culture of *Porphyridium* sp. was performed in winter and extracellular polysaccharide values are obtained from 200 to 1000 mg.L^{-1} [18]. In contrast to Setyaningsih et al. [13], where extracellular polysaccharide values were obtained from 12,500 - 21,500 mg.L^{-1} for a culture time of 12 days. Differences in extracellular polysaccharide values can be influenced by differences in the culture medium used, which include differences in the nutrient composition of each medium, in addition to differences in temperature and illumination

Table 1. Extracellular Polysaccharide Components (EPS)

P. *cruentum* Culture Stock (mL.L^{-1})	EPS (mg.L^{-1})
150	10,000
200	12,000
250	15,000

ISSN. 2087-2852
E-ISSN. 2338-1655

Biologically extracellular polysaccharides function to protect microalgae cells, play a role in ion exchange or reservoir, as a barrier wall that is difficult to penetrate by gas and water. It is also serves as a place of excretion of vitamins and hormones [1]. The number of EPS obtained shows good microalgae growth, and good cell metabolic processes, to produce continuous extracellular compounds. The resulting extracellular polysaccharides will be a source of nutrients for cells in the growth process. The more cell division occurs, the EPS excretion process will increase, and can extend the growth phase of microalgae caused by the availability of nutrient reserves of EPS.

The chemical composition of EPS is identified from the expression of the functional group via the FTIR test. The graph in Figure 2 shows the chemical compounds read through the functional groups such as wavelength absorption 3442.769 indicating the presence of hydroxylate bond (-OH), wavelength absorption at 2239.846 indicates the presence of carboxylic acid bond (-COOH), the CO bond is indicated by a long absorption wave 1625.614, while wavelength absorption 1438.650 and 1362.350 indicate the presence of phenol bonds, as well as at 1200-800 wavelength absorption indicates the presence of polysaccharide bonds.

Hasanah in 2016 performed FTIR test on *P. cruentum* EPS found that extracellular type of extracellular polysaccharide sugar was identified only maltoheptose composed of seven maltose disaccharides which is a component of glucose [10]. In contrast, Raposo et al. in 2014, found *P. cruentum* EPS was tested by GCMS (Gas Cromatografy Mass Spectrometry) method in which extracellular polysaccharides were identified to contain several major sugar components, including galactose (26.5-36.5 M%), glucose (22.5-24% M), and arabinose (16 M%). While other sugar components such as mannose, fucose, xylose, and rhamnose were also detected with low concentrations of 11, 9, 7 and 4 M% [14].

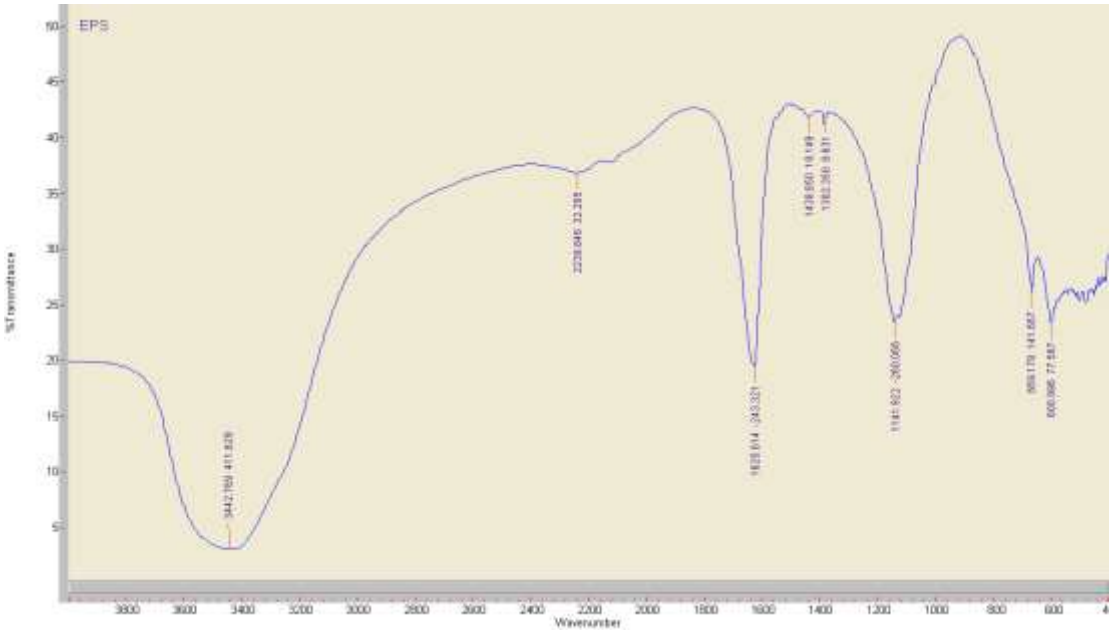

Figure 2. Extracellular polysaccharide functional group (EPS) *Porphyridium cruentum*, using FTIR test at 4000-500 cm^{-1} wavelength.

It was reported that EPS in *P. cruentum* composition with several different fractionation treatments using TLC (Thin-layer Chromatography) and GC measurements, so it was known that EPS content included Xyl, Glc, and Gal sugar [19]. Through the method of m-hydroxybiphenyl assay, sodium rhodizonate assay and IR spectrophotography, it was found that EPS sugar content included uronic acid and sulfate compound, through IR spectrophotography on band 820 cm^{-1} indicated hydroxyl primer sulfate group. This shows that the EPS extract contains sugar D- and L-Gal (Fig. 3).

Through a previous study of Geresh et al. in 1990 [20], it found α-D-glucopyranosyluronic acid-(1 → 3)-L-galactopyranose disaccharide from hydrolyzate acid *Porphyridium* sp. It indicates the configuration of each of GlcA and Gal are D- and -

ISSN. 2087-2852
E-ISSN. 2338-1655

L. This disaccharide type is known as the polysaccharide constituent part for several types of red microalgae.

Differences in sugar composition in the EPS testing, allegedly caused by hydrolysis factors that have not been optimal, in this case may be the time of hydrolysis used has not been able to break the chemical bonds EPS Porphyridium cruentum so that no overall chemical composition EPS detected. The amount of galinisic acid hydrolyzed with 0.2 M H2SO4 at 80°C reached 2.5% for 28 hours and at 100°C reached 6% for 16 hours w/w [21]. It shows that hydrolysis values can be influenced by the time and temperature used. In addition Hasanah [10] confirmed the factors that can affect the hydrolysis level can be the time, temperature, type and concentration of the sample, and used solvent.

One of the ingredients that can be used as an immunostimulant is a polysaccharide compound [22]. Polysaccharides are a classification of carbohydrates which are a combination of monosaccharide molecules composed of over 6 molecules of monosaccharides, and they can be hydrolyzed back into many monosaccharide molecules. Polysaccharide compounds have the ability to stimulate the body's immune system [7]. EPS can also be β-mannan, β-glucan, xanthan, dextran, curdlan and gellan, which have many benefits in various fields such as stabilizers, emulgators, gelling or thickener, and possess the ability to bind water well so as to maintain texture remain soft during storage time in the food industry. On the other hand in the field of health EPS is able to show anti-tumor activity, and able to improve health through increased immune power and can lower cholesterol [23].

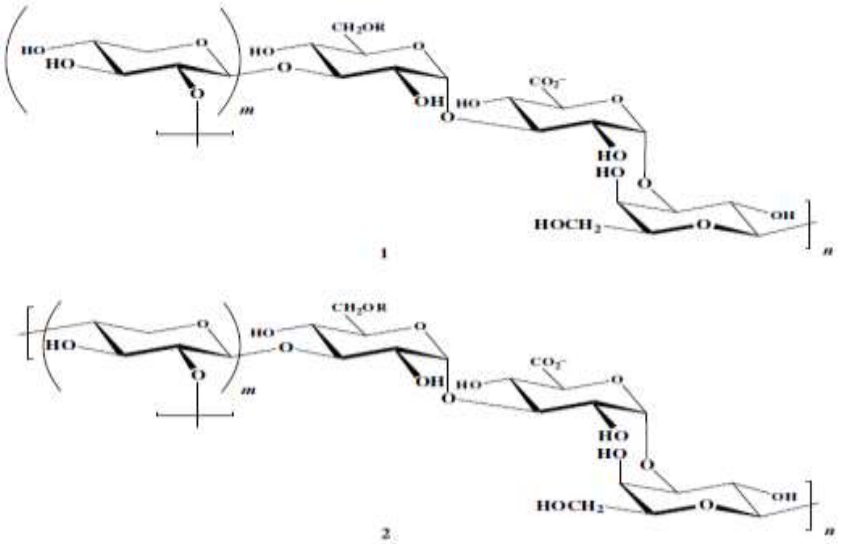

Figure 3. Unit Polysaccharide 1). Terminal Gal, 2). Xyl Terminal [19]

CONCLUSION

Variation of *P. cruentum* culture showed different EPS results, with a density of 25% capable of producing the highest EPS extract of 15,000 mg.L^{-1}. Increased chemical content of P. *cruentum* may be affected by culture modification by the addition of various fertilizers and vitamin supplements. The chemical composition of the dominant EPS is obtained by compounds of hydroxylate bonds including polysaccharides which can be utilized in the health and industrial fields.

REFERENCES

[1] Borowitzka, M.A., L.J. Borowitzka. 1988. Micro-algal biotechnology. Cambridge University Press. Cambridge.

[2] Kusmiyati, N.W.S. Agustini. 2007. Uji aktivitas antibakteri dari mikroalga *P. cruentum*. *Jurnal Biodiversitas.* 8(1). 48-53.

[3] Madigan, T.D., J.M. Martinko, J. Parker. 2009. Brock biology of microorganism, 12th Ed. Pearson/Benjamin Cummings. San Francisco.

[4] Sharma, O.D. 1986. Textbook of algae. Tata Mc. Grow Hill Publishing Company Limitted. New Delhi.

[5] Garcia, I.R., J.L.G. Guerrero. 2008. Evaluation of the antioxidant activity of three microalgal species for use as dietary supplements and in the preservation of foods. *Food Chem.* 108(3). 1023-1026.

ISSN. 2087-2852
E-ISSN. 2338-1655

[6] Kosasih, Y. 2011. Aktivitas komponen antibakteri aikroalga *Porphyridium cruentum* terhadap berbagai jenis bakteri patogen. Bachelor Thesis. Department of Aquatic Product Technology, Bogor Agricultural University. Bogor.

[7] Manilal A., S. Sujith, G.S. Kiran, J. Selvin, C. Shakir, R. Gandhimathi, A.P. Lipton. 2009. Antimicrobial potential and seasonality of red algae collected from the southwest coast of India tested against shrimp, human and phytopathogens. *Ann. Microbiol.* 59(2). 207-219.

[8] Fuentes, M.M.R., J.L.G. Sanchez, J.M.F. Sevilla, F.G.A. Fernandez, J.A.S. J.A.S. Pérez, E.M. Grima. 1999. Outdoor continous culture of *Porphyridium cruentum* in a tubular photobioreactor: quantitative analysis of the daily cyclic variation of culture parameters. *Progress Ind. Micobiol.* 35. 271-288.

[9] Fuentes, M.M.R., G.G.A., Fernandez, J.A.S. Perez, J.L.G. Guerrero. 2000. Biomass nutrient profiles of the microalga *Porphyridium cruentum*. *Food Chem.* 70. 345-353.

[10] Hasanah, 2016. Pemisahan biomassa dan eksopolisakarida *Porphyridium cruentum* menggunakan ultrafiltrasi serta pengaruhnya terhadap aktivitas inhibisi α-Glukosidase. Master Thesis. Aquatic Product Technology Graduate School, Bogor Agricultural University. Bogor.

[11] Irwani, A. Ridlo, Widianingsih, 2013. Optimalisasi total lipid mikroalga *Porphyridium cruentum* melalui pembatasan nutrien dan fotoperiod. *Buletin Oseanografi Marina.* 2(2). 16-23.

[12] Rahman, D.A. 2011. Aktivitas antihiperglikemik dari biomassa dan polisakarida ekstraseluler *Porphyridium cruentum* sebagai Inhibitor α-Glukosidase. Bachelor Thesis. Department of Aquatic Product Technology, Bogor Agricultural University. Bogor.

[13] Setyaningsih, I., E. Salamah, D.A. Rahman. 2013. Komposisi kimia dan aktivitas antihiperglikemik biomassa dan polisakarida ekstraseluler dari mikroalga Porphyridium cruentum. Jurnal Pengolahan Hasil Perikanan Indonesia. 16(1). 79-85.

[14] Raposo M.F., A.M. de Morais, R.M. de Morais. 2014. Influence of sulphate on the composition and bacterial and antiviral properties of the exopolysaccharide from *Porphyridium cruentum*. *Life Sci.* 101(1-2). 56-63.

[15] Mishra, A., B. Jha. 2009. Isolation and characterization of extracellular polymeric substances from microalgae *Dunaliella salina* under salt stress. *Bioresour. Technol.* 100. 3382-3386.

[16] Dermoun, D., D. Chaumont, J.M. Thebault, A. Dauta. 1992. Modelling of growth of *Porphyridium cruentum* in connection with two interdependent factors: light and temperature. *J. Bioresour. Technol.* 42. 113-117.

[17] Prayitno, J. 2015. Pola pertumbuhan dan pemanenan biomassa dalam fotobioreaktor mikroalga untuk penangkapan karbon. *Jurnal Teknologi Lingkungan.* 17(1). 45-52.

[18] Singh S., S.A. Arad, A. Richmond. 2000. Extracellular Polysaccharide production in outdoor mass cultures of *Porphyridium* sp. in Flat Plate Glass Reactors. *J. Appl. Phycol*. 12. 269-275.

[19] Geresh, S., S. Arad, O. Levy-Ontman, W. Zhang, Y. Tekoah, R. Glaser. 2009. Isolation and characterization of poly- and oligosaccharides from the red microalga *Porphyridium* sp. *Carbohydr. Res.* 344(3). 343-349.

[20] Geresh, S., O. Dubinsky, S. Arad, D. Christiaen, R. Glaser. 1990. Structure of 3-O-(alpha-D-glucopyranosyluronic acid)-L-galactopyranose, an aldobiouronic acid isolated from the polysaccharides of various unicellular red algae. Carbohydr. *Res.* 208. 301-305.

[21] Emaga, T.H., N. Rabetafika, C.S. Blecker, M. Paquot. 2012. Kinetics of the hydrolysis of polysaccharide galacturonic acid and neutral sugars chains from flaxseed mucilage. *Biotechnol. Agron. Soc. Environ.* 16 (2). 1-14.

[22] Sakai, M. 1999. Current research status of fish immunostimulan. Aquaculture. Faculty of Agriculture, Miyazaki University. Miyazaki.

[23] Yang, F., Y. Shi, J. Sheng, Q. Hu. 2006. In Vivo immunomodulatory activity of polysaccharides derived from *Chlorella pyrenoidosa*. *Eur. Food Res. Technol.* 224(2). 225-228.

ISSN. 2087-2852
E-ISSN. 2338-1655

Optimal Control of Tumor Growth Model with Dendritic Cells as Immunotherapy

Firmansyah Reskal Motulo[1], Trisilowati[2*], Abdul Rouf[2]

[1]Master Program Mathematics, Faculty of Mathematics and Natural Sciences, University of Brawijaya, Malang, Indonesia

[2]Department of Mathematics, Faculty of Mathematics and Natural Sciences, University of Brawijaya, Malang, Indonesia

Abstract

In this paper, optimal control of tumor growth model with dendritic cells as immunotherapy is provided. The model equation can be expressed into a nonlinear differential equation system consisting of four compartments namely, tumor cells, CTL cells, helper T cells, and dendritic cells. Dendritic cells as immunotherapy are injected to the body at time t. The aim of this optimal control is to minimize the tumor cells density as well as the cost of dendritic cells to be administered to the body. Optimal control problem is carried out based on Pontryagin's maximum principle and numerical simulation is solved by using Forward-Backward Sweep methods. Simulation results show that control strategy shrinks tumor cells density which is shown by tumor cells density graph that monotonically decreases after applying dendritic cells as immunotherapy.

Keywords: immunotherapy, optimal control, Tumor cell.

INTRODUCTION

Cancer is a term that commonly used to address a group of dangerous diseases. One characteristic of cancer as an abnormal cell is uncontrolled growth. Cancer is caused by a malignant tumor, in general tumor is divided into two, namely benign tumors and malignant tumors (cancer). Cancer is formed from abnormal and unstable cells and developed through the bloodstream system and lymphatic system [1]. Cancer arises from the transformation of healthy cells into tumor cells in a multi-stage process that generated from the pre-cancerous stage to malignant tumors. This changes are commonly occurring because genetic factors and three external factors, namely physical carcinogens, such as ultraviolet radiation and ionization; chemical carcinogens such as asbestos, tobacco smoke components, aflatoxins (food's contaminant), and arsenic (drinking water's contaminant); and biological carcinogens such as infections from viruses, bacteria or certain parasites [2].

Based on WHO data in 2010, the number of cancer patients worldwide increases every year, which is firm to 7 million people with two-thirds of them are in developing countries [3]. There are several ways that can be proposed to inhibit tumor growth such as radiation and drug therapy. Also, it ultimately can be done through immunotherapy by using dendritic cells (DCs) which are known as dendritic cell vaccinations. A dendritic cell vaccine is a new form of immunotherapy used to treat cancer [4].

Dendritic cells are the most effective antigen-presenting cell because of its strategic location, such in places where microbes and foreign antigens enter the body and are located around the organs that targeted by the bacteria or abnormal cells progression [5]. Based on its function there are two types of dendritic cells, namely conventional dendritic cells (cDCs) and plasmacytoid dendritic cells (pDCs). The primary feature of cDCs is to recognize the antigens then presented to T cells ($CD4^+T$) and removed some crucial molecules, while pDCs have a role in generating interferon as antiviral in the body. In general, it can be illustrated that the part of dendritic cells against tumor or other infections started by recognizing such antigens produced by the abnormal cell, then releasing molecules such as cytokines to activate T cells by presenting antigen through the major histocompatibility complex (MHC) or human leucocyte antigen (HLA) [6].

Analysis of tumor growth model has been performed by several researchers, including Kirschner and Panetta that discussed mathematical models of tumor growth and their interactions with immunotherapy [7]. This study described the dynamics between tumor cells, immune cells, and IL-2 which prove that

* Correspondence address:
Trisilowati
Email : trisilowati@ub.ac.id
Address : Dept. Mathematics, Faculty of Mathematics and Natural Sciences, University of Brawijaya, Veteran Malang, Malang 65145.

ISSN. 2087-2852
E-ISSN. 2338-1655

immunotherapy with interleukin-2 can boost the immune system [7].

DePillis et al. in 2001 evaluated a tumor-spreading model that expressed in the form of a system of ordinary differential equations. In this study, an optimal control approach is used to evaluate the tumor growth with drug therapy. In this model, there are four subpopulations, namely tumor cells, host cells, immune cells, and drug therapy [8]. Five years later DePillis et al. developed a tumor growth model by combining immunotherapy and chemotherapy. The results of numerical simulations indicated that chemotherapy or immunotherapy alone is not sufficient to control tumor growth, furthermore it is shown that combining the two therapies can significantly remove the entire tumor [9].

In 2013, DePillis et al. analyzed the mathematical model by performing therapy on melanoma using dendritic cells [10]. In that model, they have modified the Ludewig's model describing the interaction between dendritic cells, organs, and tumor cells [11]. In the same year, Trisilowati et al. researched optimal control of dendritic cell treatment model on tumor growth. It is demonstrated that dendritic cells are used as a natural killer for tumor cells and treatment therapy which is solved using optimal control problems [12].

Sharma and Samanta in 2013 conducted a study on tumor growth models and their interactions with the immune system using chemotherapy drugs [13]. The analysis of tumor growth model is performed by investigating the effects of tumor immune interactions and chemotherapy drugs which are expressed in four components: (i) T cells that can not attack and destroy tumor cells directly, but release the interleukin-2 cytokine that stimulates CTLs (Cytotoxic T-Lymphocytes) and convert it into active CTL cells, (ii) active CTL cells that can attack, destroy, or even swallow tumor cells, (iii) tumor cells, and (iv) chemotherapy drugs [13]. Sharma and Samanta also applied the model in optimal control problem in order to minimize the amount of drugs to be used in reducing the number of tumor growth. Furthermore, in 2017, Rangel-Reyes et al. conducted an optimal control study of the murine model to measure the effectiveness of dendritic cells [14]. The model consists of tumor cells, $CD4^+$T cells as helper cells, $CD8^+$T or CTL cells, dendritic cells, IL-2, TGF-β^+T as inhibitory cells, IFN-γ which increases regulation of MHC class 1, and the number of MHC class 1 for each melanoma cell [14].

As described in previous study, dendritic cell has an important role in regulating and controlling the tumor growth [15,16]. In addition, dendritic cell has a potential application in cancer treatment. This treatment is often considered as a safe treatment compared with other therapies [17]. Therefore, in this research the effect of dendritic cell as immunotherapy in cancer treatment is observed. Mathematical model on Sharma and Shamanta [13] is modified by changing the chemotherapy compartment with dendritic cell as immunotherapy. Optimal control is then applied to the model to find the number of dendritic cells to be administered so as minimize the number of tumor cells as well as the cost of the treatment. Optimal control problems is solved using Pontryagin's maximum principle to obtained the optimal system. The interpretation is performed based on the results of a numerical simulation on MATLAB software by using Sweep Forward-Backward method.

MATERIAL AND METHOD

Construction Model

In this article, optimal control of the tumor growth model consists of four compartments in the form of nonlinear differential equations. Further, each compartment express the density of tumor cells, cell CTLs, helper T cells, and dendritic cells.

Determination of Optimal Control Problems

Optimal control settlement is about determining the state, costate, and stationary condition to obtain optimal solutions [18]. In the field of mathematics, optimal control is generally used as a strategy to minimize or maximize a particular objective functional. Therefore, in this paper, the aim of optimal control is to reduce the number of tumor cell as well as the cost of treatment.

Numerical Simulation

Numerical simulation is conducted to support the analytical results. At this stage, the simulation is approached by using Sweep Forward-Backward method on MATLAB software.

RESULT AND DISCUSSION

Model Formulation

The model in this paper is govern by the ordinary differential equations which consist of four state variables:

(i) T , the tumor cells.

(ii) I_H , the CTL cells.

ISSN. 2087-2852
E-ISSN. 2338-1655

(iii) I_R, the helper T cells.

(iv) C, the dendritic cells.

The growth rate of tumor cell is assumed to grow logistically with the terms $r_1T(1-p_1T)$. The presence of active CTL cells in the body can eradicate the tumor cells which is represented by a term $-\alpha_1 T I_H$. In addition, to inhibit the development of tumor cells, a dendritic cell vaccination is given by a response of q_1, thus the rate of tumor cells killed by dendritic cell is denoted by -q_1CT.

The presence of helper T cells serves to stimulate CTLs by releasing an interleukin-2, thus forming an active CTL cell with the terms $\beta I_H I_R$. Active CTL cells have function to destroy or attack the presence of tumor cells in the body, they become inactive after interacting with tumor cells. Then the density of CTLs cells is reduced by a term $-\alpha_2 T I_H$. In addition, the density of CTL cells decrease because of the decay rate of active CTLs with the terms $-dI_H$.

The density of helper T cells is influenced by the growth of such cell that are assumed to grow logistically with the terms $r_2 I_R(1-p_2 I_R)$. Based on its function, the presence of helper T cells in the body can not attack and destroy tumor cells directly, but by stimulating CTLs cells into active CTLs cells causing a reduction in helper T cell density with term $-\beta I_H I_R$. The presence of dendritic cell vaccination may affect helper T cells resulting in an increase in helper T cell density with the term $q_2 C I_R$.

Dendritic cells are a type of cell that can be used in the process of inhibiting tumor growth by providing vaccination of these cells to patients with the tumor. To impede the tumor growth, dendritic cell is injected to the body at time t which is denoted by $u(t)$. Furthermore, dendritic cells decay with the rate γ, so that their density is reduced by a term$-\gamma C$.

Based on the description above, we can obtain equation system for tumor growth model as follows.

$$\begin{aligned}
\frac{dT}{dt} &= r_1T(1-p_1T) - q_1CT - \alpha_1 T I_H,\\
\frac{dI_H}{dt} &= \beta I_H I_R - \alpha_2 T I_H - dI_H,\\
\frac{dI_R}{dt} &= r_2 I_R(1-p_2 I_R) - \beta I_H I_R + q_2 C I_R,\\
\frac{dC}{dt} &= u - \gamma C.
\end{aligned} \qquad (1)$$

Optimal Control Problems

The optimal control strategy used in the tumor growth model is a way to inhibit the development of tumor cell density. In this study, optimal control is performed by using dendritic cells as exterminators of tumors, thus in the system of equations (1) variable control with dendritic cells are denoted by $u(t)$. The optimal control problem on the tumor growth model is expressed by the following objective functional

$$J(u) = \int_0^{t_f} \left(T + \tfrac{1}{2}Au^2\right) dt,$$

where *A* represents the weight quantity of controlling dendritic cell vaccination. Next, we determine the optimal solution indicated by u^*, so that

$$J(u^*) = \min\{J(u) : u \in U\},$$

given that,

$$u = \{0 \le u \le 1, t \in [0,T]\}.$$

Before determining the optimal solution (u^*), Hamiltonian function is first established to obtain state equations, costate equations, and stationary conditions. The Hamiltonian function is obtained based on the objective functional and constraints on the system (1) which ere expressed in the form

$$\begin{aligned}
H &= f(t,\vec{x},u) + \sum_{i=1}^{4} \sigma_i(t) g_i(t,\vec{x},u),\\
&= T + \frac{1}{2}Au^2 + \sum_{i=1}^{4} \sigma_i(t)\, g_i(t,\vec{x},u),
\end{aligned}$$

Given that T is the number of tumor cells to be minimized, σ_i is costate variable, and g_i is the right-hand side of the system (1).

$$\begin{aligned}
H =& T + \frac{1}{2}Au^2 + \sigma_1(r_1T(1-p_1T) - q_1CT - \alpha_1 T I_H)\\
&+\sigma_2(\beta I_H I_R - \alpha_2 T I_H - dI_H) + \sigma_3(r_2 I_R(1-p_2 I_R)\\
&-\beta I_H I_R + q_2 C I_R) + \sigma_4(u - \gamma C).
\end{aligned}$$

Furthermore, based on Hamiltonian function then state equation can be obtained as follows.

State Equations

The state equation of the tumor growth model of the system (1) is derived from Hamiltonian function toward a system of the costate variable (1) with the following steps

$$\vec{x} = \frac{\partial H}{\partial \sigma_i} = g_i(t,\vec{x},u), \quad \text{given that} \quad i = 1,2,3,4$$

ISSN. 2087-2852
E-ISSN. 2338-1655

Thus, it is obtained

$$\frac{dT}{dt} = \frac{\partial H}{\partial \sigma_1} = r_1 T(1 - p_1 T) - q_1 CT - \alpha_1 T I_H,$$
$$\frac{dI_H}{dt} = \frac{\partial H}{\partial \sigma_2} = \beta I_H I_R - \alpha_2 T I_H - d I_H,$$
$$\frac{dI_R}{dt} = \frac{\partial H}{\partial \sigma_3} = r_2 I_R(1 - p_2 I_R) - \beta I_H I_R + q_2 C I_R,$$
$$\frac{dC}{dt} = \frac{\partial H}{\partial \sigma_4} = u - \gamma C.$$

with initial conditions $T(0) \geq 0$, $I_H(0) \geq 0$, $I_R(0) \geq 0$, $C(0) \geq 0$. Furthermore, the costate equation is obtained based on the Hamilton function and given as in the following sections.

Costate Equations

The costate equation model of tumor growth with dendritic cells as control is obtained by the completion stage as follows.

$$\frac{d\sigma_i}{dt} = -\frac{\partial H}{\partial x_i}, \quad \text{given that} \quad \partial x_i = T, I_H, I_R, C$$

Thus, we have

$$\frac{d\sigma_1}{dt} = -\frac{\partial H}{\partial T} = -(1 + r_1\sigma_1 - 2r_1 p_1 T\sigma_1 - \alpha_1 I_H \sigma_1 - q_1 C\sigma_1 - \alpha_2 I_H \sigma_2),$$
$$\frac{d\sigma_2}{dt} = -\frac{\partial H}{\partial I_H} = -(-\alpha_1 T\sigma_1 + \beta I_R \sigma_2 - \alpha_2 T\sigma_2 - d\sigma_2 - \beta I_R \sigma_3),$$
$$\frac{d\sigma_3}{dt} = -\frac{\partial H}{\partial I_R} = -(\beta I_H \sigma_2 + r_2\sigma_3 - 2r_2 p_2 I_R \sigma_3 - \beta I_H \sigma_3 + q_2 C\sigma_3),$$
$$\frac{d\sigma_4}{dt} = -\frac{\partial H}{\partial C} = -(-q_1 T\sigma_1 + q_2 I_R \sigma_3 - \gamma\sigma_4),$$

with transversality conditions

$$\sigma_1(T) = \sigma_2(T) = \sigma_3(T) = \sigma_4(T) = 0.$$

Stationer Conditions

In the optimal control problem of the tumor growth model, the stationary condition is obtained from the partial derivative of Hamiltonian function toward u, that is

$$\frac{\partial H}{\partial u} = 0,$$

Thus, we obtained

$$\frac{\partial H}{\partial u} = Au + \sigma_4,$$
$$Au + \sigma_4 = 0,$$
$$Au = -\sigma_4,$$
$$u = -\frac{\sigma_4}{A}.$$

Given that $0 \leq u \leq 1$, thus we get the equation as follows

$$u^* = \begin{cases} -\frac{\sigma_4}{A}, & \text{if } 0 \leq -\frac{\sigma_4}{A} \leq 1 \\ 0, & \text{if } -\frac{\sigma_4}{A} \leq 0 \\ 1, & \text{if } -\frac{\sigma_4}{A} \geq 1. \end{cases}$$

In compact notation,

$$u^* = \min\left\{\max\left\{0, -\frac{\sigma_4}{A}\right\}, 1\right\}.$$

Furthermore, the optimal system of tumor growth models is obtained by substituting u^* on the system of state and costate equation. Then, we obtained

$$\frac{dT}{dt} = r_1 T^*(1 - p_1 T^*) - q_1 C^* T^* - \alpha_1 T^* I_H^*,$$
$$\frac{dI_H}{dt} = \beta I_H^* I_R^* - \alpha_2 T^* I_H^* - d I_H^*,$$
$$\frac{dI_R}{dt} = r_2 I_R^*(1 - p_2 I_R^*) - \beta I_H^* I_R^* + q_2 C^* I_R^*,$$
$$\frac{dC}{dt} = u - \gamma C^*,$$
$$\frac{d\sigma_1}{dt} = -1 - r_1\sigma_1 + 2r_1 p_1 T^*\sigma_1 + \alpha_1 I_H^*\sigma_1 + q_1 C^*\sigma_1 + \alpha_2 I_H^*\sigma_2,$$
$$\frac{d\sigma_2}{dt} = \alpha_1 T^*\sigma_1 - \beta I_R^*\sigma_2 + \alpha_2 T^*\sigma_2 + d\sigma_2 + \beta I_R^*\sigma_3,$$
$$\frac{d\sigma_3}{dt} = -\beta I_H^*\sigma_2 - r_2\sigma_3 + 2r_2 p_2 I_R^*\sigma_3 + \beta I_H^*\sigma_3 - q_2 C\sigma_3,$$
$$\frac{d\sigma_4}{dt} = q_1 T^*\sigma_1 - q_2 I_R^*\sigma_3 + \gamma\sigma_4,$$

Numerical method and simulations

In this section, numerical simulations are conducted by using the initial value $(T, I_H, I_R, C) = (150, 50, 75, 35)$ and parameter values as in Table 1. Based on the graph of numerical simulation, we can easily know every alteration that happened to each subpopulation T, I_H, I_R, C toward time (t).

The graph of the solution in Figure 1. is shown by $u_{max} = 1$, the weight quantity $A = 0.5$, and parameter values as presented in Table 1.

Table 1. Paramer values for simulation

r_1	0.0544,
r_2	0.009,
p_1	0.002,
p_2	0.0003,
α_1	0.0005,
α_2	0.00008,
q_1	0.0008,
q_2	0.0004,
β	0.0005,
d	0.0412,
γ	0.01,

ISSN. 2087-2852
E-ISSN. 2338-1655

Based on the parameter values, it is obtained that the solution graph on the subpopulation of the tumor cells grow to the high number, however it decreases after the immunotherapy is applied. This result suggests that dendritic cells can be used to minimize tumor cell density. Also, the presence of dendritic cells provides a positive effect on the density of helper T cells that serve to stimulate CTL cells, in turn can eradicate the presence of a tumor cell. Increasing the response received by CTL cells are followed by increasing the active CTLs cell density (I_H). Thus, the function of active CTL cells in eradicating the tumor is more optimal (see Fig. 1).

Figure 2 shows the amount of dendritic cell as immunotherapy used in eliminating tumor cells for a given of time. Therapeutic control is provided at maximum value at 1 unit should administered since t = 0, until it begins to decrease at t ranges from 120 to reach zero when t = 200. This result states that no more immunotherapy is given.

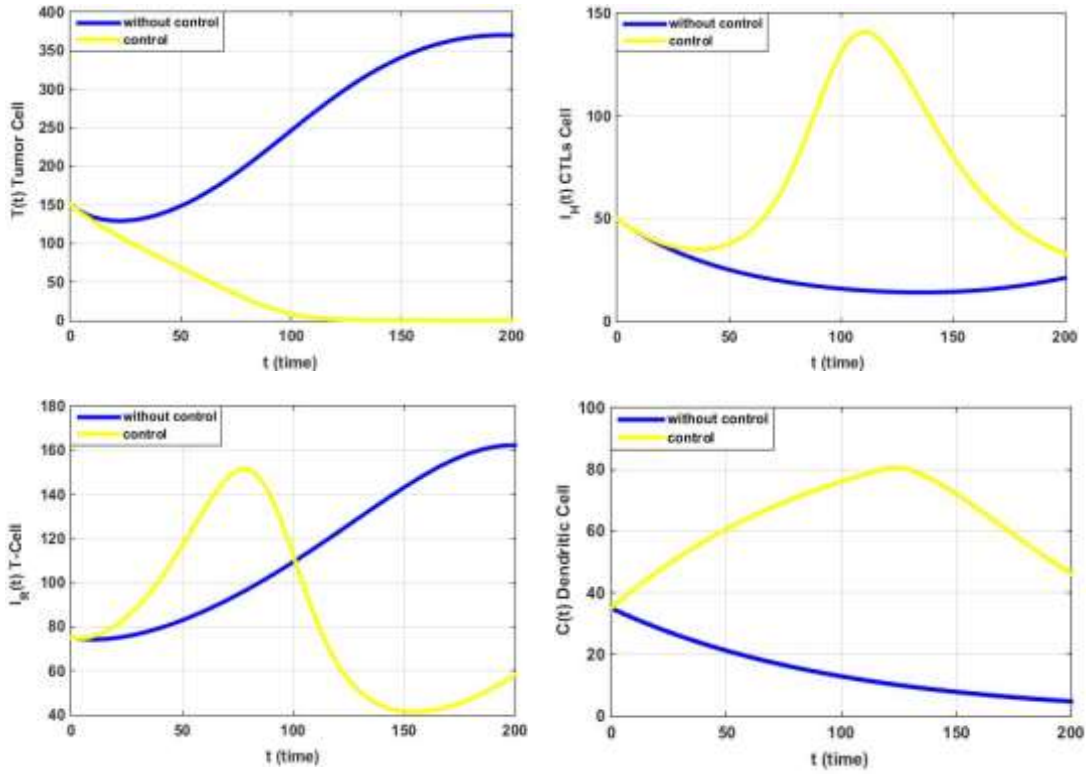

Figure 1. The evolution of subpopulation density T, I_H, I_R, C for $t \in [0,200]$

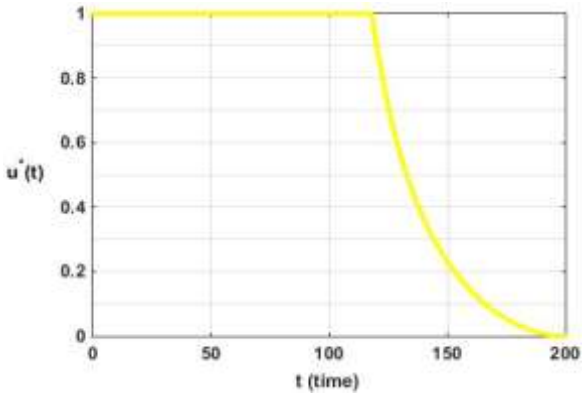

Figure 2. The control profile of immunotherapy, $u(t)$

ISSN. 2087-2852
E-ISSN. 2338-1655

CONCLUSION

In this paper, we have analyzed an optimal control of tumor growth model with immunotherapy. The effect of dendritic cells as immunotherapy is observed. Optimal system has been derived by using Pontryagin's principle to establish state, costate equation and stationary condition. The results of numerical simulations show that immunotherapy using dendritic cells is effective in reducing the number of tumor cell density. Thus it suggests that occupying dendritic cells as immunotherapy can be used as cancer treatment for the patient in the future.

REFERENCES

[1] Chalimah, I. N. 2017. Benign tumors and malignant tumors: What is the difference? Available at: http://schema.org/7806/.

[2] World Health Organization. 2017. Cancer. Available at: http://www.who.int/factsheets/fs297/en/.

[3] World Health Organization. 2010. Prevalence of Cancer in Indonesia and Worldwide. Hospital Management, Center for Health Policy and Management. Faculty of Medicine, Gadjah Mada University. Available at: http://www.manajemenrumahsakit.net.

[4] Palucka, K.U., H. Ueno, J. Fay, J. Banchereau. 2010. Dendritic cells and immunity against cancer. *J. Internal Med.* 269. 64-73.

[5] Bratawijaya, K.G. 2006. Basic immunology, 7th Ed. Medical Faculty, University of Indonesia. Jakarta.

[6] Malissen, B., E. Reinherz, R. Stanfield, I. Wilson. 2012. Chapter 3: the induced responses of innate immunity. In: Murphy, K. (Ed). Janeway's immunobiology 8th Ed. Garland Science Taylor and Paris Group. London and New York. 97-147.

[7] Kirschner, D., J.C. Panetta. 1998. Modeling immunotherapy of the tumor-immune interaction. *J. Math. Biol.* 37. 235-252.

[8] DePillis, L.G., A.E. Radunskaya. 2001. A mathematical tumor model with immune resistance and drug therapy; an optimal control approach. *J. Theor. Med.* 3(2). 79-100.

[9] DePillis, L.G., W. Gu, A.E. Radunskaya. 2006. Mixed immunotherapy and cemotherapy of tumors; modeling, application and biological interpretation. *J. Theor. Biol.* 208. 841-862.

[10] DePillis, L.G., A. Gallegos, A.E. Radunskaya. 2013. a model of dendritic cell therapy for melanoma. *Front. Oncol.* 3. 56.

[11] Ludewig, B.B., P. Krebs, T. Junt, H. Metters, J. Ford, R.M. Anderson. 2004. Determining control parameters for Dendritic Cell-Cytotoxic T Lymphocyte interaction. *Eur. J. Immunol.* 2407-2418.

[12] Trisilowati, S.W. McCue, D.G. Mallet. 2013. An optimal control model of dendritic cell treatment of a growing tumour. *ANZIAM Journal.* 54, (CTAC 2012), C664-C680.

[13] Sharma, S., G.P. Shamanta. 2013. Dynamical behavior of a tumor-immune system with chemotherapy and optimal control. *J. Nonlinear Dyn.* 13. 608598.

[14] Rangel-Reyes, J.C., J.C. Chimal-Eguia, E. Castillo-Montiel. 2017. Dendritic immunotherapy improvement for and optimal control murine model. *Comput. Math. Methods Med.* 9. 5291823.

[15] Munich, S., A. Sobo-Vujanovic, W.J. Buchser et al. 2012. Dendritic cell exesomes directly kill tumor cells and activate natural killer cells via TNF superfamily ligands. *OncoImmunology.* 1(7). 1074-1083.

[16] Hanke, N.D. Alizadeh, E. Katsanis, N. Larmonier. 2013. Dendritic cell tumor killing activity and its potential applications in cancer immunotherapy. *Crit. Rev. Immunol.* 33(1), 1-21.

[17] Sabado, R.L., N. Bhardwaj. 2013. Dendritic cell immunotherapy. *Ann. NY Acad. Sci.* 1284(1). 31-45.

[18] Lenhart, S., J.T. Workman. 2007. Optimal control applied to biological models. Taylor and Francis Group. New York.

ISSN. 2087-2852
E-ISSN. 2338-1655

Heavy Metal Copper (Cu) Distribution in Water and Its Bioaccumulation in Green Mussel (*Perna viridis*) in Coastal Area of Ujung Pangkah, Gresik District

Muhammad Qodri Fitra[1]*, Diana Arfiati[2], Bambang Semedi[2]

[1]Master Program of Aquaculture, Faculty of Fisheries and Marine Sciences, University of Brawijaya, Malang, Indonesia

[2]Faculty of Fisheries and Marine Sciences, University of Brawijaya, Malang, Indonesia

Abstract

Environmental pollution in the form of increased concentration of heavy metal Copper (Cu) becomes the main factor that can affect water quality and inhibit green mussel culture (*Perna viridis*) in Ujung Pangkah Coastal Area of Gresik District. The purpose of this research is to analyze concentration of heavy metal Copper (Cu) on water and its bioaccumulation in green mussel (*P. viridis*) in Ujung Pangkah waters, Gresik District. This research will be conducted from June to August 2017. The method used in this research is descriptive method. Sampling of seawater and mussel by purposive sampling. Cu heavy metal content in Ujung Pangkah waters, Gresik District has 0.003 – 0.006 ppm in July and 0.002 – 0.006 ppm in August. That value is still safe below predetermined quality standards. The results of heavy metal measurement test in shellfish has 0.159 to 0.69 ppm in July and 0.162 – 0.71 ppm in August. The high concentrations of Cu heavy metals in Ujung Pangkah waters are simultaneous to the bioaccumulation concentration in the green mussel. The higher concentration in the waters, the higher the bioaccumulation in the green mussels. And vice versa. The distribution of Cu heavy metal concentration at point 4 is the highest. While at point 1 has the lowest Cu heavy metal concentration.

Keywords: Copper, Bioaccumulation, Green Mussel, Heavy Metal, *Perna viridis*.

INTRODUCTION

The waters of Ujung Pangkah of Gresik District is the downstream of Bengawan Solo. So that the northern waters of Gresik District accommodate various types of compounds derived from industrial waste along the river and tributaries. Ujung Pangkah Coastal Area, Gresik District is a quite large producer of green shells (*Perna viridis*). Based on the data of fisherman catch from the Marine and Fisheries Office of Gresik [1], in 2013 obtained results in September reached 240 tons. However, contamination occurring in aquatic environments has become one of the main factors that may inhibit the survival of green mussels [2]. This type of shellfish is a typical type of organism that can accumulate heavy metals, and shells have low mobility. The adaptation, presence of heavy metals in the organism are thought to represent the existence of heavy metals contained in their habitat [3]. However, some study showed that the increased Cu concentration will decreasing the level of filtration of green mussels simultaneously [4], even mortality [5].

The dangers of heavy metal accumulation will not only affect the shells, but the organisms above the trophic level will also affect in humans where the effects of poisoning can be caused, among others, disruption of the kidney system, digestive gland or resulting in the fragility of the bone [6]. Heavy metals can cause special effects in living organisms, such as Minamata disease, cleft lip, nervous system damage, birth defects, carcinogenicity, and disruption of the immune function. Thus it can be said that all of the heavy metals can be toxic which will poison the living body when accumulated in the body for a long time [7].

There are some heavy metals that were found exceed the standard quality of one of the metal content of Copper (Cu), i.e. It reach 0.218 $mg.L^{-1}$ while quality standard [8] is equal to 0.02 $mg.L^{-1}$. Green mussel (*P. viridis*), which dominates the territorial waters of Ujung Pangkah, Gresik allegedly affected by heavy metal pollution. So it will also affect the levels of Copper (Cu) bioaccumulation in the body of green shells (*P. viridis*). This research is aimed to analyze the concentration of heavy metal Copper (Cu) on water and its bioaccumulation in green mussel

* Correspondence address:
Muhammad Qodri Fitra
Email : m.qodrifitra@gmail.com
Address : Faculty of Fisheries and Marine Sciences, University of Brawijaya, Veteran Malang, Malang 65145.

ISSN. 2087-2852
E-ISSN. 2338-1655

(*P. viridis*) in Ujung Pangkah waters, Gresik District.

MATERIALS AND METHODS

This research was conducted from June to August 2017 in Ngemboh Village, Ujung Pangkah Sub-district, Gresik District. We used descriptive method. Sampling of Heavy metal parameter data on water and green mussel was done by ex-situ.

Determination of Sampling Point

Sampling locations were determined based on difference of land use using Global Positioning System (GPS) as many as five sampling spot that showed at Figure 1. Sampling spot 1 located in an area near the Dalegan coast with coordinates 60 53' 57, 7" S and 1120 29' 45, 4" E. Sampling spot 2 located in a residential area with coordinate 60 53' 59, 5" S and 1120 30' 12, 8" E. Sampling spot 3 located in an industry area of shipbuilding and repair with coordinate 60 53' 20, 1" S and 1120 29' 42, 9" E. Sampling spot 4 located in near waste area of river ngimbo with coordinate 60 53' 16, 2" S and 1120 29' 49, 4" E. Sampling spot 5 located in near Bengawan Solo river estuary wint coordinate 60 53' 57, 1" S and 1120 29' 36, 0" E.

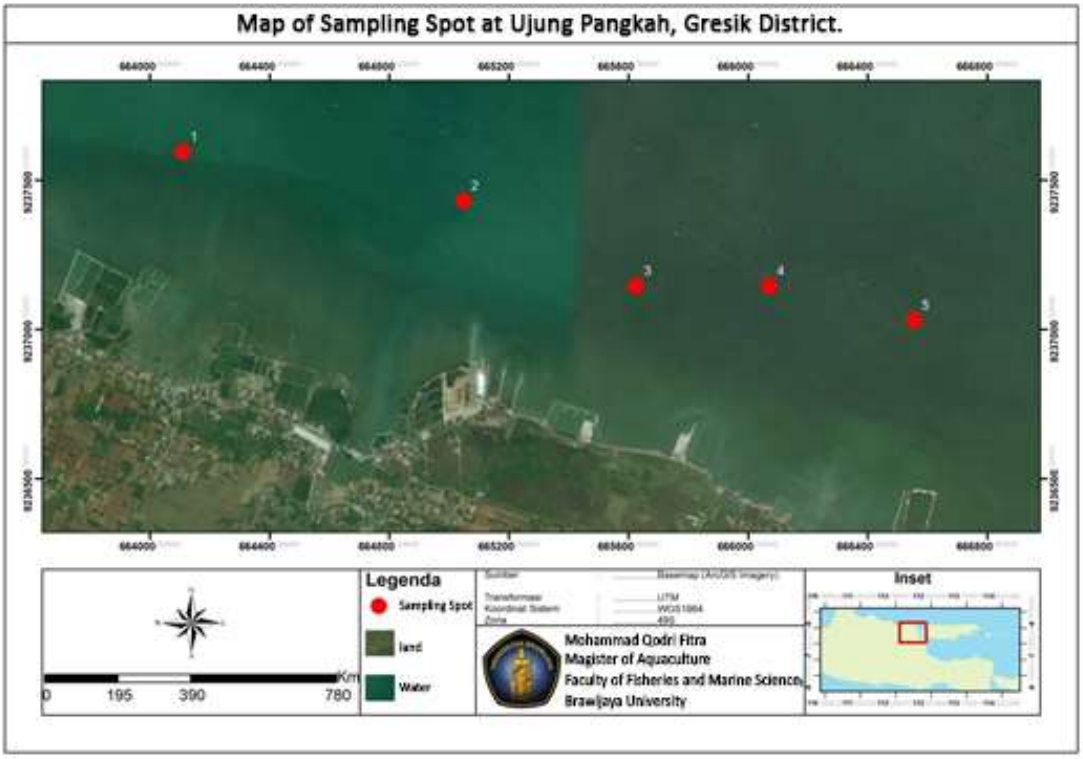

Figure 1. Sampling Spot at Ujung Pangkah, Gresik District

Sampling Procedure

Sampling was done by taking samples of sea-water and mussels (*P. viridis*) to determine the concentration level of heavy metal content Cu from each sampling point. It then used to determine the distribution of heavy metal content in Ujung Pangkah water.

Sampling Analysis

Measurement of sample in this research is done by two way, i.e. directly (*in situ*) in field and indirectly (*ex situ*) or analyzed in the laboratory. Physical and chemical parameters consist of temperature, DO, pH and salinity which will be used as research supporting data. Physical and chemical parameters of the waters are measured directly. Analysis of Cu heavy metals concentration in water and mussel samples was conducted in laboratory using Atom Absorbtion Spectrophotometer (AAS) method. The analysis was conducted in Laboratory of Chemistry, Department of Chemistry, University of Brawijaya.

RESULT AND DISCUSSION

Heavy Metal Cu Concentration on Water

The result of Cu level analysis at Ujung pangkah water location in July has the highest value at the sample point 3 and point of sample 4, while the Cu with the lowest value found at point 1. Cu content can be seen in Figure 2.

ISSN. 2087-2852
E-ISSN. 2338-1655

The high Cu content at sample point 3 and 4 is caused by the estuary of Bengawan Solo River and adjacent to the ship painting factory so that in this region, the value of Cu heavy metals is still below the standard quality threshold. The lowest Cu concentration at sample point 1 is due to the fact that it is far from factory activity and also the activity of the fisherman so that the Cu heavy metal content in this area is low.

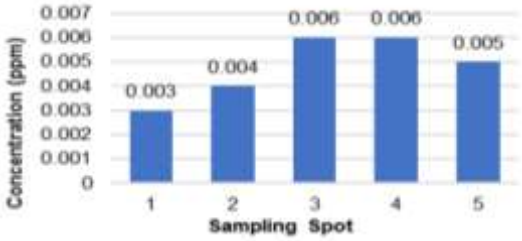

Figure 1. Concentration of Cu in Water on July 2017

The content of heavy metal Cu in Ujung Pangkah waters in August can be seen in Figure 3. The content of heavy metal Cu in waters with the highest value is at sample point 4 and lowest at sample point 1.

The highest value is at sample point 4, this is because it is adjacent to the activities of the ship repair factory and the surrounding fisherman activities. While the lowest heavy metal content of Cu at the sample point 1 due to the area far from the activities of fishermen and factory activities.

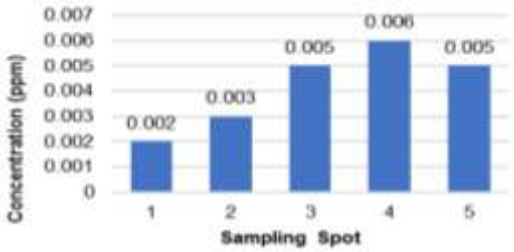

Figure 2. Concentration of Cu in Water on August 2017

Heavy metals entering the natural waters will become part of the water and sediment suspension system through the process of absorption, precipitation, and ion exchange [4]. At the sample points 3 and 4, high Cu values are thought to be caused by a number of community activities that produce Cu wastes. The main source of Cu heavy metals is the activities of fishing boats or ports, disposal of household waste and copper industry waste [9].

Distribution of Heavy Metal Copper (Cu)

Based on Figure 2, analysis of the distribution of Cu proceed to the analysis of Geographic Information Systems (GIS) so that the output obtained is made in the form of a map. The resulting map can be seen in Figure 4.

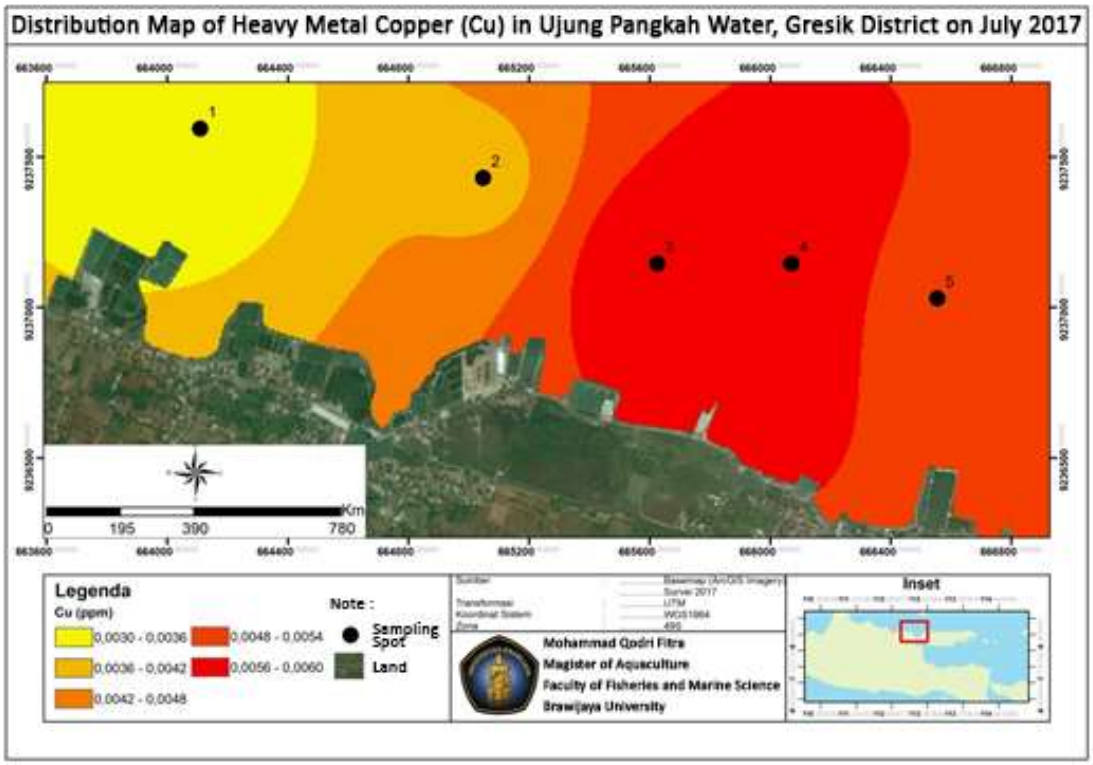

Figure 3. Distribution Map of Heavy Metal Copper (Cu) in Ujung Pangkah Water on July 2017

ISSN. 2087-2852
E-ISSN. 2338-1655

In the map, it can be seen that the distribution of Cu heavy metals in Ujung Pangkah waters, Gresik District in July the highest Cu content value is at the sample points 3 and 4. While the lowest Cu content is obtained at sample point 1.

From the data of heavy metals in the waters in Figure 3, we obtained a map of the results of heavy metal distribution that can be seen in Figure 5. The distribution of Cu heavy metal concentration at point 4 is the highest. At the sample points 3 and 5 are the points containing the second highest heavy metal contamination. While at point 1 has the lowest Cu heavy metal concentration compared to the other point.

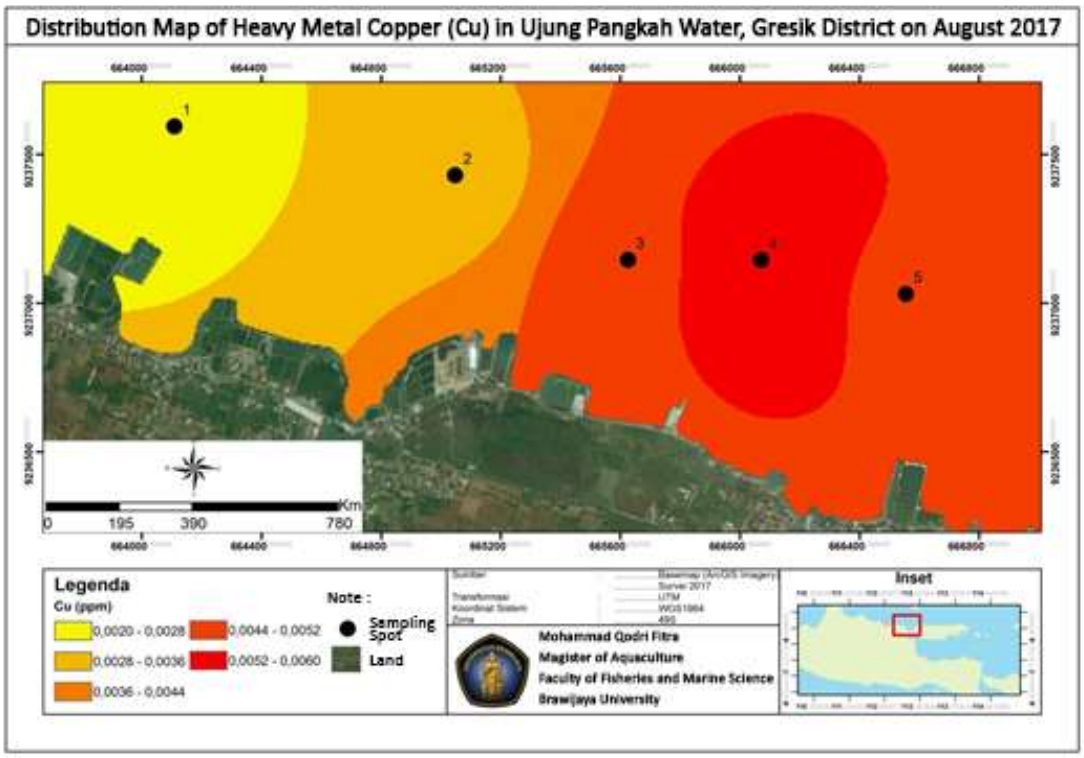

Figure 4. Distribution Map of Heavy Metal Copper (Cu) in Ujung Pangkah Water on August 2017

Heavy Metal Cu in Green mussel (*Perna viridis*)

Green mussel (*P. viridis*) is a filter feeder organism because of its ability to get food by filtering the water around the place of life. Bivalves are commonly used as test organism for heavy metal content due to its filterer and sedentary filter. The concentration data of Cu heavy metals on green mussel in July can be seen in Figure 6 and August in Figure 7.

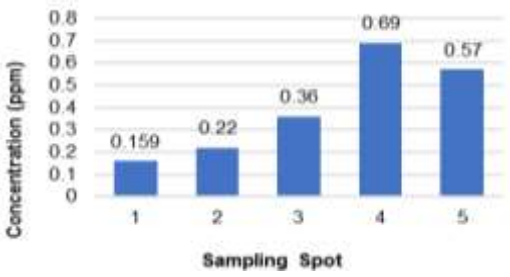

Figure 5. Heavy metal Cu in Green Mussel (*P. viridis*) on July 2017

Based on the graph above, the heavy metal content of Cu in green mussel in July ranged from 0.159 ppm - 0.69 ppm where the highest value of the content obtained at the sample point 4. This is because the location at the point of sample 4 adjacent to the activity of the plant and river estuary Bengawan Solo so the level of pollution is higher. While the lowest value is at the point of sample 1 where the location is far from the activities of fishermen and industrial activities.

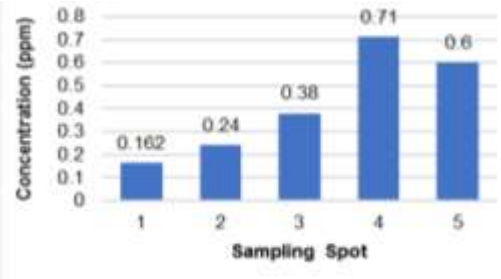

Figure 6. Heavy Metal Cu in Green Mussel (*P. viridis*) on August 2017

The content of Cu heavy metals in green shells in August ranged from 0.162 ppm - 0.71 ppm with the highest value being at sample point

ISSN. 2087-2852
E-ISSN. 2338-1655

4. This is the same as the graph in July that the highest value of Cu heavy metal on green shells is also at the sample point 4. While the lowest Cu value in the waters is at the point of sample 1 where July is also the lowest value obtained at sample point 1.

Heavy metals that enter into the waters can be accumulated by the animal body one of them bivalves [6]. The concentration value of Cu heavy metal in green shells is proportional to Cu concentration in the waters at the same point. This means that the accumulation of heavy metal Cu in the waters will affect the level of accumulation in the body of green kerrang. The higher Cu content in the waters then the Cu levels in the body kerrang will also increase and vice versa. Heavy metals in seashells other than from sea water also come from food then undergo biomagnification [7].

Correlation Analysis

The content of heavy metals in green shells (*P. viridis*) is relatively higher when compared with heavy metal content in the waters. The result of Pearson correlation analysis show perfect correlation (Table 1).

Table 1. Correlation analysis of metallothionein (MT) on Water and Mussel in July 2017

		MTMussel	MTWater
MTMussel	Pearson Correlation	1	.772
	Sig. (2-tailed)		.126
	N	5	5
MTWater	Pearson Correlation	.772	1
	Sig. (2-tailed)	.126	
	N	5	5

Table 2. Correlation analysis of metallothionein (MT) on Water and Mussel in August 2017

		MTMussel	MTWater
MTMussel	Pearson Correlation	1	.926*
	Sig. (2-tailed)		.024
	N	5	5
MTWater	Pearson Correlation	.926*	1
	Sig. (2-tailed)	.024	
	N	5	5

This indicates that the rate of accumulation of green shells against heavy metals is quite high. Heavy metals entering the aquatic environment will undergo precipitation and then be absorbed by the shells present in the waters. Shellfish is one of the most efficient biota in accumulating heavy metals [9]. This is because the shells that live in the waters move very slowly, and the food is a detritus, so the chances of entering heavy metals into the body is very large. Heavy metal concentrations are high in water, there is a tendency for heavy metals concentrations to be high in the sediments, and the accumulation of heavy metals in demersal animal bodies is also higher [10].

CONCLUSION

The high concentrations of Cu heavy metals in the Ujung Pangkah waters are directly proportional to the bioaccumulation concentration of Cu in the green mussel. The higher concentration in the waters, the higher the bioaccumulation in the green kerrang, and vice versa. The distribution of Cu heavy metal concentration at point 4 is the highest. While at point 1 has the lowest Cu heavy metal concentration.

REFERENCES

[1] Office of Marine and Fisheries Gresik Regency. 2013. Produksi perikanan laut kerang hijau tahun 2011-2012. Office of Marine and Fisheries Gresik District. Gresik.

[2] Cappenberg, H.A.W. 2006. Pengamatan komunitas moluska di perairan Kepulauan Derawan, Kalimantan Timur. *Oseonologi dan Limnologi di Indonesia.* 39.

[3] Rijalinoor. 2003. Studi kandungan logam berat Pb di saluran Kenjeran dan kerang di muara saluran. *Info Teknik.* 4(1). 34-43.

[4] Suryono, C.A. 2006. Kecepatan filtrasi kerang hijau *Perna viridis* terhadap *Skeletonema* sp pada media tercemar logam berat timbal (Pb) dan tembaga (Cu). *Ilmu Kelautan.* 11(3). 153-157.

[5] Sze, P. W. C., S.Y. Lee. 2000. Effects of chronic copper exposure on the green mussel *Perna viridis*. *Mar. Biol.* 137(3). 379-392.

[6] Matagi, S.V., D. Swai, R. Mugabe. 1998. Heavy metal removal mechnisms in wetlands. *Afr. J. Trop. Hidrobiol. Fish.* 8. 23-35.

[7] Liu, L., L. Fasheng, D. Xiong. 2006, Heavy metals contamination and their distribution in different size practions of the surficial sediment of Hathe River, China. *Environ. Geol.* 50. 431-438.

[8] Government Regulation of the Republic of Indonesia. 2001. No.82 about management

ISSN. 2087-2852
E-ISSN. 2338-1655

of water quality and control on water pollution. Republic of Indonesia. Jakarta.

[9] Juniawan, A., B. Rumhayati, B. Ismuyanto. 2013. Karakteristik Lumpur Lapindo dan fluktuasi logam berat Pb dan Cu pada Sungai Porong dan Aloo. *Sains Terapan.* 7(1). 50-59.

[10] Ramakritinan, C.M., C. Rathisri, A.K. Kumaraguru. 2012. Acute toxicity of metals: Cu, Pb, Cd, Hg and Zn on marine molluscs, *Cerithedia Cingulata* G., and *Modiolus Philippinarum* H. *Indian J. Geo-Marine Sci.* 41(2). 141-145.

ISSN. 2087-2852
E-ISSN. 2338-1655

Patellar Giant-Cell Tumor: a Case Report

Istan Irmansyah Irsan[1,2], Satria Pandu Persada Isma[1,2], Rakhmad Aditya Hernawan[1,2*]

[1]Department of Orthopaedic and Traumatology, Faculty of Medicine, University of Brawijaya, Malang, Indonesia
[2]Saiful Anwar Hospital, Malang, Indonesia

Abstract

Giant cell tumor (GCT) found mostly in the long bones metaphysis or epiphysis. GCT usually occur between the ages of a third and fourth decade and locally aggressive. Giant-Cell Tumor seldom affects the patella. Multicentric forms rarely reported. A fourteen-year-old female with a lump at her left patella since one-year associated with slight pain that aggravated by activity for six months. Plain X-ray left knee AP, and lateral views reveal expansile lytic lesion in left patella with thinning of the anteroinferior cortex and sclerotic septa within. MRI of left knee shows approximately 3x2x2 cm heterogeneous lobulated expansile soft tissue mass in left patella extending up to the patellofemoral joint with fluid-fluid appearance. From fine needle aspiration cytology, resulting giant-cell tumor with the differential diagnosis of an aneurysmal bone cyst. The operation already performed. Curettage, bone graft, and a biopsy taken. An immunocytochemical smear was performed and confirmed as a patellar giant-cell tumor. Six months after excision of the tumor, the patient complained no arthralgia and have a full range of motion for the knee.

Keywords: Giant-cell tumor, knee lump, knee pain, patella.

INTRODUCTION

Many cases of giant cell tumor (GCT) found in long bones metaphysis or epiphysis. GCT usually occur between the ages of a third and fourth decade, it is locally aggressive but also has metastatic potential [1,2]. This lesion most often located around the knee joint, originates at the epiphysis, spreads to the metaphysis and makes the cortex erode in 25% of the cases. Ten percent of these tumors have a malignant course [3]. The reported incidence of patellar GCT was less than one percent [4]. This article reported a left patellar GCT which diagnosed on fine needle aspiration cytology, magnetic resonance imaging and already performed excision, curettage, and bone cement.

CASE REPORT

A fourteen-year-old female at Malang, East Java, presented with a lump since one-year that grows progressively at her left patella associated with slight pain that has aggravated with activity for six months. It measured 42 cm in its diameters with a normal skin surface. There are no pulmonary and other systemic symptoms. The other laboratory result was within limits.

The patient underwent plain left anteroposterior (AP) and lateral views knee x-ray. Radiograph reveal expansive lytic lesion in left patella with sclerotic septa within and thinning of the anteroinferior cortex (Fig. 1).

Figure 1. The lateral and anteroposterior plain x-ray shows expansive lytic lesion in the left patella

The patient underwent MRI of the left knee. T_1 and T_2 weighted images obtained in sagittal and axial planes (Fig. 2 and 3). MRI of left knee shows approximately 3x2x2 cm heterogeneous lobulated expansive soft tissue lump in left patella extending up to the articular surface, and a fluid-fluid level observed. The possible differential diagnosis from MRI includes the giant-cell tumor or an aneurysmal bone cyst. Luckily, the articular cartilage at the posterosuperior part is still intact.

For diagnosis confirmation, fine needle aspiration performed at the patellar antero-inferior portion. Histopathological finding still cannot differentiate whether this is the giant-cell tumor or an aneurysmal bone cyst although

* Correspondence address:
Rakhmad Aditya Hernawan
Email : aditflea@gmail.com
Address : Dept. Orthopaedic & Traumatology, Faculty of Medicine, University of Brawijaya, Veteran Malang, Malang 65145.

multi-nucleated giant cell was already found (Fig. 4).

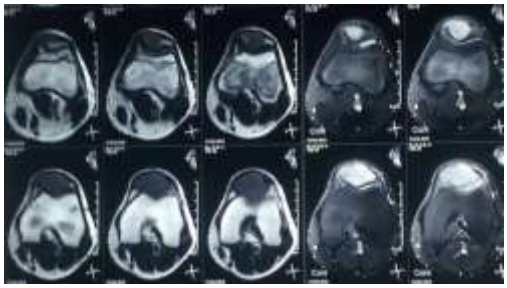

Figure 2. T_1 and T_2 axial MRI show defect in an anteroinferior aspect of the patella

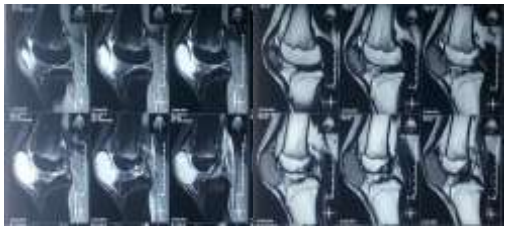

Figure 3. Sagittal T_1 and T_2 MRI show a fluid-fluid level

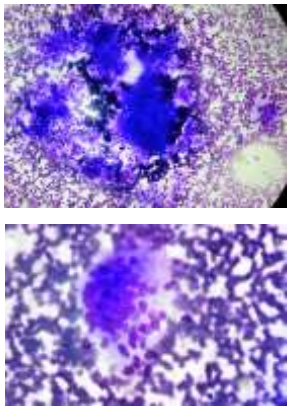

Figure 4. Multi-nucleated giant cell from fine needle aspiration

We performed lesion curettage and bone substitution with general anesthesia. These procedures performed through the longitudinal incision at approximately 10 cm above the area. The incision was made with an oval shape, the periosteum was detached with a raspatory from the patellar surface. From appearance, the tumor was solid, yellow-brown coloring with small blood retention (Fig. 5). The tumor macroscopically looks like a GCT. We curetted the contents carefully and filled approximately 5 g of calcium hydroxy-apatite ceramic to the defect and fixed it with two screws. Plain radiograph of the left knee anteroposterior (AP) and lateral views post-surgery taken to confirm the bone substitution component fills in the defect (Fig. 6).

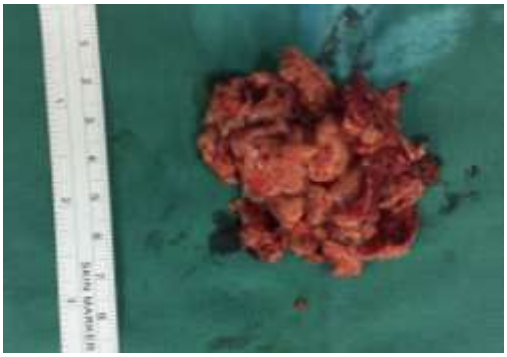

Figure 5. Macroscopically of the tumors, solid and yellow-brown coloring with small blood retention

Figure 6. Post surgery AP and lateral left knee plain x-ray

Histopathological examination was performed after the surgery and showed multi-nucleated giant cell with more than 20 nuclei, spindle-shaped short cells, calcification and bone tissues with few mitotic figures and no cellular atypia observed. By this findings, the lesion diagnosed as a GCT instead of an aneurysmal bone cyst (Fig. 7). Immunohistochemical was performed to confirm the diagnosis and found a positive result in CD68 staining (Fig. 8). The left patellar giant-cell tumor confirmed.

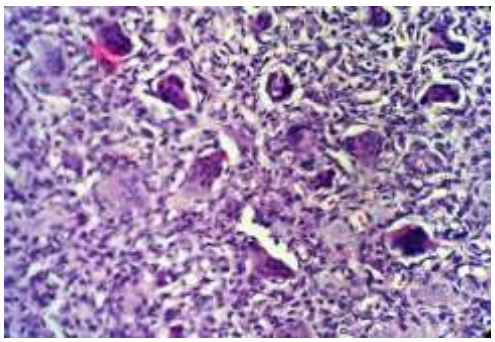

Figure 7. Histopathological examination shows multi-nucleated giant cell with more than 20 nuclei, spindle-shaped short cells, calcification and bone tissues

ISSN. 2087-2852
E-ISSN. 2338-1655

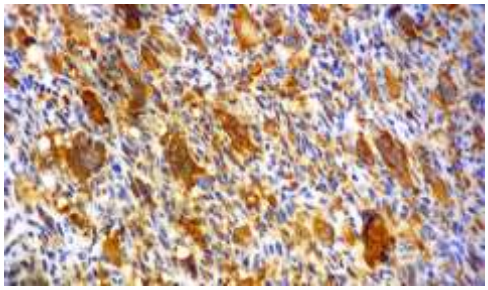

Figure 8. The immunohistochemical show positive result of CD68 staining

The knee was then protected with a splint for two weeks after the operation. One week after the surgery the suture was removed and then the patient begins to a range of motion and weight-bearing exercise. Full weight-bearing allowed four weeks after the surgery. The patient regains a full motion six months after surgery and has no arthralgia of the knee.

DISCUSSION

Bone tumors seldom affected the patella. A survey held by the Japanese Orthopedic Association, 403 primary bone tumor cases were reported from 1972 to 2003. Most of these cases, 70.5% involving the lower extremities [1]. However, tumors affected the patella were only 0.5% (75) of all cases. Of these, 71 were benign bone tumors, that is 22 was diagnosed with GCT, 14 was solitary exostosis, and 24 was chondroblastoma. The patellar GCT reported in the international literature was only less than 50 cases worldwide [2].

Clinically, the patients with patellar GCT usually complained about lump and pain at the knee [3-7]. From the inspection, we found lump, redness, swelling, and effusion. From the palpation, we found local heat, tenderness, and crepitus. An attempt to move the affected part shows the decrease of motion range [3-7]. The laboratory results in severe cases showed a serum alkaline phosphatase (ALP) increasing and also erythrocyte sedimentation rate (ESR) [8].

Radiographs showed an osteolytic lesion, destruction of the bone, and sometimes, soap bubble appearance [3]. Magnetic resonance imaging (MRI) showed expansive soft tissue mass of the patella, and also some evidence of adjacent tissues and sclerotin [8]. On GCT patient, the chest x-ray is necessary to determine a possibility of lung metastasis and also bone scintigraphy for metastasis on other bones.

A fine needle or incisional biopsy are recommended to establish the diagnosis. Microscopically, GCT featuring multinucleated giant cells, a few mitotic spindle-shaped short cells, and bone tissue calcification should be distinguished from a chondroblastoma or an aneurysmal bone cyst. An aggressive GCT histologically showed a nuclear atypia with compact stroma, hyperchromatic, frequent mitotic figures, and the unevenly distributed giant cells [7].

Curettage that combines with cryosurgery may be the choice in the early stage of patellar GCT with the risk of recurrence about 35% [10]. For Enneking stage 2 GCT, the therapy should be partial patellectomy or curettage intralesional with bone substitution and extensor mechanism reconstruction is the first choice in the management of patellar GCT. But for Enneking stage 2 to 3 GCT, patellectomy combined with adjuvant treatment for metastasis is recommended [8]. In the advanced cases, only treatment left that offers best functional results is resection [2]. Novel treatment includes using osteoarticular grafts for reconstruction after patellar resection in advanced cases may be a feasible option [10].

CONCLUSION

Patellar GCT can be mistaken for other tumors of soft tissues and bone. Fine needle or biopsy would be diagnostic if an adequate specimen is obtained and canal so confirms with immunohistochemical staining. In the early stage, curettage accompanied with bone substitution and cryosurgery may be attempted, and patellectomy for the late stage. For future reconstruction procedure, osteoarticular grafts can be used after resection that may be a feasible option for the advanced cases.

REFERENCES

[1] Singh, V.P., N. Kannan, H.G. Mukhopadhyay, S. Mukherjee, R. Lakhtakia. 1996. Giant cell tumor of bone: an unusual metastatic pattern. *Med. J. Armed Forces India*. 52(4). 260-262

[2] Paudel, S., P. Kayastha, P. Pokhrel, A. Shah, R.K. Ghimire, M.A. Ansari. 2012. Giant cell tumor of patella. *J. Inst. Med.* 34. 58-60.

[3] Hutagalung, E.U., S. Gumay, B. Budiatmoka 2005. Neoplasma tulang: diagnosis dan terapi. Galaxy Puspa Mega. Bekasi. 41-43.

[4] Yoshida, Y., T. Kojima, M. Taniguchi, S. Osaka, Y. Tokuhashi. 2012. Giant-cell tumor of the patella. *Acta Med. Okayama.* 66. 73-76.

[5] Ofluoglu, O., R. Donthineni. 2007. Iatrogenic seeding of a giant cell tumor of

ISSN. 2087-2852
E-ISSN. 2338-1655

the patella to the proximal tibia. *Clin. Orthop. Relat. Res.* 465. 260-264.

[6] Malhotra, R., L. Sharma, V. Kumar, A.R. Nataraj. 2010. Giant cell tumor of the patella and its management using a patella, patellar tendon, and tibial tubercle allograft. *Knee Surg. Sports Traumatol. Arthrosc.* 18. 167-169.

[7] Chakravarty, U., G. Chakraverty. 2009. Late presentation of GCT of the patella*. Int. J. Orthop. Surg.* 12-13.

[8] Song, M., Z. Zhang, Y. Wu, K. Ma, M. Lu. 2015. Primary tumors of the patella. *World J. Surg. Oncol.* 13. 163.

[9] Christopher, D. 2002. Pathology and genetics of tumours of soft tissue and bone. International Agency for Research on Cancer. France. 309-312.

[10] Carnevale, P.G. 1987. Sometimes malignant tumors of bone, in Campbell's operative orthopedics, 7th Ed. St. Louis. Mosby. 765-805.

ISSN. 2087-2852
E-ISSN. 2338-1655

Rosella Flower Extract Prevent Increasing of Interleukin-6 and Amyloid-β Levels in Brain Tissue of Heated Diet-Treated Rats

Ardhiyanti P. Ratna[1,2*], Setyawati Soeharto[3], Edi Widjajanto[4], Silvy A. Falyani[1], Pia B. Batmomolin[1]

[1]Master Program in Biomedical Sciences, Faculty of Medicine, University of Brawijaya, Malang, Indonesia
[2]Laboratory of Histology, Faculty of Medicine, Al Azhar Islamic University, Mataram, Indonesia
[3]Laboratory of Pharmacology, Faculty of Medicine, University of Brawijaya, Malang, Indonesia
[4]Laboratory of Clinical Pathology, Faculty of Medicine, University of Brawijaya, Malang, Indonesia

Abstract

Heated food is a source form of various types Advanced Glycation Endproducts (AGEs). One of which is N-carboxymethyl-lysine (CML) that is often used as a sign of the formation of AGEs in the diet. The accumulation of AGEs in the brain can trigger neurodegenerative conditions. It also accelerates the accumulation of Amyloid β and proinflammatory cytokines which exacerbate neurodegeneration. *Hibiscus sabdariffa* L or rosella known to have antiglication, antioxidant, and anti-inflammatory effects. This study aims to prove the effect of food heating to the increasing levels of CML serum and evaluate the effects of daily intake of Rosella extract IL-6 levels and Amyloid β in the Wistar rats' brain given a diet high of AGEs. This experimental study with post test only control group design was conducted using 25 white male rats Wistar strain (*Rattus novergicus*) which were divided into 5 groups namely positive control, negative control, the treatment group with rosella dose 200 mg.kgBW^{-1}, 300 mg.kgBW^{-1}, and 400 mg.kgBW^{-1}. The high diets of AGEs are given for 12 weeks, and it was added to the rosella extract with various doses on the 9th to 12th weeks. The examination of CML serum level, interleukin 6 brain level, and Amyloid β of the brain was carried by ELISA. This study found differences between CML serum level of rats which fed a standard diet and the one that was given a heated diet (p= 0.0001). It also found that rosella flower extract can prevent the increasing levels of interleukin 6 and Amyloid β in the brain tissue of rats which were given a heated diet, and both effective doses were on 200 mg.kgBW^{-1}.

Keywords: Advanced Glycation End products, Amyloid β, Interleukin 6, N-carboxymethyl-lysine, Rosella.

INTRODUCTION

Over the last few decades, the consumption of highly processed foods and the ones that contain high sugar and fat has increased dramatically [1]. Changes in diet patterns have resulted in the increased of *Advanced Glycation Endproducts* (AGEs) which is formed in foods during a warm-up process. AGEs is a Maillard reaction product, where the component of sugars in food react with proteins, causing cross-reaction protein, and produce a brownish color with the formation of flavor and aroma components. Various forms of AGEs were produced during the process of heating food [2]. One of which is N-carboxymethyl-lysine (CML) that is often used as a sign of the formation of AGEs in the diet [3].

In the decade of the 80s, Monnier and Cerami, the pioneer in aging process with the theory of glycosylated non-enzymatic, revealed the presence of crosslinks between the long-lived protein, which is mediated by AGEs, that led to a decrease in the function of cells and tissues inthe natural aging process [4]. The role of AGEs in the aging process in the brain or neurodegenerative first revealed in the mid-1990s [5]. Distribution of AGEs are also found in various compartments and parts of the human brain and led to allegations of links between AGEs with neurodegenerative disorders [6].

In the brain, AGEs can disrupt neuronal cells through the formation of covalent bonds directly with the substrate. AGEs extracellular can affect the neurons through its surface receptor namely RAGE. RAGE is a member of the immunoglobulin superfamily that can bind to a large group of ligands such as AGEs and amyloid β (Aβ) [7]. The interaction of the ligand-receptor activates signal transduction pathways that are mediated by receptors and affected the cell function [6].

The accumulation of AGEs will also accelerate the accumulation of Aβ [7]. A study also showed there is an activation of the pathway of mitogen-activated kinase protein (MAPK) in response to

* Correspondence address:
Ardhiyanti Puspita Ratna
Email : ardhiyanti.pr@gmail.com
Address : Biomedical Program, Faculty of Medicine, University of Brawijaya, Veteran Malang, Malang 65145.

the Aβ fibrils in the aftermath of inflammatory signals of kinase-dependent tyrosine on microglia. Microglial cells exposed to Aβ will secrete inflammatory mediators, one is interleukin 6 [8]. Therefore, AGEs known to play an important role in the development of neurodegenerative diseases [7]. The biggest problem posed by the effects of neurodegenerative disorders is very damaging, but until now, its success rate of treatment is low [9].

Over the past few years, the derived flavonoids have been found helpful in the treatment of neurodegenerative diseases [10]. Flavonoid is a component of polyphenols found in plant food and is divided into six groups: flavonols, flavones, isoflavones, flavanones, flavanols, and anthocyanins [11].

Anthocyanin is a polyphenol in the group of flavonoids that are known as antioxidants [12]. Anthocyanins inhibit glycation and scavenging activity against DPPH and anion superoxide. Anthocyanin resistance mechanism against glycation occurs through barriers against auto-oxidation of monosaccharides [13]. Anthocyanin also hinder the process of glycation and AGEs binding to its receptor as well as the prevention of lipid peroxidation and inhibition of *polyol pathway* [14].

Hibiscus sabdariffa L. known as Rosella is known to contain phenolic acid compounds such as hibiscus acid and anthocyanins as delphinidin-3-sambubioside and cyanidin-3-sambubioside [13]. Research conducted by Peng et al. in 2011 found that Rosella was also able to reduce lipid peroxidation in mouse models of diabetes [15]. Later, research carried by Ademiluyi et al. in 2013 found an anthocyanin content of 121.5 mg.100g^{-1} Rosella [14]. This study aims to prove the effect of heated food on elevated levels of CML and determine the effect of daily intake Rosella extract on the levels of IL-6 and Amyloid β in wistar rats' brain which given a heated diet.

MATERIAL AND METHOD

Subject

This research was experimental study, using post test-only control group design. The animals that were used were white male rats (*Rattus norvegicus*) Wistar strain, 10-12 weeks of age with 150-180 grams baseline weight. The animals obtained from the Laboratory of Animal Physiology, Faculty of Science and Technology, Maulana Malik Ibrahim State Islamic University Malang. There were 25 animals as samples which were calculated based on the Federer formula. The whole animal was treated in accordance with the provisions of the Helsinki Convention. Ethical Clearance was obtained from the Research Ethics Committee of Health Research Ethics Faculty of Medicine, the University of Brawijaya, issued number 278/EC/KEPK/ 07/2016.

The rats were placed in the individual cages with an area of 500m^2 in a well-ventilated room and sufficient lighting, where the light-dark cycle was set every 12 hours. Its room temperature ranged from 20-26°C. The cages were cleaned regularly and the husks were replaced every day. After the rats were adapted for one week in a research environment, it then divided into five groups with 5 rats each group that was selected randomly. The negative control group (KN) was given a standard diet BR1 (21-23% protein, 5% fat, 40-45% starch, 5% crude fiber) which was not heated. Positive control group (KP) were given a high AGEs diet, such as BR1's feeds which was heated using an oven with the temperature of 150^{o}C for 15 minutes. R_1 was a group of rats fed a high AGEs diet and rosella flower extract ethanol at a dose of 200 mg.kgBW^{-1}. R_2 was a group of rats fed a high AGEs diet and ethanol extracts of rosella a dose of 300 mg.kgBW^{-1}. R_3 was a group of rats fed a high AGEs diet and extract ethanol of rosella flower at a dose of 400 mg.kgBW^{-1}. The Rosella was obtained from Materia Medika Hall Batu City.

During the first 8 weeks, KP, R_1, R_2 and R_3 groups were given BR1 heated feed diet only, while KN was fed by BR1 which was not heated. Next, in the 9th week, the levels of *N-Carboxymethyl-lysine* (CML) serum in all groups was measured. Then, the KN group was fed by not heated BR1 diet, while the R_1, R_2, R_3 groups were fed BR1 heated and ethanol extract of rosella various doses orally, and the KP group was only fed by BR1 heated only. The treatment was held for 4 weeks.

At the 13th week, the rats were fasted for 8 hours, then terminated by cervical dislocation method. Next, the organ removal was done from the brain directly. Surgery was performed in the cranial area that is on the skull, the brain was separated and the third medial or part of the cerebrum was taken. Then, the brain tissue was put in a pot filled with Phosphate Buffer saline-azide (PBS-azide) pH 7.4.

Data Collection

After 8 weeks feeding of a high AGEs diet, then the levels of *N-Carboxymethyl-lysine* (CML)

ISSN. 2087-2852
E-ISSN. 2338-1655

serum in all groups was measured at the 9th week. Measurement of serum CML aimed to examine the differences between each group and to ensure increasing of CML serum level before starting treatment with an extract of rosella. At the 9th week, the rat's blood was taken through the medial canthus orbita using a hematocrit micropipette. Blood was collected in 2 mL tube. Furthermore, it was centrifuged at 3000 rpm for 20 minutes. Next, take the supernatant and perform protocol conformance checks CML ELISA Kit (BT Laboratory catalog no.E1374Ra). Rats that had taken blood was returned to the cage and continued its research procedures.

The measurement of interleukin 6 (Il-6) and amyloid β of the brain tissue were performed using ELISA method. After the rats were terminated at week 13th and the brain was taken, then was examined for levels of Interleukin 6 and amyloid β in the tissue. Sample preparation was done by taking 0.5 gram of brain tissue then ground it up, then added with 300 μL mixture PIC and RIPA buffer solution, then the mixture is homogenized by vortex and incubated at 37°C for 10 minutes, and the supernatant was taken. The supernatant was obtained to examine levels of interleukin 6 according to the protocol of ELISA Kit IL-6 (BT Laboratory catalog no.E0135Ra) and the protocol ELISA Kit Aβ (BT Laboratory catalog no.E0093Ra).

Data analysis

Data were analyzed statistically. Data normality was tested by the Shapiro-Wilk test. Homogeneity of data was tested by Levene's test. CML levels to compare the differences between the groups fed standard diet and high AGEs diet conducted independent t-test. Effect of Rosella extract on levels of IL6 and β Amyloid in the brain was tested by ANOVA followed by Tukey HSD Post Hoc test. The significance level used more than 95% (p-value <0.05).

RESULT AND DISCUSSION

Levels of serum CML

The measurements of serum levels of CML in mice fed with standard diet and the group fed high AGEs diet showed that serum levels of CML in the group fed with heated diet are higher than those fed standards. The average serum levels of CML in the group fed which was heated by 159 ± 8.23 ng.mL^{-1}, whereas in the standard feed group 51.6 ± 33.66 ng.mL^{-1}, as shown in Figure 1. In the independent t-test obtained by value t-count -6930 with p-value 0.001. A P-value less than 0.05 (P <0.05) shows that there are significant differences between the CML levels of rats that were fed with oven-heated diet and the non-heated diet. So there is an increased level of serum CML of rats that given oven heated diet.

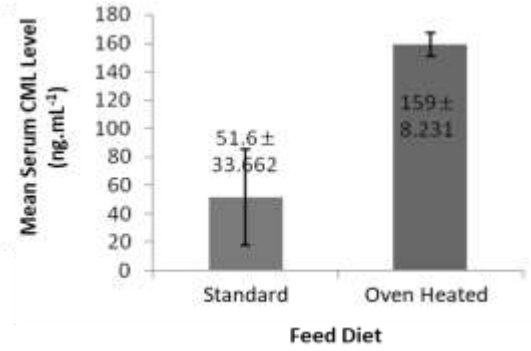

Figure 1. The Mean of CML serum levels
Description: Standard is group that given non heated BR-1 diet, oven heated is group that given oven heated BR-1 diet

Brain tissue levels of Interleukin 6

Measurements result of interleukin 6 levels in rat brain tissue showed that KP group is higher than other groups, while the R3 group showed the lowest results. The average levels of interleukin 6 from each group is KN 2.21 ± 3.602 ng.mL^{-1}, KP 14.8 ± 7.08 ng.mL^{-1}, R_1 4.014 ± 0.513 ng.mL^{-1}, R_2 2.402 ± 0.763 ng.mL^{-1} and R3 2.002 ± 0.639 ng.mL^{-1}. Overview of Mean interleukin 6 levels in the brain tissue of mice shown in Figure 2.

Based on the results of the ANOVA test, was obtained p-value of 0.000, less than α = 0.05 (p <0.05). So it can be concluded that there is a significant influence on the administration of Rosella extract with several different doses on levels IL-6 in the brain tissue of mice.

Since the administration of rosella flower extract has a significant effect on brain levels of IL-6, then continued with Post hoc testing by comparing with other groups to seek which dose is most effective. Based on the test results Tukey HSD known that the decrease of brain levels of IL-6 was significantly demonstrated in all groups that were given rosella flower extract, either a dose of 200 mg.kgBW^{-1}, 300 mg.kgBW^{-1}, or a dose of 400 mg.kgBW^{-1}. Groups of rats given the extract of Roselle at all doses had average levels of the IL-6 brain did not differ significantly with the negative control group mice. This shows that the rosella extract can reduce levels of the IL-6 brain to near rats given feed without heating.

On the correlation between changes in the rosella extract dose levels of IL-6, -0.649

ISSN. 2087-2852
E-ISSN. 2338-1655

correlation coefficient with p-value 0.002 (p <0.05). This suggests a significant association between changes in the rosella extract dose levels of IL-6. -0.649 Correlation coefficient indicates the level of the relationship is strong enough, where the negative sign indicates the opposite relationship. This means that increasing doses of the rosella extract will be followed by a decrease in the levels of IL-6 and vice versa.

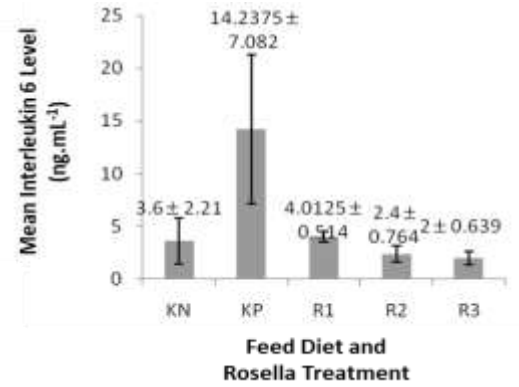

Figure 2. Mean of Interleukin 6 Levels of Brain Tissue

Description:

KN = negative control (standard feed, without extract)

KP = positive control, fed with heated-food without extract

R_1 = treatment group 1 (fed with heated food + Rosella flower ethanol extract 200 mg.kgBW^{-1})

R_2 = treatment group 2 (fed with heated food + Rosella flower ethanol extract 300 mg.kgBW^{-1})

R_3 = treatment group 3, (fed with heated food + Rosella flower ethanol extract 400 mg.kgBW^{-1})

Amyloid β levels of brain tissue

Measurement of amyloid β levels in rat brain tissue KP group showed a higher level than other groups, while the R_3 group showed the lowest results. The average levels of Amyloid b from each group was KN 21.3 ± 4.655 pg.mL^{-1}, KP 93. 454 ± 4.024 pg.mL^{-1}, R1 23.04 ± 2.364 pg.mL^{-1}, R2 20.18± 1.556pg.mL^{-1} and R3 15.54± 2.77 pg.mL^{-1}. Mean level of amyloid β in the brain tissue of rats shown in Figure 3.

Based on the results of the analysis using ANOVA, obtained p-value of 0.000, less than α = 0.05 (p <0.05), so that can be concluded that there is a significant influence on the administration of rosella extract with several different doses on amyloid β levels in rats brain tissue.

As the administration of rosella flower extract had significant effect on amyloid β levels. then continued with Post hoc test by comparing with other groups to seek which rosella extract dosage is most effective. Based on the test results Tukey HSD known that decreased levels of Amyloid b significantly demonstrated in all groups were given a rosella flower extract, either a dose of 200 mg.kgBW^{-1}, 300 mg.kgBW^{-1} body weight, or a dose of 400 mg.kgBW^{-1}. Groups of rats given the rosella extract at all doses had average levels of amyloid β brain did not differ significantly with the negative control group rats. This shows that the rosella extract can lower brain levels of amyloid β to nearly rats given feed without heating.

On the correlation between changes in the rosella extract dose levels of amyloid β, the correlation coefficient was – 0.837 with p-value 0.000 (p <0.05). This suggests a significant association between changes in the rosella extract dose levels of Amyloid β. -0.649 Correlation coefficient indicates the level of the relationship is strong enough, where the negative sign indicates the opposite relationship. This means that increasing doses of the extract of roselle will be followed by decreased levels of Amyloid b and vice versa.

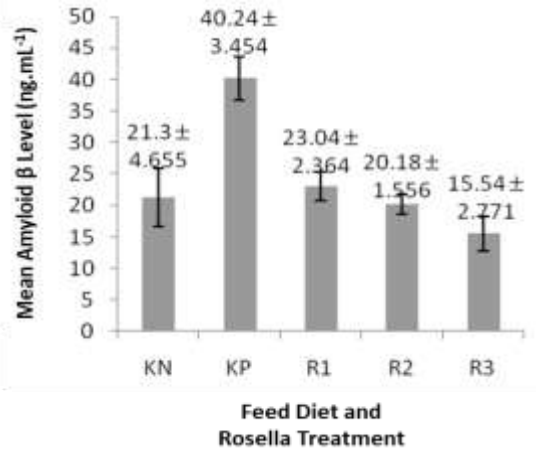

Figure 3. Mean levels of Amyloid β of brain tissue

Description:

KN = negative control (standard feed, without extract)

KP = positive control, fed with heated-food without extract

R_1 = treatment group 1 (fed with heated food + Rosella flower ethanol extract 200 mg.kgBW^{-1})

R_2 = treatment group 2 (fed with heated food + Rosella flower ethanol extract 300 mg.kgBW^{-1})

R_3 = treatment group 3, (fed with heated food + Rosella flower ethanol extract 400 mg.kgBW^{-1})

DISCUSSION

This study aims to prove the effect of food heating on the increase of circulating AGEs, especially CML. It also evaluates the effect of ethanol extract of roselle flowers on levels of interleukin 6 and amyloid β in the brain tissue of rats were given a high AGEs diet. Animals used were white rats (*Rattus novergicus*) male Wistar

ISSN. 2087-2852
E-ISSN. 2338-1655

strain by the age of 10-12 weeks. Selection of the rats as a research subject is because rats are the experimental animals were easily controlled and blood or tissues can be collected in relatively high amounts. In addition the study treatment is given orally, then the use of rats is very helpful, because the presence of stomach valve, that make rats can't vomit [25]. The age of rats of 2-3 months can be analogized as adolescence in humans [16].

Animals were fed heated BR1. BR1 feed compositions containing 21-23% protein, 5% fat, 40-45% starch and 5% crude fiber. Heating was conducted using the oven for 15 minutes at 150°C. The heating method draws on previous research, in which the heating of the meat by baking at a temperature of 150^0C for 15 minutes, which is able to increase CML doubled compared with the controls [1].

The feeding was carried out for 8 weeks, then the experimental animals treated with rosella flower extract for 4 weeks, while still given heated diet. Rosella extract is done in three doses of 200 mg, 300 mg, and 400 mg. The range of doses taken based on the results of previous research, which is known the dose of extract rosella 288 mg.kgBW^{-1} able to demonstrate an anti-inflammatory effect on the rat model of diabetes induced by Streptozotocin [17]. The feeding for 12 weeks analogous to exposure to food processed by heating in humans during 6.5 years. Known comparison of the human years equal to 13 days in rats [16]. Long-term exposure of heated food potentially be a source of AGEs for humans, accumulation of AGEs is higher in tissues and circulation, has the potential to be pathogenic, which will develop into a variety of chronic diseases [18].

In this study, we found that the CML serum level of the group that given oven heated food is higher than the standard group (p= 0.0001). N-carboxymethyl-lysine (CML) is often used as a marker of the formation of AGEs in the diet. CML can be formed from Amadori product that is fructolysin, produced an unstable intermediate and then oxidized to form CML [3]. The process of formation of Amadori product in the Maillard reaction occurs during the processing of meal by heating. The reaction will turn food into a brownish color, aroma onset, as well as produce better taste. When the food is heated at high temperatures, a chemical reaction between an amino acid group with a reducing sugar which will improve the taste and gives a brownish color. This reaction is used in the food industry to change the flavor, color, and aroma of food [19].

Heated diet in this study aims to improve the content of AGEs, in this case, the CML. AGEs are formed during the cooking process such as roasting, frying or baking. Food processing involving high temperatures will lead to the accumulation of AGEs in the body increases dramatically [20]. Dietary AGEs are known to be important resources for the overall amount of AGEs in the body. Methods of cooking with dry heat can increase levels of dietary AGEs. The increase in AGEs in the method can achieve a 100-fold compared with raw foods [2].

Once consumed, 10% of AGEs or also known as glycotoxin will be absorbed into the circulation, 2/3 will remain in the body, and only 1/3 that excreted through renal after 3 days of consumption [21]. Unexcreted glycotoxin will react with cells and tissues, it's also active and causes pathological effects. Total accumulation of exogenous glycotoxin may exceed endogenous glycotoxin [22]. This explanation is consistent with the findings obtained in this study, where the average level of CML serum of rats fed a diet high in AGEs, which are induced by heated diet, almost 3-fold higher compared to the group standard diet.

In this study, after rats were induced by administration of a high AGEs diet from the heated food, then the rats were treated with the rosella extract (*Hibiscus sabdariffa* L). Then we explored the effect on the levels of interleukin 6 (IL-6) in the brain tissue of rats were given high AGEs diet. The results showed a significant effect on the extract of Roselle with several different doses of the levels of IL-6 on brain tissue of rats, which was obtained p-value of 0.000 ($p < 0.05$). Results of post hoc test showed a dose of 200 mg is an effective dose for lowering the levels of brain IL-6. While the correlation test obtained a strong relationship between the provision of roselle extract with decreased levels of IL-6.

Rosella has many active compound content which is able to act as anti-oxidants. Rosella contain flavonoids, anthocyanins, alkaloids, b-sitosterol and ascorbic acid [22]. Per 100 grams of rosella contained 140.13 mg of ascorbic acid and total anthocyanins as much as 622.91 mg. It is known that anthocyanins have antioxidant effects that high compared to other antioxidants, such as vitamin E, ascorbic acid and β-carotene [23].

Anthocyanins, such as cyanidin and delphinidin, is able to inhibit the expression of

ISSN. 2087-2852
E-ISSN. 2338-1655

inflammatory mediators [23]. Delphinidin 3-sambubioside (DP3-Sam), one of Hibiscus anthocyanin which is derived from Hibiscus sabdariffa petals. In cell models, DP3-Sam and delphinidin (Dp) can reduce levels of inflammatory mediators such as iNOS, NO, IL-6, MCP-1 and TNF-α induced by LPS, via down regulation of pathways signal NF κB and MEK1/2 – ERK1 / 2 [24]. In the study conducted Mardiah et al, 2015, found that the extract of roselle 288mg / day can reduce the inflammation in rats induced by streptozotosin, through the mechanism of barriers to free radicals [17]. This is consistent with recent research that indicate a significant influence of rosella extract on levels of IL-6 brain.

The results of this study also found that there is a significant influence on the awarding of rosella flower extract with several different doses to levels of amyloid β (Aβ) of the brain. Known p-value of 0.000 ($p < 0.05$). Results of post hoc test show an effective dose is in the dose of 200 $mg.kgBW^{-1}$.In addition correlation coefficient was -0.837 with p-value 0.000 ($p < 0.05$). This suggests a significant relationship between dose changes rosella extract with Aβ levels. Where the rosella extract dose increase will be followed by decreased levels of Aβ.

Neurodegeneration induced by oxidative stress that is associated with the increasing of the Aβ deposits. Aβ will attach to the neuron membrane or glial cell and generate oxygen-dependent free radicals which then cause lipid peroxidation and protein oxidation. Aβ causes the release of lipid membranes of neurons, resulting in disruption of homeostasis and loss of neuronal function. The loss of membrane integrity that caused by free radicals generated by Aβ leads to dysfunction of cellular, such as the inhibition of ion-motive ATPase inhibition retrieval systems glutamate from Na^+-dependent glial cells as a consequence of excitatory neuron receptors N-methyl-D-aspartate (NMDA) which can cause a loss of synapses in neurons, loss of calcium homeostasis, loss of transporter protein function, impaired signaling pathway, and activation of nuclear transcription factors and apoptotic pathways [25].

Anthocyanins can protect neurons from damage induced by the accumulation of Aβ. Anthocyanins are known to maintain homeostasis of calcium (Ca^{2+}) intracellularly. Disruption of homeostasis of Ca^{2+} itself apart will disrupt membrane integrity and function of the synapse and triggers activation of apotosis mediated by mitochondrial disorders [26]. Other studiy also found that the disruption of homeostasis of Ca^{2+} is also responsible for the increased production of peptide Aβ, resulting in a cycle of degenerative which resulted in increased apoptosis and impaired function of the synapse. Anthocyanin is a free radical scavenger potent and able to detoxify the oxidative damage by reducing ROS and or strengthen the work of enzymatic antioxidants [27]. the results of these studies support the results of recent research which shows that rosella extract has significant effect on brain levels of Aβ.

CONCLUSION

This study concluded that the heated diet may increase the CML serum levels by 3 times compared to the non-heated diet. It also found that Rosella flower extract at a dose of 200 mg/day effectively prevent the increasing of interleukin 6 and Amyloidβ leveles in the brain tissue of rats that were given a high AGEs from the heated feed.

REFERENCES

[1] Henle, T. 2009. Maillard reaction of proteins and advanced glycation end products (AGEs) in food. In: Stadler, R.H., D.R. Lineback (Eds). Process-Induced Food Toxicants. John Wiley & Sons, Inc. Hoboken, NJ. 215-242.

[2] Uribarri, J., S. Woodruff, S. Goodman, W. Cai, X. Chen, R. Pyzik, A. Yong, G.E. Striker, H. Vlassara. 2010. Advanced glycation end products in foods and a practical guide to their reduction in the diet. *J. Am. Diet. Assoc.* 110. 911-916.

[3] Ames, J.M. 2008. Determination of Nε-(Carboxymethyl)lysine in foods and related systems. *Ann. NY Acad. Sci.* 1126. 20-24.

[4] Jerums, G., S. Panagiotopoulos, J. Forbes, T. Osicka, M. Cooper. 2009. Evolving concepts in advanced glycation, diabetic nephropathy, and diabetic vascular disease. *Arch. Biochem. Biophys.* 419. 55-62.

[5] Simard, E., T. Söllradl, J.S. Maltais, J. Boucher, P. D'Orléans-Juste, M. Grandbois. 2015. Receptor for Advanced Glycation End-Products signaling interferes with the vascular smooth muscle cell contractile phenotype and function. PLoS ONE 10(8). e0128881.

[6] Srikanth, V., B. Westcott, J. Forbes, T.G. Phan, R. Beare, A. Venn, S. Pearson, T. Greenaway, V. Parameswaran, G. Münch,

ISSN. 2087-2852
E-ISSN. 2338-1655

2013. Methylglyoxal, cognitive function and cerebral atrophy in older people. *J. Gerontol. A Biol. Sci. Med. Sci.* 68(1). 68-73.

[7] Takuma, K., F. Fang, W. Zhang, S. Yan, E. Fukuzaki, H. Du, A. Sosunov, G. McKhann, Y. Funatsu, N. Nakamichi, T. Nagai, H. Mizoguchi, D. Ibi, O. Hori, S. Ogawa, D.M. Stern, K. Yamada, S.S. Yan. 2011. RAGE-mediated signaling contributes to intraneuronal transport of amyloid-beta and neuronal dysfunction. *Proc. Natl. Acad. Sci. USA.* 106. 20021-20026.

[8] Li, J., D. Liu, L. Sun, Y. Lu, Z. Zhang. 2012. Advanced Glycation End Products and neurodegenerative diseases: mechanisms and perspective. *J. Neurol. Sci.* 317. 1-5.

[9] Yamamoto, A., A. Simonsen. 2011. The elimination of accumulated and aggregated proteins: a role for aggrephagy in neurodegeneration. *Neurobiol. Dis.* 43. 17-28.

[10] Vauzour, D., A.R. Mateos, G. Corona, M.J.O. Concha, J.P.E. Spencer. 2010. Polyphenols and human health: prevention of disease and mechanisms of action. *Nutrients*. 2. 1106-1131.

[11] Spencer, J.P., D. Vauzour, C. Rendeiro. 2009. Flavonoids and cognition: the molecular mechanisms underlying their behavioural effects. Arch. Biochem. Biophys. 492. 1-9.

[12] Shipp, J., E.M. Abdel-Aal. 2010. Food applications and physiological effects of anthocyanins as functional food ingredients. *Open Food Sci. J*. 4. 7-22.

[13] Ubani, C.S., P.E. Joshua, A.N. Oraeki. 2010. Influence of aqueous extract of *Hibiscus sabdariffa* calyces on lipid profile of phenobarbitone induces Wistar albino rats. *J. Pharm. Res.* 3(2). 319-324.

[14] Ademiluyi, A.O., G.Oboh, O.J. Agbebi. 2013. Anthocyanin – rich red dye of *Hibiscus Sabdariffa* calyx modulates Cisplatin-induced Nephrotoxicity and oxidative stress in rats . *Int. J. Biomed. Sci.* 9(4). 243-248

[15] Peng, X., K.W. Cheng, J. Ma, B. Chen, C.T. Ho, C. Lo, F. Chen, M. Wang. 2008. Cinnamon bark proanthocyanidins as reactive carbonyl scavengers to prevent the formation of advanced glycation end products. *J. Agr. Food Chem.* 56. 1907-1911.

[16] Sengupta, P. 2013. The laboratory rat: relating its age with humans. *Int. J. Prev. Med.* 4(6). 624-630.

[17] Mardiah, F.R. Zakaria, E. Prangdimurti, R. Damanik. 2015. Anti-inflammatory of purple roselle extract in diabetic rats induced by Streptozotocin. *Proc. Food Sci.* 3. 182-189.

[18] Fang, H., L. Wang, S. Zhang, H. Liu, J. Li. 2014. Advanced glycation end products (AGEs) formation in high protein foods processing model system. *J. Chinese Inst. Food Sci. Technol.* 14. 28-34.

[19] Tamanna, N., N. Mahmood. 2015. Food processing and maillard reaction products: effect on human health and nutrition. *Int. J. Food Sci.* 1-6.

[20] Contreras, C.L., K.C. Novakofski. 2010. Dietary advanced glycation end products and aging. *Nutrients*. 2. 1247-1265.

[21] Degen J, H. Beyer, B. Heymann, M. Hellwig, T. Henle. 2014. Dietary influence on urinary e xcretion of 3-deoxyglucosone and its metabolite 3-deoxyfructose. *J. Agric. Food Chem.* 62. 2449-2456.

[22] Semba, R.D., E.J. Nicklett, L. Ferrucci. 2010. Does accumulation of Advanced Glycation End Products contribute to the aging phenotype? *J. Gerontol. Med. Sci.* 65A(9). 963-975.

[23] Hou, D.X., T. Yanagita, T. Uto, S. Masuzaki, M. Fujii. 2005. Anthocyanidins inhibit cyclooxygenase-2 expression in LPS-evoked macrophages:structure–activity relationship and molecular mechanisms involved. *Biochem. Pharmacol.* 70. 417-425.

[24] Sogo, T., N. Terahara, A. Hisanaga, T. Kumamoto, T. Yamashiro, S. Wu, K. Sakao, D.X. Hou. 2015. Anti-inflammatory effects of Delphinidin 3-Sambubioside. *Biochem. Mol. Biol. Int.* 41(1). 58-65.

[25] Richardsz, S.S., R.A. Sweet. 2009. Dementia. In: Sadock, B.J., V.A. Sadock, P. Ruiz. Comprehensive text book of psychiatry Vol 1, 9th Ed. Lippincott Williams and Wilkins. Philadelphia. 1176-1185.

[26] Kawahara, M., M. Kato-Negishi. 2011. Link between aluminum and the pathogenesis of Alzheimer's disease: the integration of the aluminum and amyloid cascade hypotheses, *Int. J. Alzheimer Dis.* DOI: 10.4061/2011/276393.

[27] Butterfield, D.A., A.M. Swomley, R. Sultana. 2013. Amyloid beta-peptide (1-42)-induced oxidative stress in Alzheimer disease: importance in disease pathogenesis and progression. *Antioxid. Redox Signal.* DOI:10.1089/ars.2012.5027.

ISSN. 2087-2852
E-ISSN. 2338-1655

Dynamical Analysis of Predator-Prey Model Leslie-Gower with Omnivore

Rina Exviani[1]*, Wuryansari Muharini Kusumawinahyu[2], Noor Hidayat[3]

[1]Master Program of Mathematics, Faculty of Mathematics and Natural Sciences, University of Brawijaya, Malang, Indonesia
[2]Department of Mathematics, Faculty of Mathematics and Natural Sciences, University of Brawijaya, Malang, Indonesia

Abstract

This article discussed a dynamical analysis on a model of predator-prey Leslie-Gower with omnivores which is modified by Lotka-Volterra model with omnivore. The dynamical analysis was done by determining the equilibrium point with its existing condition and analyzing the local stability of the equilibrium point. Based on the analysis, there are seven points of equilibrium. Three of them always exist while the four others exist under certain conditions. Four points of equilibrium, which are unstable, while the others three equilibrium point are local asymptotically stable under certain conditions. Moreover, numerical simulations were also conducted to illustrate the analytics. The results of numerical simulations agree with the results of the dynamical analysis.

Keywords: local stability, omnivore, predator-prey models, the equilibrium point.

INTRODUCTION

Lotka-Volterra model was firstly introduced Lotka in 1925 and Volterra in 1926 [1]. Lotka-Volterra's study has produced a simple model of predation or interaction between two species in an ecosystem. They also have introduced classical Lotka-Volterra model, which is currently developed by researchers [2].

In 1948, Leslie discussed Lotka-Volterra model and found impossibility in a model, which is infinity in predator growth [3]. Therefore, Leslie and Gower introduced a new name's predator-prey model, which is modification of Lotka-Volterra's model. The model is known as Leslie-Gower Predator-Prey Model. Leslie-Gower have modified Lotka-Volterra's *predator-prey* model by assuming that the predation of predator is limited, which means that the predation of predator will not more carrying capacity of prey. Leslie-Gower two dimension models as:

$$\begin{aligned}\frac{dx}{dt} &= (r_1 - a_1 y - b_1 x)x,\\ \frac{dy}{dt} &= \left(r_2 - a_2\frac{y}{x}\right)y.\end{aligned} \qquad \textbf{(1)}$$

with $x(t)$ state the population density of prey and $y(t)$ state the population density of predator.

In 2015, Andayani and Kusumawinahyu [4] a three species predator – prey model, the third species are omnivores. This model is constructed by assumming there are just three species in such an ecosystem. The first species, called as prey (rice plant), the prey for the second and the third species. The second species, called as predator (carrion), only feeds on the first species and can extinct with prey. The third species, namely omnivores (mouse), eat the prey and carcasses of predator. Consequently, omnivores of predator only reduces the prey population but does not affect the predator growth. Assumed that the prey population grow logistically and any competition between omnivores [5]. Based on these assumption, the mathematical model representing those growth density of population rates by nonlinear ordinary differential equation system, namely

$$\begin{aligned}\frac{dx}{dt} &= x(1 - y - z - bx),\\ \frac{dy}{dt} &= y(-c + x)\\ \frac{dz}{dt} &= z(-e + fx + gy - \beta z).\end{aligned} \qquad \textbf{(2)}$$

In this model, $x(t), y(t)$ and $z(t)$ the density of prey, predator, and omnivore populations, respectively. All parameter of model (2) are positive. The death rates of the predator and omnivore are denoted by c and e, respectively. The parameter f rivalry toward prey that effect increases of omnivore population, while the parameter g rivalry toward prey that effect increases of omnivore population. Parameter b and β carrying the capacity of the prey and omnivore, respectively [5]. The aim of this study is a dynamical analysis on a model of predator-prey

* Correspondence address:
Rina Exviani
Email : rhinaexviani@gmail.com
Address : Dept. Mathematics, Faculty of Mathematics and Natural Science, University of Brawijaya, Veteran Malang, Malang 65145.

ISSN. 2087-2852
E-ISSN. 2338-1655

Leslie-Gower with omnivores which is modified by Lotka-Volterra model with omnivore.

MATERIAL AND METHOD

In this study, predator-prey model by Leslie-Gower with omnivore. This model is constructed by assumming the third species are omnivores. This model is constructed by assumming there are just three species in such an ecosystem. The first species, called as prey (rice plant), the prey for the second and the third species. The second species, called as predator (carrion), only feeds on the first species and can extinct with prey. The third species, namely omnivores (mouse), eat the prey and carcasses of predator. Consequently, omnivores of predator only reduces the prey population but does not affect the predator growth. Assumed that the prey population grow logistically and any competition between omnivores.

Literature Study

Literature study related to the research process, such as the literature discussing the Leslie-Gower model, Lotka-Volterra model, omnivore, and forward-backward sweep method [7-12]. We also used other supporting references in problem solving in this study. In the Lotka-Volterra predator-prey model with omnivore, namely:

$$\frac{dx}{dt} = x(1 - y - z - bx),$$
$$\frac{dy}{dt} = y(-c + x),$$
$$\frac{dz}{dt} = z(-e + fx + gy - \beta z).$$

on this system has only five equilibrium point's, namely:

$$E_0 = (0,0,0)$$
$$E_1 = \left(\frac{1}{b},0,0\right)$$
$$E_2 = (c,1-bc,0)$$
$$E_3 = \left(\frac{e+\beta}{f+\beta b},0,\frac{f-be}{f-\beta b}\right)$$
$$E_4 = \left(c,\frac{\beta(1-bc)-(fc-e)}{g+\beta},\frac{g(1-bc)+f(fc-e)}{g+\beta}\right)$$

To accommodate biological meaning, the existence conditions for the equilibria require that they are nonnegative. It is obvious that E_0 dan E_1 always exist, E_2 exist if $bc < 1$, E_3 exist if $f > be$ and E_4 the densities of omnivores and predators $1 - bc$ has to be positive. Then, E_4 exist if $bc < 1$ and $0 < fc - e < \beta(1 - bc)$.

While, predator-prey model by Leslie-Gower with omnivore has seven equilibrium points (Table 1). So the predator-prey model by Leslie-Gower model with omnivores is more concrete in this case.

Table 1. Equilibrium Points of predator-prey model by Leslie-Gower with omnivore

Equilibrium Points	Existence Requirement
$E_1 = (0,0,0)$	-
$E_2 = \left(0,\frac{kr_2}{a_2},0\right)$	-
$E_3 = \left(\frac{r_1}{b_1},0,0\right)$	-
$E_4 = (0,y_4,z_4)$	$c_3 kr_2 > a_2 c_1$
$E_5 = (x_5,0,z_5)$	$r_1 c_2 > b_1 c_1$
$E_6 = (x_6,y_6,0)$	$a_2 r_1 > b_2 kr_2$
$E_7 = (x_7,y_7,z_7)$	$c_4 r_1 + c_1 b_3 > \frac{c_1}{c_3}(b_2 c_4 + b_3 c_3)$

MATHEMATICAL MODEL

This study constructs Lotka-Volterra's *predator-prey* model with omnivore (2). This model is developed by modify the predator that previously used Lotka-Volterra's form to Leslie-Gower's, which was examined by Leslie-Gower. This is based on the fact that predator depends on the available number of prey to establish. Therefore, the model is stated to be in the following equation system (3):

$$\frac{dx}{dt} = x(r_1 - b_1 x - b_2 y - b_3 z),$$
$$\frac{dy}{dt} = y\left(r_2 - \frac{a_2}{x+k}y\right), \quad \textbf{(3)}$$
$$\frac{dz}{dt} = z(-c_1 + c_2 x + c_3 y - c_4 z)$$

with $x = x(t)$, $y = y(t)$, and $z = z(t)$ state the population density of prey, predator, and omnivore. All of the parameters are positive in value. Parameters r_1 and r_2 respectively show intrinsic growth of prey and predator. b_1 is the coeffcient of competition between prey, b_2 is the predator interaction coefficient between predator to prey and b_3 is a predatory interaction between omnivores against prey. Whereas a_2 is an interaction parameter between predators and parameter k is a parameter of protection against

ISSN. 2087-2852
E-ISSN. 2338-1655

predators. Parameter c_1 is omnivorous natural death, c_2 partially omnivorous predictor coefficient to prey, c_3 as predator coefficient of predator carcass, c_4 is competition between omnivorous population. While, tribal form $\frac{(a_2 y)}{(x+k)}$ can be interpreted as scarcity of prey may stimulate predators to replace foot sources with other alternatives. Therefore, it is assumed that predators depend not only on prey, but predators can eat other than prey in the prey environment. So in this article it is modeled by adding a positive constant k to the division.

RESULT AND DISCUSSION

All parameters of Equation (3.1) in this study are assumed positive in value. Parameters r_1 and r_2 consecutively show intrinsic growth of prey and predator. b_1 is the competition coefficient among preys, b_2 is the predation interaction coefficient between predator and prey, and b_3 is the predation interaction between omnivore and prey. Meanwhile, a_2 is the interaction parameter among predators, and parameter k is the protection parameter against predator. Parameter c_1 is the natural death of omnivore, c_2 is the predation coefficient of omnivore on prey, c_3 is the predation coefficient on the carcass of predator, and c_4 is the competition among omnivore populations.

Equilibrium Point and Existence

The point of Equilibrium (3) is solution for sytem:

$$x(r_1 - b_1 x - b_2 y - b_3 z) = 0,$$
$$y\left(r_2 - \frac{a_2}{x+k} y\right) = 0,$$
$$z(-c_1 + c_2 x + c_3 y - c_4 z) = 0.$$

The system has seven points of equilibrium, namely $E_1 = (0,0,0)$, $E_2 = \left(0, \frac{kr_2}{a_2}, 0\right)$, and $E_3 = \left(\frac{r_1}{b_1}, 0,0\right)$ in which the three points exist unconditionally, equilibrium point $E_4 = \left(0, \frac{r_2 k}{a_2}, \frac{c_3 r_2 k - c_1 a_2}{c_4 a_2}\right)$ exists with the condition of $c_3 r_2 k > a_2 c_1$, equilibrium point $E_5 = \left(\frac{r_1 c_4 + b_3 c_1}{c_2 b_3 + c_4 b_1}, 0, \frac{c_2 r_1 - c_1 b_1}{c_2 b_3 + c_4 b_1}\right)$ exists if $z = c_2 r_1 > c_1 b_1$, equilibrium point $E_6 = \left(\frac{r_1 a_2 - b_2 r_2 k}{a_2 b_1 + b_2 r_2}, \frac{r_2 (r_1 + b_1 k)}{a_2 b_1 + b_2 r_2}, 0\right)$ exists if $a_2 r_1 > b_2 k r_2$. Equilibrium point $E_7 = (x_7, y_7, z_7)$ with

$$x_7 = \frac{a_2 r_1 c_4 + a_2 c_1 b_3 - r_2 k b_2 c_4 - r_2 k c_3 b_3}{a_2 b_1 c_4 + a_2 c_2 b_3 + r_2 b_2 c_4 + r_2 c_3 b_3}$$
$$y_7 = \frac{r_2 (r_1 c_4 + c_1 b_3 + k b_1 c_4 + k c_2 b_3)}{a_2 b_1 c_4 + a_2 c_2 b_3 + r_2 b_2 c_4 + r_2 c_3 b_3}$$
$$z_7 = \frac{r_1 r_2 c_3 + r_1 a_2 c_2 + b_1 r_2 k c_3 - b_1 a_2 c_1 - b_2 r_2 c_1 - b_2 r_2 k c_2}{r_2 b_2 c_4 + r_2 c_3 b_3 + a_2 b_1 c_4 + a_2 c_2 b_3}$$

exists if $r_1 c_4 + b_3 c_1 > \frac{c_1}{c_3}(b_2 c_4 + b_3 c_3)$.

Stability Analysis

The local stability of system (3) for each equilibrium point is as follows.

a) $E_1 = (0,0,0)$ is unstable

b) $E_2 = \left(0, \frac{r_2 k}{a_2}, 0\right)$ is stable if $r_1 a_2 < b_2 r_2 k$ and $c_3 r_2 k > c_1 a_2$

c) $E_3 = \left(\frac{r_1}{b_1}, 0,0\right)$ is unstable

d) $E_4 = \left(0, \frac{r_2 k}{a_2}, \frac{c_3 r_2 k - c_1 a_2}{c_4 a_2}\right)$ is stable if $c_4 r_1 + c_1 b_3 < \frac{k r_2}{a_2}(b_2 c_4 + b_3 c_3)$

e) $E_5 = \left(\frac{r_1 c_4 + b_3 c_1}{c_2 b_3 + c_4 b_1}, 0, \frac{c_2 r_1 - c_1 b_1}{c_2 b_3 + c_4 b_1}\right)$ is unstable

f) $E_6 = \left(\frac{r_1 a_2 - b_2 r_2 k}{a_2 b_1 + b_2 r_2}, \frac{r_2 (r_1 + b_1 k)}{a_2 b_1 + b_2 r_2}, 0\right)$ is unstable

g) $E_7 = (x_7, y_7, z_7)$.

This stability analysis uses the criteria of Routh-Hurwitz $\lambda^3 + A\lambda^2 + B\lambda + C = 0$. The characteristic equation will have negative roots if and only if $A > 0, C > 0$ and $AB > C$. Therefore, it can be concluded that $AB - C > 0$. If the condition is met, the equilibrium point of E_7 will be stable.

Proof

i. Jacobi matrix system (3) for E_1 is $J(E_1) = \begin{bmatrix} r_1 & 0 & 0 \\ 0 & r_2 & 0 \\ 0 & 0 & -c_1 \end{bmatrix}$. The three Eigen values of the matrix $J(E_1)$ are positive, so E_1 is unstable.

ii. Jacobi matrix $E_2 = \left(0, \frac{r_2 k}{a_2}, 0\right)$ is

$$J = \begin{bmatrix} r_1 - \frac{b_2 r_2 k}{a_2} & 0 & 0 \\ \frac{r_2^2}{a_2} & -r_2 & 0 \\ 0 & 0 & -c_1 + \frac{c_3 r_2 k}{a_2} \end{bmatrix},$$

which has eigen values $\lambda_1 = r_1 - \frac{b_2 r_2 k}{a_2}$, $\lambda_2 = -r_2$, $\lambda_3 = -c_1 + \frac{c_3 r_2 k}{a_2}$

ISSN. 2087-2852
E-ISSN. 2338-1655

. The equilibrium point (E_2) stable, if $r_1 a_2 < b_2 r_2 k$ and $c_3 r_2 k > c_1 a_2$.

iii. Jacobi matrix on equilibrium point $E_3 = \left(\frac{r_1}{b_1}, 0, 0\right)$ is

$$J = \begin{bmatrix} -r_1 & -\frac{r_1 b_2}{b_1} & -\frac{r_1 b_3}{b_1} \\ 0 & r_2 & 0 \\ 0 & 0 & -c_1 + \frac{c_2 r_1}{b_1} \end{bmatrix},$$

has eigen values $\lambda_1 = -r_1,\ \lambda_2 = r_2,\ \lambda_3 = -c_1 + \frac{c_3 r_1}{b_1}$ so E_3 unstable.

iv. Jacobi matrix on equilibrium point $E_4 = \left(0, \frac{r_2 k}{a_2}, \frac{c_3 r_2 k - c_1 a_2}{c_4 a_2}\right)$ is

$$J = \begin{bmatrix} r_1 - b_2 y_4 - b_3 z_4 & 0 & 0 \\ \frac{r_2^2}{a_2} & -r_2 & 0 \\ c_2 z_4 & c_3 z_4 & -c_1 - 2c_4 z_4 + c_3 z_4 \end{bmatrix},$$

because $x = 0, r_2 \frac{a_2}{x+k} y = 0,$ and $-c_1 + c_2 x + c_3 y - c_4 z = 0.$ so E_4 stable if

$$\lambda_1 = r_1 - \frac{b_2 k r_2}{a_2} - \frac{b_3}{a_2 c_4}(k r_2 c_3 - a_2 c_1) < 0,$$

$$\frac{r_1 a_2 c_4 - b_2 k r_2 c_4 - b_3 k r_2 c_3 + b_3 a_2 c_1}{a_2 c_4} < 0,$$

$$c_4 r_1 + c_1 b_3 < \frac{k r_2}{a_2}(b_2 c_4 + b_3 c_3).$$

v. Jacobi matrix on the equilibrium point $E_5 = \left(\frac{r_1 c_4 + b_3 c_1}{c_2 b_3 + c_4 b_1},\ 0,\ \frac{c_2 r_1 - c_1 b_1}{c_2 b_3 + c_4 b_1}\right)$

$$J(E_5) = \begin{bmatrix} r_1 - 2b_1 x_5 - b_3 z_5 & -b_2 x & -b_3 x \\ 0 & r_2 & 0 \\ c_2 z_5 & c_3 z_5 & -c_1 - 2c_4 z_5 + c_2 x_5 \end{bmatrix}$$

with,

$r_1 - b_1 x - b_2 y - b_3 z = 0 \Rightarrow r_1 - b_1 x_5 - b_3 z_5 = 0,$

$y = 0,$

$-c_1 + c_2 x + c_3 y - c_4 z = 0 \Rightarrow -c_1 + c_2 x_5 - c_4 z_5 = 0,$

so

$$J(E_5) = \begin{bmatrix} -b_1 x_5 & -b_2 x & -b_3 x \\ 0 & r_2 & 0 \\ c_2 z_5 & c_3 z_5 & -c_4 z_5 \end{bmatrix},$$

$$|J(E_5) - \lambda I| = \begin{vmatrix} -b_1 x_5 - \lambda & -b_2 x & -b_3 x \\ 0 & r_2 - \lambda & 0 \\ c_2 z_5 & c_3 z_5 & -c_4 z_5 - \lambda \end{vmatrix},$$

$$= (r_2 - \lambda_1) \begin{vmatrix} -b_1 x_5 - \lambda & -b_3 x \\ c_2 z_5 & -c_4 z_5 - \lambda \end{vmatrix} = 0.$$

The equilibrium point E_5 result $\lambda_1 = r_2 > 0$ so unstable l.

vi. Jacobi matrix on the equilibrium point $E_6 = \left(\frac{r_1 a_2 - b_2 r_2 k}{a_2 b_1 + b_2 r_2}, \frac{r_2(r_1 + b_1 k)}{a_2 b_1 + b_2 r_2}, 0\right)$

$$J(E_6) = \begin{bmatrix} r_1 - 2b_1 x_6 - b_2 y_6 & -b_2 x_6 & -b_3 x_6 \\ \frac{a_2 y^2}{(x+k)^2} & r_2 \frac{2a_2 y}{x+k} & 0 \\ 0 & 0 & -c_1 + c_2 x_6 + c_3 y_6 \end{bmatrix},$$

with,

$r_1 - b_1 x - b_2 y - b_3 z = 0 \Rightarrow r_1 - b_1 x_6 - b_3 y_6 = 0,$

$r_2 \frac{a_2}{x+k} y = 0 \Rightarrow \frac{y}{x+k} = \frac{r_2}{a_2} \rightarrow \left(\frac{y}{x+k}\right)^2 = \frac{{r_2}^2}{{a_2}^2},$

$z = 0,$

so

$$J(E_6) = \begin{bmatrix} -b_1 x_6 & -b_2 x & -b_3 x \\ \frac{{r_2}^2}{a_2} & -\frac{a_2 y}{x+k} & 0 \\ 0 & 0 & -c_1 + c_2 x_6 + c_3 y \end{bmatrix},$$

$$|J(E_6) - \lambda I| = \begin{vmatrix} -b_1 x_6 - \lambda & -b_2 x & -b_3 x \\ \frac{{r_2}^2}{a_2} & -\frac{a_2 y}{x+k} - \lambda & 0 \\ 0 & 0 & J_{33} - \lambda \end{vmatrix},$$

$$= (J_{33} - \lambda)\left[(\lambda + b_1 x)\left(\lambda + \frac{a_2 y}{x+k}\right) + \frac{b_2 {r_2}^2}{a_2} x\right] = 0,$$

$$= (J_{33} - \lambda)\left[\lambda^2 + \left(b_1 x + \frac{a_2 y}{x+k}\right)\lambda + \frac{b_1 a_2 y}{x+k} + \frac{b_2 {r_2}^2}{a_2} x\right] = 0.$$

result $\lambda_1 < 0,$ with used characteristic as follow $\lambda_1 \lambda_2 > 0 \,\Lambda\, \lambda_1 + \lambda_2 < 0$ proven that E_6 unstable.

vii. Jacobi matrix on equilibrium point $E_7 = (x_7, y_7, z_7)$

$$J(E_7) = \begin{bmatrix} b_1 x_7 & -b_2 x_7 & -b_3 x_7 \\ \frac{a_2 y^2}{(x+k)^2} & r_2 \frac{2a_2 y}{x+k} & 0 \\ c_2 z_7 & c_3 z_7 & -c_1 z_7 \end{bmatrix},$$

$$J(E_7) = \begin{bmatrix} -b_1 x_7 & -b_2 x & -b_3 x \\ \frac{{r_2}^2}{a_2} & -r_2 & 0 \\ c_2 z_7 & c_3 z_7 & -c_1 z_7 \end{bmatrix},$$

Same of characteristic with use cofactor expansion second line,

$$|J(E_7) - \lambda I| = \begin{vmatrix} -b_1 x_7 - \lambda & -b_2 x_7 & -b_3 x_7 \\ \frac{{r_2}^2}{a_2} & -r_2 - \lambda & 0 \\ c_2 z_7 & c_3 z_7 & -c_1 z_7 - \lambda \end{vmatrix},$$

ISSN. 2087-2852
E-ISSN. 2338-1655

$$= -\frac{r_2^2}{a_2}\begin{vmatrix} -b_2x_7 & -b_3x_7 \\ c_3z_7 & -c_1z_7-\lambda \end{vmatrix} + (-r_2-\lambda)\begin{vmatrix} -b_1x_7-\lambda & -b_3x_7 \\ c_2z_7 & -c_1z_7-\lambda \end{vmatrix} = 0,$$

$$= -\frac{1}{a_2}(a_2b_1c_4\lambda x_7z_7 + a_2b_1c_4r_2x_7z_7 + a_2b_3c_2\lambda x_7z_7 + a_2b_3c_2r_2x_7z_7$$
$$+b_2c_4r_2^2x_7z_7 + b_3c_3r_2^2x_7z_7 + a_2b_1\lambda^2x_7 + a_2b_1\lambda r_2x_8 + a_2c_4\lambda^2z_7$$
$$+a_2c_4\lambda r_2z_7 + b_2\lambda r_2^2x_7 + a_2\lambda^3 + a_2\lambda^2r_2),$$

With declaration as:

$$\lambda^3 + A\lambda^2 + B\lambda + C = 0,$$

with,

$$A = c_4z_7 + b_1x_7 + r_2 > 0,$$
$$B = b_1c_4x_7z_7 + b_3c_2x_7z_7 + b_1r_2x_8 + c_4r_2z_7 + a_2r_2^2x_7 > 0,$$
$$C = \frac{a_2b_1c_4r_2x_7z_7 + a_2b_3c_2r_2x_7z_7 + b_2c_4r_2^2x_7z_7 + b_3c_3r_2^2x_7z_7}{a_2}.$$

Based on criteria Routh-Hurwitz, the equilibrium point E_7 local asymptotically stable if $A > 0$, $C > 0$ and $AB - C > 0$.

Numerical Simulation

Numerical simulations are performed to see the validity of numerical analysis using the fourth-orde Runge-Kutta method to ilustrate the results of the analysis. There are several cases that are simulated in the discussion of this study, as follows.

Simulation I

Simulation I (Fig. 1) show E_2 exists, and conditions of stable E_2 are $r_1a_2 < b_2kr_2$ and $c_1a_2 > c_3kr_2$, Parameter being used $r_1 = 0.5$, $b_1 = 0.05$, $b_2 = 0.6$, $b_3 = 0.1$, $r_2 = 0.7$, $a_2 = 0.2$, $k = 0.3$, $c_1 = 0.9$, $c_2 = 0.25$, $c_3 = 0.2$, $c_4 = 0.2$

Thus, the equilibrium points of E_1 exists, E_2 exist, E_3 exists, and E_5 exists. The numerical simulation to equilibrium point $E_2 = (0{,}1.05{,}0)$. This is relevant to the analysis result which states that equilibrium E_2 is stable.

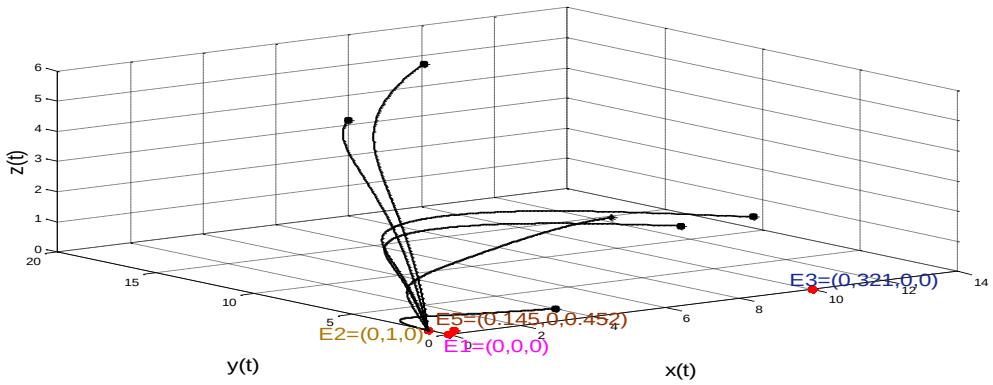

Figure 1. Portrait Phase System Equation 3.1 for simulation I

Simulation II

Simulation II, the stability conditions of E_2 are changed into $r_1a_2 > b_2kr_2$ and $c_1a_2 < c_3kr_2$, parameter
$r_1 = 0.8, b_2 = 0.4, b_3 = 0.1, b_1 = 0.05, r_2 = 0.7$, $a_2 = 0.2, k = 0.3, c_1 = 0.3, c_2 = 0.25$, $c_3 = 0.6, c_4 = 0.2$. Thus, it produces E_4 exists, E_5 exists, E_6 exists. Then, E_7 exists and is stable toward equilibrium point, so the initial value shows that E_7 is stable.

ISSN. 2087-2852
E-ISSN. 2338-1655

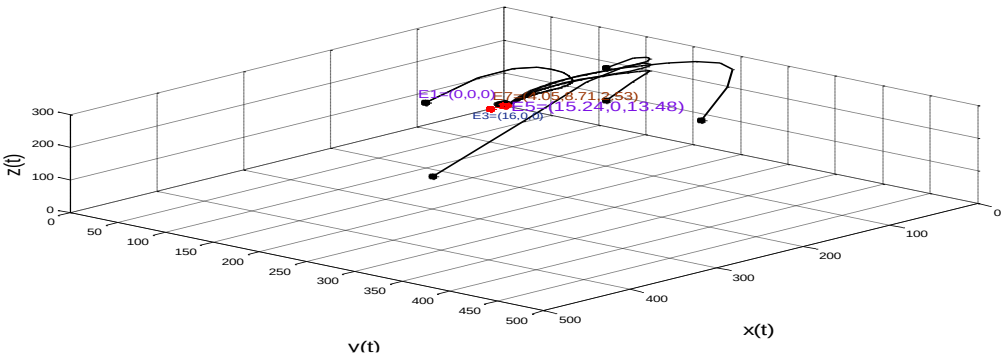

Figure 2. Portrait Phase System Equation 3.1 for Simulation II

Simulation III

The stability conditions in simulation III of E_2 are changed into $r_1 a_2 > b_2 k r_2$ dan $c_1 a_2 > c_3 k r_2$, parameter $r_1 = 0.8, b_2 = 0.4, b_3 = 0.1, b_1 = 0.05, r_2 = 0.7, a_2 = 0.2, k = 0.3, c_1 = 0.9, c_2 = 0.25, c_3 = 0.2, c_4 = 0.2$. Thus, it produces E_1 exists, E_2 exists, E_3 exists, E_5 exists, and E_6 exists, but, in this case, it does not go to any point, so it exists but is unstable.

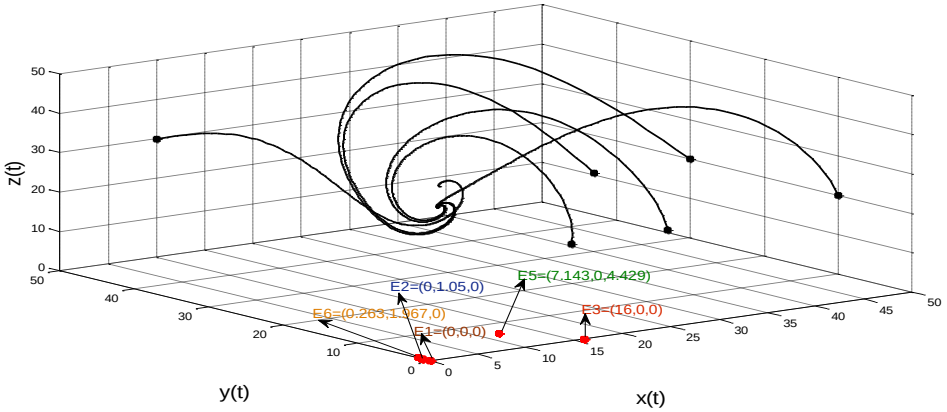

Figure 3. Portrait Phase System Equation 3.1 for Simulation III

Simmulation IV

The stability conditions in simulation IV, of E_2 are changed into $r_1 a_2 < b_2 k r_2$ dan $c_1 a_2 < c_3 k r_2$, parameter $r_1 = 0.5, b_2 = 0.6, b_3 = 0.1, b_1 = 0.05, r_2 = 0.7, a_2 = 0.2, k = 0.3, c_1 = 0.3, c_2 = 0.25,$ $c_3 = 0.6, c_4 = 0.2$. Thus, it produces E_1 exists, E_2 exists, E_3 exists, E_4 exists, and E_5 exists and unstable.

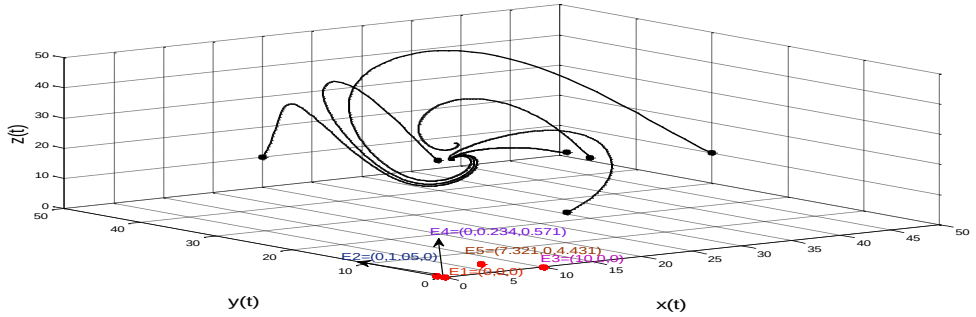

Figure 4. portrait phase system equation 3.1 for simulation IV

ISSN. 2087-2852
E-ISSN. 2338-1655

Simulation V:

Stability condition $c_4 r_1 + c_1 b_3 < \frac{r_2 k}{a_2}(b_2 c_4 + b_3 c_3)$, the fifth simulation is conducted to show the stability characteristics of equilibrium point E_4. Based on the existence condition and the stability of equilibrium point E_4, parameter $r_1 = 0.5, b_2 = 0.4, b_3 = 0.1, b_1 = 0.05, r_2 = 0.9, a_2 = 0.2, k = 0.5, c_1 = 0.3, c_2 = 0.25, c_3 = 0.6, c_4 = 0.2$. Thus, it produces E_1 exists, E_2 exists, E_3 exists, E_4 exists, and E_5 exists towards equilibrium point E_4. This is relevant to the analysis result which states that the equilibrium point is stable.

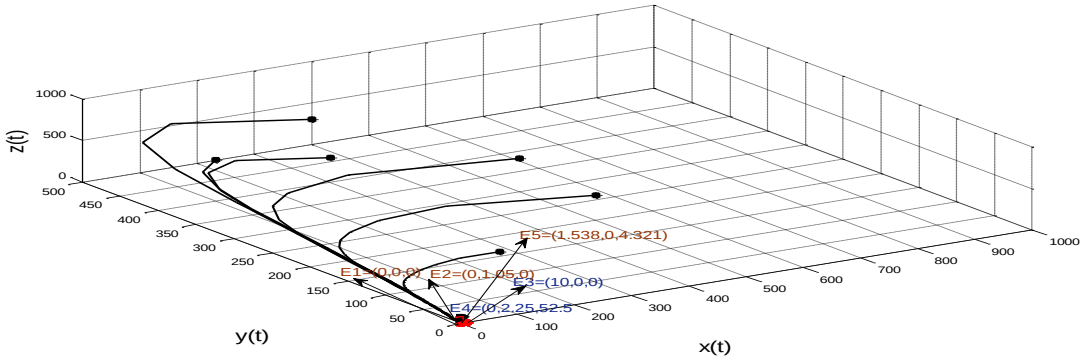

Figure 5. Portrait Phase System Equation 3.1 for Simulation V

CONCLUSION

The conclusions that are drawn based on the discussion of the thesis are as follows. Predator-prey model by Leslie-Gower with omnivore is obtained in a form of common differential equation system. There are seven equilibrium points in the model, there are three of them, i.e. E_1, E_2 and E_3, unconditionally exist and the other four, i.e. E_4, E_5, E_6 and E_7, conditionally exist. Of the seven equilibrium points, three of them, E_1, E_2, E_4 dan E_7, have stability condition.

REFERENCES

[1] Jeffrey, R. C. 2012. Introduction to numerical methods. Lecture Notes for Matth 3311. The Hong Kong University of Science and Technology. Kowloon, Hongkong.

[2] Murray, J.D. 2002. Mathematical biology I: an introduction, 3rd Ed. Springer. New York.

[3] Mohammadi, H., M. Mahzoon. 2013. Effect of weak prey in Leslie-Gower Predator-Prey Model. *Appl. Math. Comput.* 224, 196-204.

[4] Andayani, P., W.M. Kusumawinahyu. 2015. Global Stability Analysis on a Predator-Prey Model with Omnivora. *Appl. Math. Sci.* 9(36). 1771-1782.

[5] Previte, J.P., K.A. Hoffman. 2010. Chaos in Predator-Prey Model with an Omnivore. *Math. Biol.* 92(1). 1-7.

[6] Huo, H.F., X. Wang, C. Carlos. 2011. Dynamics of a stage structured Leslie-Gower Predator- Prey Model. *Appl. Math.* Article ID 149341.

[7] Chen, L., F. Chen. 2009. Global stability in Leslie-Gower Predator-prey model With feedback controls. 22(9). 1330-1334.

[8] Tanabe, K., T. Namba. 2005. Omnivory creates chaos in simple food web models. *Ecology.* 86(12). 3411-3414.

[9] Nagle, R.K., E.B. Saff, A. D. Snider. 2004. Fundamentals of differential equations and boundary value problems, 6th Ed. Pearson Education Inc. USA.

[10] Mattheij, R., J. Molenaar. 2002. Ordinary differential equation in theory and practice. Society for Industrial and Applied Mathematics. New York.

[11] Korobeinikov, A. 2001. A Lyapunov Function for Leslie-Gower Predator-Prey Models. *Appl. Math. Lett.* 14(6). 697-699.

[12] Polis, G.A., C.A. Myers, R.D. Holt. 1989. The ecology and evolution of intraguild predation: potential competitors that eat each other. *Annu. Rev. Ecol. Evol. Syst.* 20(1). 297-330.

ISSN. 2087-2852
E-ISSN. 2338-1655

MANUSCRIPT SUBMISSION

FOCUS AND SCOPE

Journal of Experimental Life Science (JELS) is scientific journal published by Graduate Program of Brawijaya University as distribution media of Indonesian researcher's results in life science to wider community. JELS is published in every four months. JELS published scientific papers in review, short report, and life sciences especially nanobiology, molecular biology and cellular biology. JELS is scientific journal that published compatible qualified articles to academic standard, scientific and all articles reviewed by expert in their field.

Journal of Experimental Life Science (JELS) have vision to become qualified reference media to publish the best and original research results, and become the foundation of science development through invention and innovation on cellular, molecular, and nanobiology rapidly to community.

Journal of Experimental Life Science (JELS) have objectives to published qualified articles on research's results of Indonesian researchers in life science scope. JELS encompasses articles which discuss basic principles on nature phenomenon with cellular, molecular, and nanobiology approach.

PEER REVIEW PROCESS

Publication of articles by JITODE is dependent primarily on their validity and coherence, as judged by peer reviewers, who are also asked whether the writing is comprehensible and how interesting they consider the article to be. All submitted manuscripts are read by the editorial staff and only those articles that seem most likely to meet our editorial criteria are sent for formal review. All forms of published correction may also be peer-reviewed at the discretion of the editors. Reviewer selection is critical to the publication process, and we base our choice on many factors, including expertise, reputation, and specific recommendations. The editors then make a decision based on the reviewers' advice, from among several possibilities:

Accepted, with or without editorial revisions
Invite the authors to revise their manuscript to address specific concerns before a final decision

Rejected, but indicate to the authors that further work might justify a resubmission

Rejected outright, typically on grounds of specialist interest, lack of novelty, insufficient conceptual advance or major technical and/or interpretational problems

PUBLICATION FREQUENCY

JELS publish 2 Issues per year until 2017. JELS started to publish 3 Issues per year since 2018.

OPEN ACCESS POLICY

This journal provides immediate open access to its content on the principle that making research freely available to the public supports a greater global exchange of knowledge.

COPYRIGHT NOTICE

Authors who publish with this journal agree to the following terms:

Authors retain copyright and grant the journal right of first publication with the work simultaneously licensed under a Creative Commons Attribution License that allows others to share the work with an acknowledgement of the work's authorship and initial publication in this journal.

Authors are able to enter into separate, additional contractual arrangements for the non-exclusive distribution of the journal's published version of the work (e.g., post it to an institutional repository or publish it in a book), with an acknowledgement of its initial publication in this journal.

Authors are permitted and encouraged to post their work online (e.g., in institutional repositories or on their website) prior to and during the submission process, as it can lead to productive exchanges, as well as earlier and greater citation of published work (The Effect of Open Access).

PRIVACY STATEMENT

The names and email addresses entered in this journal site will be used exclusively for the stated purposes of this journal and will not be made available for any other purpose or to any other party.

ETHICS PUBLICATION

Research that using animal, human, and clinical testing is should already have ethical clearance certificate from authorized institution.

Title Typed in Bold, Capitalize each First Letter of Each Word, Except Conjunctive, *Scientific name* should not be Abbreviated (Calibri 14 Bold Center, should not exceed 12 words, except conjuctive)

First Author[1]*, Second Author[2], Third Author[3] (Calibri 12 Center, without title)

[1]First Author Affiliation, Correspondence author should be indicated by * symbol (Calibri 9 Center)
[2]Department of Biology, Faculty of Mathematics and Natural Sciences, University of Brawijaya, Malang, Indonesia
[3]Laboratorium of Physiology, Faculty of Medicine, University of Brawijaya, Malang, Indonesia

Abstract (Calibri 9 Bold Center)

This article illustrates preparation of your paper using MS-WORD (.doc or .rtf). Manuscript was numbered consecutively. Main text typed in two columns (67 characters), except title and abstract in one column. The manuscript should be written in English. The length of manuscript should not exceed 10 pages including table and figure in this format using A4 paper single space. The text should be in the margin of 3 cm up, down and left side, 2.5 cm on right side. Abstract includes the research purposes, research method and research results in one paragraph of *essay,* not *enumerative*. No citation in abstract. Abstract should not exceed 200 words. Keywords typed after abstract. (Calibri 9 Justify).

Keywords: manuscript, English, format, 5 words maximum (Calibri 9 Left)

INTRODUCTION* (Calibri 10 Bold, Left, Capslock)

All submitted manuscripts should contain original research which not previously published and not under consideration for publication elsewhere. Articles must be written in ENGLISH and manuscripts may be submitted for consideration as research report articles, short reports or reviews.

The introduction explains the background of the problem, the study of literature and research purposes. Some initial introduction paragraphs explain the problem and background to these problems [1]. The next few paragraphs explain the study of literature that contains recent knowledge development which is directly related to the issues. The last paragraph of the introductory section contains a description of the purposes of the study. (Calibri 10 Justify)

MATERIAL AND METHOD (Calibri 10 Bold, Left, Capslock)

This section describes the types of methods (qualitative, quantitative or mixed-method) with details of methods of data collection and data analysis [2]. This section also describes the perspective that underlying the selection of a particular method. (Calibri 10 Justify)

Correspondence address: (Calibri 8 Bold, Left)
Full name of correspondence author
Email : sapto@jurnal.ub.ac.id
Address : afiliation address include post code

Data Collection (Calibri 10 Bold, Left)

Explain the data collection methods, i.e. surveys, observations or archive, accompanied by details of the use of such methods. This section also describes the population, sampling and sample selection methods. (Calibri 10 Justify)

The use of English language should followed proper grammar and terms. Name of organism shoul be followed by its full scientific name in the first mention, in *italic* [3]. Author of the scientific name and the word of "var." typed regular. Example: *Stellaria saxatillis* Buch. Ham. First abbreviation typed in colon after the abbreviated phrase.

Author must use International Standard Unit (SI). Negative exponent used to show the denominator unit. Example: g l^{-1}, instead of g/l. The unit spaced after the numbers, except percentage [4]. Example: 25 g l^{-1}, instead of 25gl^{-1}; 35% instead of 35 %. Decimal typed in dot (not coma). All tables and figures should be mentioned in the text.

RESULT AND DISCUSSION (Calibri 10 Bold, Left, Capslock)

This section contains the results of the analysis and interpretation or discussion of the results of the analysis. Describe a structured, detailed, complete and concise explanation, so that the reader can follow the flow of analysis and thinking of researchers [5]. Part of the results study should be integrated with the results of the

analysis and the results and discussion are not separated.

Table

Table should be submitted within the manuscript and in separated file of *Microsoft Excel* (xls.). Table whould not exceed 8 cm (one column) and 17 cm (two columns). Table should be embedded in different page after references.

Table should be numbered in sequence. Table title should be brief and clear above the table, with uppercase in initial sentence. Vertical line should not be used. Footnote use number with colon and superscripted. Symbol of (*) or (**) was used to show difference in confidence interval of 95 and 99%.

Table 1. Example of the Table (Calibri 8.5 Left)

No	Point (Calibri 8.5 Justify)	Description
1		
2		
3		
4		
5		

Sources: Journal of PPSUB (Calibri 8.5 Left)

Figures

Figures should be in high resolution and well contrast in JPEG or PDF with the following conditions:

- Monochrome image (line art), figures of black and white diagram (solid/no shades of gray), resolution 1000-1200 dpi (dot per inch).
- Combination Halftone, combine figure and text (image containing text) and coloured graphic or in grayscale format. Resolution 600-900 dpi.
- Halftone, coloured figure or grayscale format without text. Resolution 300 dpi.
- Black and white figure should be in the grayscale mode, while coloured figures should be in RGB mode.
- Figure should not exceed the width of 8 cm (one column), 12.5 cm (1.5 columns) or 17 cm (two columns).
- Figures title typed clearly below the figure.
- Figure with pointing arrow should be grouped (grouping).
- Figures were recommended in black and white.
- Legend or figure description should be clear and complete. If compressed, the figure should be readable.
- Statistic graphic should be supplemented with data sources.
- If the figures come from the third party, it should have the copyright transfer from the sources.

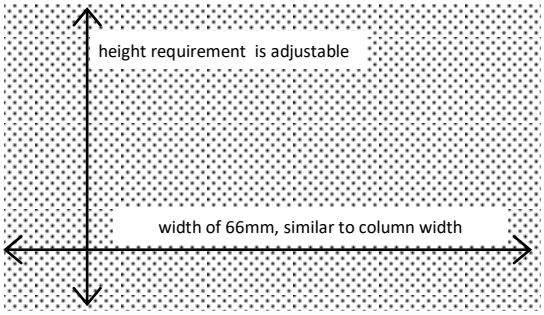

Figure 1. Illustration of Dimensional Figure of one column width. Figure dimension adjusted to the width of one column. Name the figure (diagram) written below the image. (Calibri 8.5 Justify)

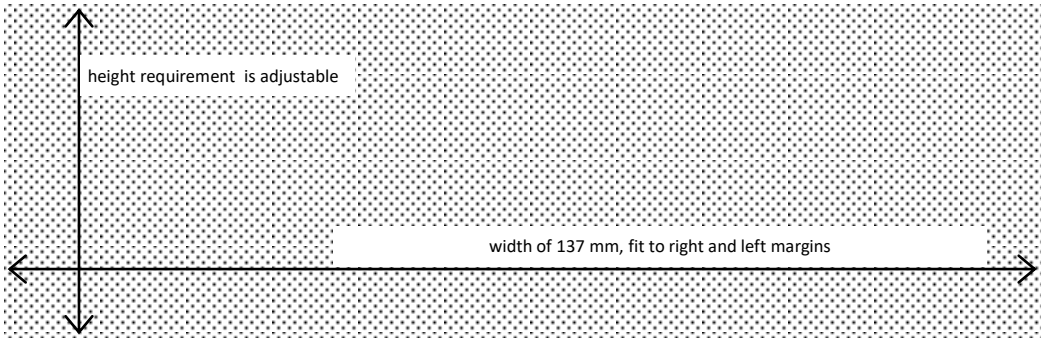

Figure 2. . Illustration of Dimensional Figure of two column width. Figure dimension adjusted to the width of two columns (137 mm). Figure were align top or bottom of the page. (Calibri 8.5 Justify)

References

1. Primary references include journal, patent, dissertation, thesis, paper in proceeding and text book.
2. Avoid self citation.
3. Author should avoid reference in reference, popular book, and internet reference except journal and private ana state institution.
4. Author was not allowed to use abstract as references.
5. References should been published (book, research journal or proceeding). Unpublished references or not displayed data can not be used as references.
6. References typed in numbering list (format number 1,2,3,…), ordered sequentially as they appear in the text (system of Vancouver or author-number style).
7. Citation in the manuscript typed only the references number (not the author and year), example: Obesity is an accumulation of fat in large quantities which would cause excessive body weight (overweight) [1]. Obesity is a risk factor of diabetic, hypertension dan atherosclerosis [2].

CONCLUSION (Calibri 10 Bold, Left, Capslock)

Conclusion of the study's findings are written in brief, concise and solid, without more additional new interpretation. This section can also be written on research novelty, advantages and disadvantages of the research, as well as recommendations for future research.(Calibri 10 Justify)

ACKNOWLEDGEMENT (Calibri 10 Bold, Left, Capslock)

This section describes gratitude to those who have helped in substance as well as financially. (Calibri 10 Justify)

REFERENCES (Calibri 10 Bold, Left, Capslock)

[1]. (Calibri 10 Justify, citation labelling by references numbering)
[2]. Vander, A., J. Sherman., D. Luciano. 2001. Human Physiology: The Mecanisms of Body Function. McGraw-Hill Higher Education. New York. (Book)
[3]. Shi, Z., M. Rifa'i, Y. Lee, K. Isobe, H. Suzuki. 2007. Importance of CD80/CD86-CD28 interaction in the recognation of target cells by $CD8^{+}CD122^{+}$ regulatory T cells. *Journal Immunology.* 124. 1:121-128. (Article in Journal)
[4]. Syafi'i, M., Hakim, L., dan Yanuwiyadi, B. 2010. Potential Analysis of Indigenous Knowledge (IK) in Ngadas Village as Tourism Attraction. pp. 217-234. In: Widodo, Y. Noviantari (eds.) Proceed-ing *Basic Science National Seminar 7* Vol.4. Universitas Brawijaya, Malang. (Article within conference proceeding)
[5]. Dean, R.G. 1990. Freak waves: A possible explanation. p. 1-65. *In* Torum, A., O.T. Gudmestad (eds). Water wave kinetics. CRC Press. New York. (Chapter in a Book)
[6]. Astuti, A.M. 2008. The Effect of Water Fraction of *Stellaria* sp. on the Content of TNF-α in Mice (*Mus musculus* BALB-C). Thesis. Department of Biology. University of Brawijaya. Malang. (Thesis)

Cover Images:

3D Structure of EGCG (*Epigallocatechin-3-Gallate*)
Green Tea Component

Created by:
Widodo, S.Si.,M.Si.,Ph.D MED Sc.

Address:

Building B, 1st Floor, Graduate School, University of Brawijaya
Jl. Mayor Jenderal Haryono 169, Malang, 65145
Telp: (0341) 571260 ; Fax: (0341) 580801
Email: jels@ub.ac.id
Web: jels.ub.ac.id

9 772087 285007